

MILLER, STRATVERT & TORGERSON, P.A.
LAW OFFICES

RANNE B. MILLER
ALAN C. TORGERSON
ALICE T. LORENZ
GREGORY W. CHASE
LYMAN G. SANDY
STEPHEN M. WILLIAMS
STEPHAN M. VIDMAR
SETH V. BINGHAM
TIMOTHY R. BRIGGS
RUDOLPH LUCERO
DEBORAH A. LACEY
GARY L. GORDON
LAWRENCE R. WHITE
SHARON P. GROSS
VIRGINIA ANDERMAN
MARTE D. LIGHTSTONE
J. SCOTT HALL*
THOMAS R. MACK
TERRI L. SAUER
JOEL T. NEWTON
THOMAS M. DOMME
RUTH O. PREGENZER
JEFFREY E. JONES

MANUEL I. ARRIETA
ROBIN A. GOBLE
JAMES R. WOOD
DANA M. KYLE
KIRK R. ALLEN
RUTH FUESS
KYLE M. FINCH
H. BROOK LASKEY
KATHERINE W. HALL
FRED SCHILLER
PAULA G. MAYNES
MICHAEL C. ROSS
CARLA PRANDO
KATHERINE N. BLACKETT
JENNIFER L. STONE
ANDREW M. SANCHEZ
M. DYLAN O'REILLY
AMINA QUARGNALI-LINSLEY
JENNIFER D. HALL
MARY A. WOODWARD
JENNIFER L. OLSON
TODD A. SCHWARZ
JULIE A. COLEMAN

COUNSEL

PAUL W. ROBINSON
ROSS B. PERKAL
JAMES J. WIDLAND
BRADLEY D. TEPPER**
GARY RISLEY

OF COUNSEL

WILLIAM K. STRATVERT
JAMES B. COLLINS
RALPH WM. RICHARDS

ALBUQUERQUE, NM

500 MARQUETTE N.W., SUITE 1100
POST OFFICE BOX 25687
ALBUQUERQUE, NM 87125-0687
TELEPHONE: (505) 842-1950
(800) 424-7585
FACSIMILE: (505) 243-4408

FARMINGTON, NM

300 WEST ARRINGTON, SUITE 300
POST OFFICE BOX 869
FARMINGTON, NM 87499-0869
TELEPHONE: (505) 326-4521
FACSIMILE: (505) 325-5474

SANTA FE, NM

150 WASHINGTON AVE., SUITE 300
POST OFFICE BOX 1986
SANTA FE, NM 87504-1986
TELEPHONE: (505) 989-9614
FACSIMILE: (505) 989-9857

LAS CRUCES, NM

500 S. MAIN ST., SUITE 800
POST OFFICE BOX 1209
LAS CRUCES, NM 88004-1209
TELEPHONE: (505) 523-2481
FACSIMILE: (505) 526-2215

PLEASE REPLY TO SANTA FE

* NEW MEXICO BOARD OF SPECIALIZATION RECOGNIZED SPECIALIST IN NATURAL RESOURCES - OIL & GAS LAW
** NEW MEXICO BOARD OF SPECIALIZATION RECOGNIZED SPECIALIST IN REAL ESTATE LAW

June 21, 2001

BY HAND-DELIVERY

Mr. David Catanach
New Mexico Oil Conservation Division
1220 S. St. Francis
Santa Fe, New Mexico 87505

Re: NMOCD Case No. 12633; Application of David H. Arrington Oil and Gas, Inc. for
Unorthodox Well Location and Simultaneous Dedication, Lea County, New Mexico

Dear Mr. Catanach:

At the June 14, 2001 hearing on the above application, the petroleum engineering witness testimony referred to SPE literature addressing methods of calculating drainage radii from horizontal wellbores in the context of the difficulties that would be encountered in establishing, monitoring and enforcing a production penalty in this case. We offered to provide you with copies of those articles which are enclosed herewith.

Very truly yours,

MILLER, STRATVERT & TORGERSON, P.A.



J. Scott Hall

JSH/ao

Enclosure(s) – as stated

cc: Mike Stewart, Permian Resources w/o
Michael Feldewert (with enclosures)

7690/26781/Correspondence/Catanach ltr1.doc

Mike Stewart

Fax: 918-685-3874

Pages: 6

From: Paul M. Mubalik

Methods calculate area drained by horizontal wells

S.D. Joshi
Joshi Technologies
International Inc.
Tulsa

The drainage area of a horizontal well can be calculated by averaging the results obtained from two different methods. For anisotropic reservoirs, nonuniform permeability has to be included in drainage area calculations.

Well spacing

Horizontal wells, in general, give higher reserves than vertical wells. Two reasons for obtaining higher ultimate reserves are increase in the drainage area and increase in the recovery factor.

The most important reason for obtaining higher ultimate reserves from horizontal wells is the significant enhancement of the drainage area, especially as compared to vertical wells. The other reason for an increase in reserves is improvement in the recovery factors. Recovery factor is the percentage of the original oil in place that can be produced.

At the present time, the field histories tend to indicate

that the recovery factors are, in general, 2-5% higher than those for vertical wells. Until more long term histories are available, it is difficult to make an exact judgment on the improvement of recovery factors.

In a given time period, a horizontal well drains a larger reservoir volume than a vertical well. Thus, the spacing used for a horizontal well should be larger than that used for a vertical well.

The drainage area of a horizontal well also depends upon natural fracturing in a fractured reservoir.

In a naturally fractured reservoir, a horizontal well drains more volume in the direction parallel to the natural fractures than in the direction perpendicular to the natural fractures. Therefore, the well spacing requirement along a fracture trend is different than that perpendicular to the fracture trend.

It is important to note that even for a vertical well, the well spacing is based upon the reservoir parameters and economic criteria. Theoretically speaking, one can drill a single well in a large reservoir

and it will drain the entire reservoir, although it may take a very long time.

Well spacings are designed so as to maximize the oil recovery and economic benefit of production. To estimate the drainage area of a horizontal well, first one must estimate the drainage area (or well spacing) of a vertical well.

Pseudosteady state

Dimensionless time, t_D , which is used to define various regions, is given as:

$$t_D = \frac{0.000264 kt}{\phi \mu c_{ti} r_w^2} \quad (1)$$

and area-based dimensionless time

$$t_{DA} = t_D (r_w^2/A) \quad (2)$$

Thus

$$t_{DA} = \frac{0.000264 kt}{\phi \mu c_{ti} A} \quad (3)$$

where: k = permeability (md), t = time (hr), ϕ = porosity (fraction), μ = viscosity (cp), c_{ti} = initial total compressibility (psi^{-1}), A = area sq

ft, and r_w = well bore radius, ft

For a vertical well located at the center of a drainage circle or a square, the time to reach pseudosteady state is $t_{DA} = 0.1$. Substituting this in Equation 3, we have

$$t_{DA} = 0.1 = \frac{0.000264 kt}{\phi \mu c_{ti} A} \quad (4)$$

$$t_{pss} = \frac{379 \phi \mu c_{ti} A}{k} \quad (5)$$

t_{pss} = time to reach pseudosteady state in hours

$$t_{pdss} = \frac{15.79 \phi \mu c_{ti} A}{k} \quad (6)$$

t_{pdss} is the time to reach pseudosteady state in days.

Generally, oil wells are developed on 40-acre spacing and gas wells are developed on 160-acre spacing. Hence

$$40 \text{ acres} = 40 \times 43,560 \text{ sq ft/acre} = 1.7424 \times 10^6 \text{ sq ft} \quad (7)$$

$$160 \text{ acres} = 160 \times 43,560 \text{ sq ft/acre} = 6.9696 \times 10^6 \text{ sq ft} \quad (8)$$

Substituting these areas into Equation 6 gives for a 40 acre well:

$$t_{pdss} = \frac{27.512 \times 10^6 \phi \mu c_{ti}}{k} \quad (9)$$

and for a 160 acre well:

$$t_{pdss} = \frac{110.05 \times 10^6 \phi \mu c_{ti}}{k} \quad (10)$$

Equations 4 and 5 show that transient time depends on the basic reservoir properties, such as permeability, porosity, and compressibility. Time to reach pseudosteady state does not depend on well stimulation.

In the case of oil wells, normally, the time to reach pseudosteady state is of the order of a few days to months.

In contrast, for gas wells in low-permeability reservoirs, the time to reach pseudosteady state could be very long; in some cases as long as a few years.

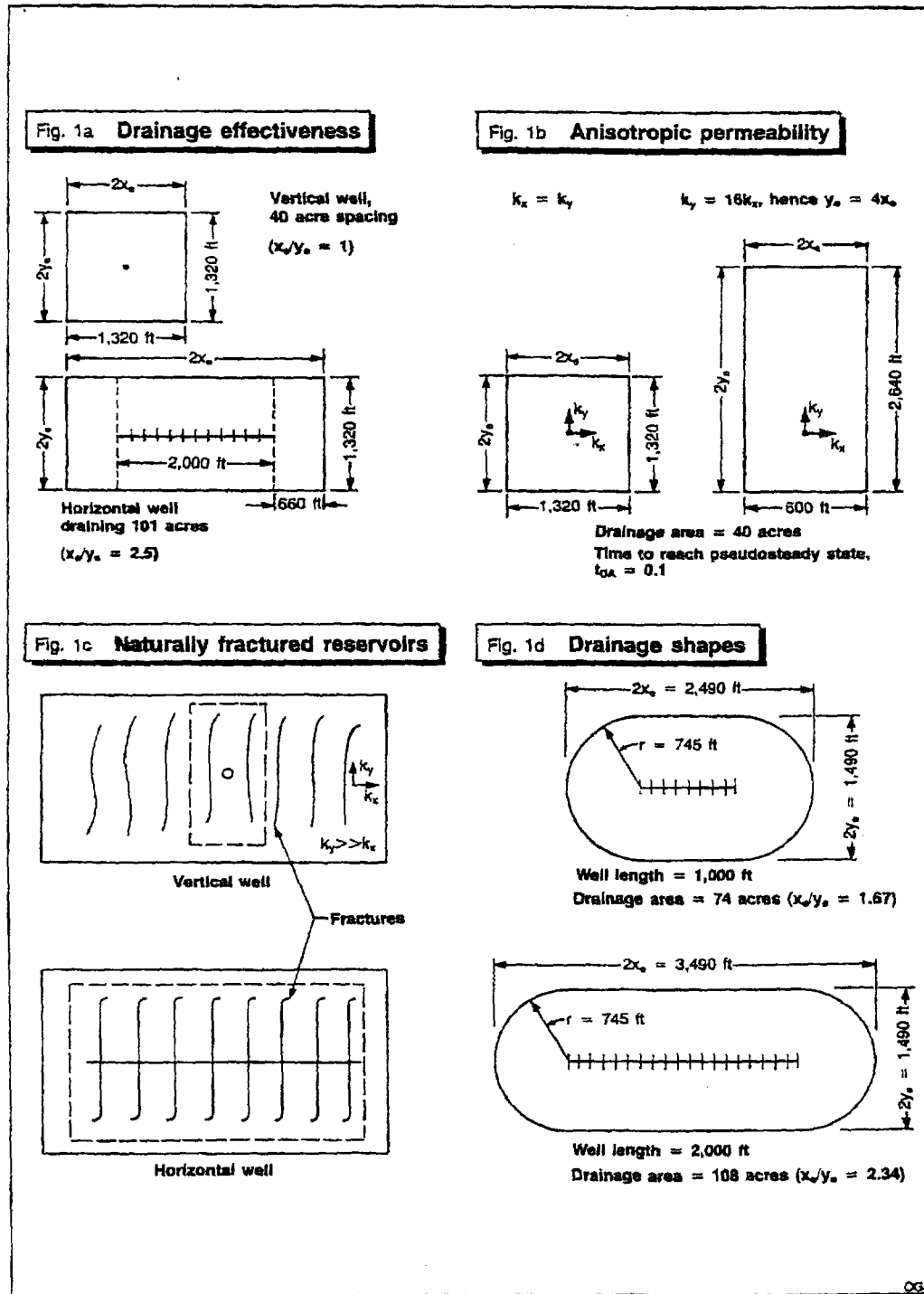
Oil well example

For an oil well drilled on 40-acre spacing, calculate the

Based on Chapter 2 of Horizontal Well Technology, Vol. 1, to be published by PennWell Publishing in late 1990.

Drainage areas

Fig. 1



wells in reservoirs with permeability less than 0.1 md, can take years for the transient state to end. In such tight reservoirs, it is very difficult to drain the reservoir economically. In these cases, methods are needed to accelerate reservoir drainage.

Infill drilling and horizontal drilling provide alternatives to drain the reservoir effectively.

The dimensionless time to reach pseudosteady state is $t_{DA} = 0.1$, as long as the well is centrally located in a drainage plane, i.e., when the well is at the center of a circle or a square ($x_e/y_e = 1$).

When the drainage area becomes rectangular, the time to reach pseudosteady state increases. For example, when one side of a drainage rectangle is five times larger than the other side ($x_e/y_e = 5$) the dimensionless time to reach pseudosteady state is $t_{DA} = 1.0$, i.e., ten times longer than a vertical well located centrally in the drainage plane.

Thus, vertical wells are unable to drain effectively rectangular drainage areas in uniform permeability reservoirs.

As shown in Fig. 1a; a long horizontal well in a given time can drain a larger area than a vertical well.

A 40-acre spacing vertical well reaches pseudosteady state in 16 days. By the same principle (Fig. 1) a 2,000 ft long well would reach pseudosteady state in a 101-acre area in 16 days.

Table 1 tells us that the time to reach pseudosteady state using vertical well draining a rectangle with dimensions $x_e/y_e = 2.5$ would be 2.5 times longer than that for a 2,000 ft long horizontal well (assumes $L \geq 1$ - the quantity y_e/x_e).

Thus, horizontal wells can be utilized to drain a larger reservoir volume than vertical wells in a given time period. This becomes very important in tight reservoirs when close vertical well spacing is required to drain the reservoir effectively.

Therefore, in a tight reservoir, horizontal wells can be used to enhance drainage volume per well in a given time period.

time to reach pseudosteady state given $\phi = 10\%$, $c_{H_2} = 0.00005 \text{ psi}^{-1}$, $k = 35 \text{ md}$, and $\mu = 4.2 \text{ cp}$ (shallow well-dead oil). Using Equation 5, $t_{pss} = 0.0002274 A = 396 \text{ hr} = 16.5 \text{ days}$.

Gas well example

Calculate the time required

to reach pseudosteady state for a gas well drilled at either 20 or 160-acre spacing in a reservoir with an initial pressure (p_i) of 1,450 psi and the reservoir properties of $\phi = 7\%$, $k = 0.03 \text{ md}$, $\mu = 0.015 \text{ cp}$, and $c_{H_2} = 0.000690 \text{ psi}^{-1}$.

Again using Equation 5 $t_{pss} = 0.00915A$. For 20

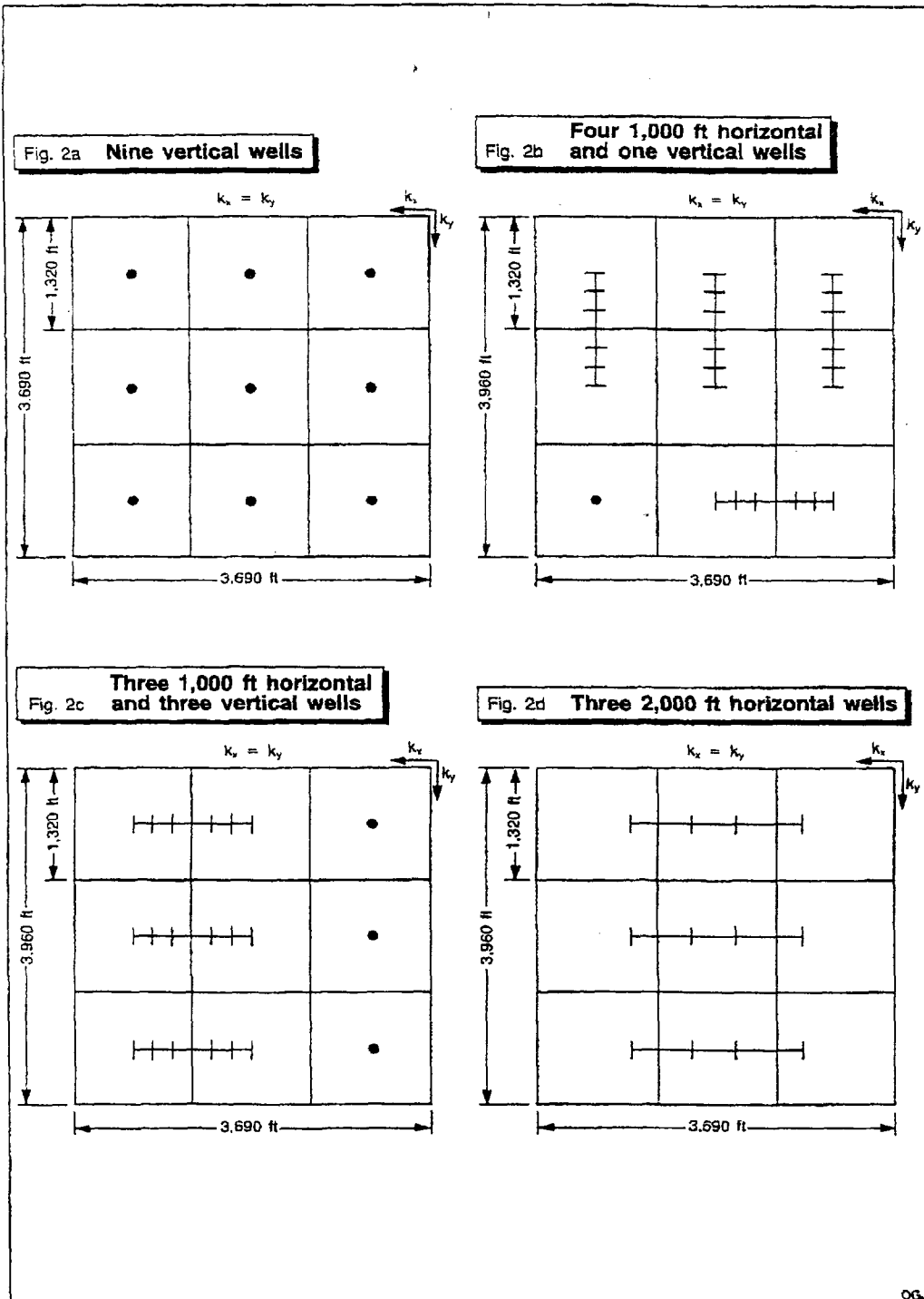
acres, $t_{pss} = 7,974 \text{ hr} = 332 \text{ days} = 0.91 \text{ years}$.

For 160 acres, $t_{pss} = 63,772 \text{ hr} = 2,657 \text{ days} = 7.3 \text{ years}$ of infinite-acting period.

As noted in the previous example, gas wells (or oil wells) drilled in a very tight reservoir, especially gas

Development patterns for 360 acres

Fig. 2



Areal anisotropy
 The discussion so far has been restricted to reservoirs with homogeneous areal permeability, namely $k_x = k_y$ (Fig. 1b). In naturally fractured reservoirs, the permeability along the fracture trend is larger than in a direction perpendicular to fractures. In such cases, a vertical well

would drain more length along the fracture trend.
 The derivation starting with Equation 11 can be used to estimate each side of a drainage area in an areally anisotropic reservoir. The equation assumes a single phase, steady-state (time independent) flow through an homogeneous formation.

$$\frac{\delta}{\delta x} (k_x \frac{dp}{dx}) + \frac{\delta}{\delta y} (k_y \frac{dp}{dy}) = 0 \quad (11)$$

Assuming constant values of k_x and k_y in x and y directions, respectively, Equation 11 is rewritten as

$$k_x \frac{d^2p}{dx^2} + k_y \frac{d^2p}{dy^2} = 0 \quad (12)$$

Multiplying and dividing throughout by $\sqrt{k_x k_y}$, Equation 12 becomes

$$\sqrt{k_x k_y} \left[\sqrt{\frac{k_x}{k_y}} \frac{d^2p}{dx^2} + \sqrt{\frac{k_y}{k_x}} \frac{d^2p}{dy^2} \right] = 0 \quad (13)$$

This can be transformed into

$$\sqrt{k_x k_y} \left[\frac{d^2p}{dx'^2} + \frac{d^2p}{dy'^2} \right] = 0 \quad (14)$$

where $y' = y \sqrt{k_x/k_y}$ (15)

and

$$y = y' \sqrt{k_y/k_x} \quad (16)$$

Thus, an areally anisotropic reservoir would be equivalent to a reservoir with effective permeability of $\sqrt{k_x k_y}$. The drainage length along the high-permeability side is larger by a factor of $\sqrt{k_y/k_x}$ than the drainage length along a low-permeability side.

Thus, if permeability along the fracture trend is 16 times larger than perpendicular to it, then drainage length along the fracture is four times larger than the length perpendicular to the fracture (Fig 1b).

In such areally anisotropic reservoirs, using vertical wells, it is difficult to drain the larger reservoir lengths in the low-permeability direction.

A horizontal well drilled along the low-permeability direction has a potential to drain a significantly larger area than a vertical well and therefore recover more reserves than vertical wells.

Thus, horizontal wells are highly beneficial in areally anisotropic reservoirs.

It is obvious that in naturally fractured formations, horizontal wells drilled in a direction perpendicular to the natural fractures are highly beneficial (Fig 1c). The success of horizontal wells in naturally fractured reservoirs, such as Austin chalk formation in Texas and Bakken formation in North Dakota, illustrates the advantage of horizontal drilling in areally anisotropic formations.

For fractured vertical wells, limited results are available to calculate the time to reach

Table 1

Start of pseudosteady state time

$t_{DA,ps}$ x_f/x_e	1	2	x_f/y_e 3	5	10	20
0.01	0.3	0.5	0.7	1.5	3.0	6.0
0.05	0.3	0.5	0.7	1.5	3.0	6.0
0.10	0.3	0.5	0.7	1.5	3.0	6.0
0.20	0.3	0.5	0.7	1.5	3.0	6.0
0.40	0.3	0.5	0.7	1.5	3.0	6.0
0.50	0.3	0.5	0.7	1.5	3.0	6.0
0.70	0.3	0.5	0.7	1.5	3.0	6.0

*For fully penetrating infinite-conductivity fractures for various penetration ratios (x_f/x_e) and different x_f/y_e ratios

pseudosteady state in square drainage boundaries.^{1,2} Khan has obtained results for fractured vertical wells in rectangular areas.³

Recently, similar results were also available for horizontal wells.^{4,5} Mutalik, et al.,⁴ calculated the time to reach the pseudosteady state for fractured vertical wells and horizontal wells in rectangular drainage areas (Tables 1 and 2).

It is important to note that there is some discrepancy in calculating the time to start pseudosteady state. For a single-phase flow in a homogeneous reservoir, the relationship between the dimensionless pressure and the dimensionless time for a well producing at a constant rate in a bounded reservoir (i.e., reservoir with a fixed drainage area) is a given, as

$$p_D = A' + 2\pi t_{DA} \quad (17)$$

where A' is a constant.

Taking derivative of Equation 17 gives

$$m = dp_D/dt_{DA} = 2\pi \quad (18)$$

Thus, in a single-phase flow calculation, pseudosteady begins when slope, m , becomes 2π .

Some engineers assume that when m reaches within 10% of 2π value, pseudosteady begins. Others use 5% criteria and a few use 1% criterion.

Depending upon the criterion used, one can estimate different values for the beginning of pseudosteady state. Different criterion can give significantly different values for the beginning of pseudosteady state.^{7,8}

At present, there is no consensus about the criterion,

but most engineers accept $t_{DA} = 0.1$ as a dimensionless time to start a pseudosteady state for a vertical well located centrally in either a circular or square drainage area.

Reference 1 does not include information about criterion that were used to calculate $t_{DA} = 0.1$, probably because these results were obtained using a numerical simulator.

The results by Mutalik, et al.⁴ for calculation of pseudosteady state for horizontal wells are probably conservative because they used a slope requirement of 5% within the value of 2π .

The above discussion indicates that before using any dimensionless time to reach pseudosteady state, it is important to critically review the criterion that has been used. This is especially important in determining well spacing in leases that last only for a short time, say less than 10 years.

In these reservoirs, knowing the beginning of pseudosteady state becomes important to drain a reservoir effectively in a limited time period.

Drainage

Due to longer well length, in a given time period under similar operating conditions, a horizontal well will drain a larger reservoir area than a vertical well. If a vertical well drains a certain reservoir volume of area in a given time, then this information can be used to calculate a horizontal well drainage area.

A horizontal well can be looked upon as a number of vertical wells drilled next to each other and completed in a limited pay-zone thickness. Then as shown in Fig. 1d,

Table 2

Dimensionless time, $t_{DA,ps}$, at the start of pseudosteady behavior*

L_D $L/2x_e$	$x_f/y_e = 1$				
1	0.2	0.4	0.6	0.8	1.0
5	0.4	0.4	0.4	0.4	0.4
10	0.4	0.4	0.4	0.4	0.4
20	0.4	0.4	0.4	0.4	0.4
50	0.4	0.4	0.4	0.4	0.4
100	0.4	0.4	0.4	0.4	0.4

L_D $L/2x_e$	$x_f/y_e = 2$				
1	0.2	0.4	0.6	0.8	1.0
5	0.6	0.6	0.6	0.6	0.2
10	0.6	0.6	0.6	0.6	0.2
20	0.6	0.6	0.6	0.6	0.2
50	0.6	0.6	0.6	0.6	0.2
100	0.6	0.6	0.6	0.6	0.2

L_D $L/2x_e$	$x_f/y_e = 5$				
1	0.2	0.4	0.6	0.8	1.0
5	2.0	2.0	2.0	2.0	0.4
10	2.0	2.0	2.0	2.0	0.6
20	2.0	2.0	2.0	2.0	0.6
50	2.0	2.0	2.0	2.0	0.6
100	2.0	2.0	2.0	2.0	0.6

*Results were obtained assuming $y_e = 933.33$ ft and $r_w = 0.225$ ft. Times are for centrally located wells for different penetrations, $L/2x_e$, and dimensionless lengths, L_D .

Table 3

Alternative well lengths

Method 1 - half circles			
Horizontal length	500 ft	1000 ft	2000 ft
Area of two half circles, acres	30 + 30 = 60	30 + 30 = 60	30 + 30 = 60
Area of central rectangle, acres	20.9	41.9	83.7
Drainage area, acres	80.9	101.9	143.7
Method 2 - ellipse			
a = Half major axis, ft	250 + 912 = 1,162	500 + 912 = 1,412	1,000 + 912 = 1,912
b = Half minor axis, ft	912	912	912
Drainage area, acres	76.4	92.9	125.8
Average of Methods 1 and 2			
Average drainage area, acres (Methods 1 + 2)	79	98	135
Number of wells for 600-acre field	8	6	5

each end of a horizontal well would drain half a circular area, with a rectangular drainage area at the center.

This concept implicitly assumes that the reservoir thickness is considerably smaller than the sides of the drainage area. It is possible to calculate the drainage area of a horizontal well by assuming an elliptical drainage area in the horizontal plane, with each end of a well as a foci of drainage ellipse. The methods to estimate

drainage areas of horizontal wells generally give fairly similar results. As a rule of thumb, a 1,000 ft long horizontal well can drain twice the area of a vertical well, while a 2,000 ft long well will drain three times a vertical well, in a given time.

Thus, it is important to use larger well spacing for a horizontal well development than that used for a vertical well development.

The following examples for drainage area calculations

are for reservoirs with uniform permeability in the areal plane. In a fractured reservoir, where permeability in one direction is higher than the other, then the well would accordingly drain a larger length in a high-permeability direction by a factor of $\sqrt{k_y/k_x}$. The k_y represents higher permeability and k_x represents lower permeability in the horizontal plane (Fig. 1c).

Horizontal wells needed

A 400-acre lease is to be developed using 10 vertical wells. An engineer suggested drilling either 1,000 or 2,000 ft long horizontal wells. Calculate the possible number of horizontal wells that will drain the lease effectively. Assume that a single vertical well effectively drains 40 acres.

If r_{ev} is a drainage radius of a vertical well, then a 40 acre vertical well drains an area of a circle = $\pi r_{ev}^2 = 40$ acres \times 43,560 sq ft/acre, $r_{ev} = 745$ ft.

Two methods can be employed to calculate horizontal well drainage area on the basis of 40 acre drainage area of a vertical well.

In Method 1 (Fig. 1d), a 1,000 ft long well will drain 74 acres. The drainage area is presented as two half circles at each end and a rectangle in the center. Similarly (Fig. 1d) a 2,000 ft long well will drain 108 acres.

In Method 2, if we assume that the horizontal well drainage area is an ellipse in a horizontal plane, then for a 1,000 ft long well:

a = half major axis of an ellipse = $(L/2) + r_{ev} = (1,000/2) + 745 = 1,245$ ft
 b = half minor axis of an ellipse = $r_{ev} = 745$ ft
 Drainage area = $\pi ab/43,560 = 67$ acres

Similarly for a 2,000 ft long well, $a = (L/2) + 745 = 1,745$ ft

$b = 745$ ft, and drainage area = $\pi ab/43,560 = 94$ acres.

The two methods give different answers for drainage area. If average areas are used the 1,000 ft well will drain 71 acres, and a 2,000 ft well will drain 101 acres. Thus, a 400-acre field can be drained by ten vertical wells, six 1,000 ft long wells, or four

2,000 ft long wells.

Horizontal wells are very appropriate for offshore and hostile environment applications where a substantial up-front savings can be obtained by drilling long horizontal wells. Because a large area can be drained with less wells, fewer slots are required on offshore platforms, and therefore, costs are significantly reduced.

Alternative well lengths

A 600-acre lease is to be developed with ten vertical wells. Another alternative is to drill 500, 1,000, or 2,000 ft long horizontal wells. Table 3 shows the possible number of horizontal wells that will drain the leases effectively. A 60 acre vertical well would drain a circle of radius, r_{ev} , of 912 ft. Area of a circle = $\pi r_{ev}^2 = 60$ acres \times 43,560 sq ft/acre, $r_{ev} = 912$ ft.

Again using the two methods described in the previous example, Table 3 shows that a 600-acre field can be effectively drained either by ten vertical wells, eight 500 ft long horizontal wells, six 1,000 ft long wells, or five 2,000 ft long wells.

Development patterns

A 360 acre lease (Fig. 2) is to be developed using nine vertical wells. How many 1,000 ft long horizontal wells could drain this reservoir effectively? How many 2,000 ft long horizontal wells could drain this effectively? What is the suggested development pattern.

As shown in one of the previous examples, if a vertical well drains 40 acres effectively, 1,000 ft and 2,000 ft long horizontal wells would drain 80 and 120 acres, respectively.

With 1,000 ft long wells, the 360 acre lease could be developed using either four horizontal wells and one vertical well or three horizontal wells and three vertical wells. The possible configurations are shown in Fig. 2.

Because a 2,000 ft long horizontal well could drain 120 acres. A 360 acre lease also can be developed using three 2,000 ft long horizontal wells.

The author . . .



Joshi

S.D. Joshi is president of Joshi Production Technologies Inc. of Tulsa, which is involved in the research and development of field applications for horizontal well technology in the U.S. and overseas. Joshi has 9 years experience in the area of horizontal well technology.

Along with Frank J. Schult of Drilling Technology Inc., Joshi teaches an industry short course on horizontal well technology through the University of Tulsa. Joshi received his PhD in mechanical engineering from Iowa State University. Prior to forming his company in 1988, Joshi was a senior research engineer in the production research department of Phillips Petroleum Co.

Anisotropic development

A well, Harris-1, drains approximately 40 acres in a 35 ft thick naturally fractured reservoir.

Pressure tests conducted between the Harris-1 and the well to the east between Harris-1 and the well to the north, indicate permeability differences along the two directions. The permeability along the east-west, k_x , is 0.5 md, while the permeability along the north-south direction, k_y , is 4.5 md. An engineer proposed to drill a 2,000 ft long horizontal well along the east-west direction. Estimate the drainage area and dimensions of each drainage area side.

Let us assume that the vertical well, Harris-1, drains a rectangle area due to anisotropy.

If the reservoir has a uniform permeability, then the well would drain a 40 acre square with each side being

$$2x_e = 2y_e = \sqrt{40 \times 43,560} = 1,320 \text{ ft}$$

The reservoir has nonuniform permeability in the areal plane with $k_x = 0.5$ md and $k_y = 4.5$ md. Hence, $k_y/k_x = 4.5/0.5 = 9$ and $\sqrt{k_y/k_x} = 3$

If the drainage rectangle has sides $2x_e$ and $2y_e$, and if we assume that Harris-1 drains only 40 acres (Equations 15 and 16):

$$(2x_e) \times (2y_e) = 40 \times 43,560$$

additionally due to anisotropy, $2y_e/2x_e = 3$.

Solving the above two equations simultaneously,

$$2x_e = 762 \text{ ft and } 2y_e = 2,286 \text{ ft}$$

Thus, for a vertical well, the drainage length along the north-south direction, which is a high permeability direction is 2,286 ft.

Hence, vertical well spacing along the north-south direction, $2y_e$, should be three times as large as along the east-west direction, $2x_e$.

Assuming that each well tip of a horizontal well drains half of a vertical well, for a 2,000 ft long horizontal well drilled along the east-west direction, the drainage length along this direction is $2x_e = 2,000 + 762 = 2,762$ ft.

Similarly, drainage length along the north-south direction will be the same as that for a vertical well which is $2y_e = 2,286$ ft.

Therefore, well spacing should be at least 2,286 ft along the north-south direction and the horizontal well tips should be spaced at least 762 ft apart.

Thus, well spacing requirements for vertical, as well as horizontal wells, are different in isotropic and anisotropic reservoirs.

References

1. Earlougher, R.C. Jr., "Advances in Well Test Analysis," Soc. of Petrol. Eng., 1977.
2. Gringarten, A.C., Ramey, H.J., Jr., and Raghavan, R., "Unsteady-State Pressure Distribution Created by a Well with a Single Infinite-Conductivity Vertical Fracture," Soc. of Petrol. Eng. Journal, pp. 347-60, August 1974.
3. Khan, A., "Pressure Behavior of a Vertically Fractured Well Located at the Center of a Rectangular Drainage Region," MS Thesis, The University of Tulsa, 1978.

4. Muhlík, P.M., Godbole, S.P., and Joshi, S.D., "Effect of Drainage Area Shapes on the Productivity of Horizontal Wells," paper 18301, SPE 83rd Annual Technical Conference Houston, Oct. 2-5, 1988.
5. Daviau, F., Mourouval, G., Bourdarot, G., and Curutcher, P., "Pressure Analysis for Horizontal Wells," SPE Formation Evaluation, December 1988, pp. 716-24.
6. Goode, P.A., and Thambyanagam, R.K.M., "Pressure Drawdown and Buildup Analysis of Horizontal Wells in Anisotropic Media," SPE Formation Evaluation, December 1987, pp. 683-97.
7. Onur, M. and Reynolds, A.C., "A New Approach for Constructing Derivative Type Curves for Well Test Analysis," SPE Formation Evaluation, March 1988, pp. 197-206.
8. Vongvuthipornchai, S., and Raghavan, R., "A Note on the Duration of the Transitional Period of Responses Influenced by Wellbore Storage and Skin," SPE Formation Evaluation, March 1988, pp. 207-14.
9. Dake, L.P., "Fundamentals of Reservoir Engineering," Elsevier Scientific Publishing Co., New York, 1978.

BOOKS

Marine Technology Reference Book, edited by Nina Morgan. Published by Butterworths, 80 Montvale Ave., Stoneham, Mass., 02180. \$195.

This reference covers most areas of marine and offshore technology. It is designed, says the publisher, to be a first point of reference for the main branches of marine technology. It will be useful for engineers who are knowledgeable in one branch of the subject and wish to learn quickly the most important basics of another branch.

The sections of the book have been written by experts in the field and cover ocean environments, offshore structures, naval architecture, submersibles and diving, marine risers and pipelines, corrosion, safety, and more.

WOAD: Worldwide Offshore Accident Databank, Statistical Report 1990, published by Veritec, P.O. Box 300, N-1322 Hovik, Norway. \$230.

Here is statistical information on all aspects of offshore safety. It is an at-a-glance reference designed for anyone engaged in offshore safety and reliability, cost/benefit analysis, and insurance.

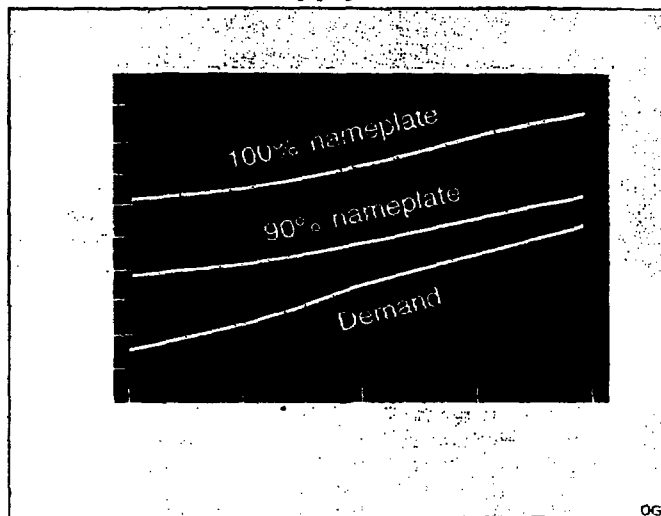
World methanol capacity/demand balance

	1989	1990	Forecast		
			1991	1992	1993
	1,000 metric tons				
Formaldehyde	6,917	7,082	7,274	7,472	7,630
DMT	537	647	653	664	670
Acetic acid	1,213	1,382	1,507	1,549	1,635
MTBE	2,197	2,426	2,944	3,569	4,055
Methyl methacrylate	492	484	540	569	585
Gasoline/fuels	195	265	270	200	235
Solvents	1,288	1,334	1,378	1,413	1,456
Others	4,168	4,564	4,675	4,798	4,890
Nontabulated countries	240	245	250	255	260
Total demand	17,347	18,419	19,491	20,499	21,416
Nameplate capacity	22,123	22,513	23,191	24,091	24,776
Capacity @ 90%	19,911	20,262	20,872	21,682	22,298
Percent utilization @ nameplate	78	82	84	85	86
Percent utilization @ 90% nameplate	87	91	93	94	96

* Estimated.

Source: Crocco & Associates Inc.

World methanol supply/demand



Methanol supplies could be pinched by mid-1990s

Global supplies of methanol could be very tight by the middle of the 1990s because of pending reformulated gasoline specifications.

Those specifications will require a minimum oxygen content in gasoline blends to reduce emissions of carbon monoxide.

Most of the oxygen requirement will be met by blending methyl tertiary butyl ether (MTBE) into gasoline. Methanol is one of the two feedstocks needed to make MTBE.

A multicient study, con-

ducted by Crocco & Associates Inc., Houston, shows that global methanol demand will grow 4.1 million metric tons/year to about 21.4 million metric tons/year in 1993 from about 17.3 million metric tons/year in 1989, an increase of some 23%. That is primarily in response to increased demand for MTBE (see chart).

Methanol nameplate production capacity will grow, however, only 12%, moving to about 24.8 million metric tons/year by 1993 from about 22.1 million metric tons/year in 1989 (see table).

Considering that only about 90% of nameplate capacity can be fully utilized, the increased demand will push methanol plant operating rates to 96% by 1993, according to Crocco & Asso-

ciates.

There are currently a few methanol plant projects under way that will add some methanol capacity. Two or three small plants in the U.S. and the Petraigas plant in New Zealand, that will clean up crude methanol to chemical grade, will start this year and add about 450,000 metric tons/year capacity, according to Crocco & Associates.

One large-scale methanol plant is under construction in Saudi Arabia, but this plant will not likely start up until 1992.

Higher methanol demand will boost methanol prices during the 1990s and spur new plant construction. But new plant facilities would take some time to construct, keeping methanol supplies tight.

In This Issue
Production

Oil&Gas Journal
September 17, 1990

METHODS CALCULATE AREA DRAINED BY HORIZONTAL WELLS

S.D. Joshi
Joshi Technologies International Inc.
Tulsa

The drainage area of a horizontal well can be calculated by averaging the results obtained from two different methods. For anisotropic reservoirs, nonuniform permeability has to be included in drainage area calculations.

WELL SPACING

Horizontal wells, in general, give higher reserves than vertical wells. Two reasons for obtaining higher ultimate reserves are increase in the drainage area and increase in the recovery factor.

The most important reason for obtaining higher ultimate reserves from horizontal wells is the significant enhancement of the drainage area, especially as compared to vertical wells. The other reason for an increase in reserves is improvement in the recovery factors. Recovery factor is the percentage of the original oil in place that can be produced.

At the present time, the field histories tend to indicate that the recovery factors are, in general, 2-5% higher than those for vertical wells. Until more long term histories are available, it is difficult to make an exact judgment on the improvement of recovery factors.

In a given time period, a horizontal well drains a larger reservoir volume than a vertical well. Thus, the spacing used for a horizontal well should be larger than that used for a vertical well.

The drainage area of a horizontal well also depends upon natural fracturing in a fractured reservoir.

In a naturally fractured reservoir, a horizontal well drains more volume in the direction parallel to the natural fractures than in the direction perpendicular to the natural fractures. Therefore, the well spacing requirement along a fracture trend is different than that perpendicular to the fracture trend.

It is important to note that even for a vertical well, the well spacing is based upon the reservoir parameters and economic criteria. Theoretically speaking, one can drill a single well in a large reservoir and it will drain the entire reservoir, although it may take a very long time.

Well spacings are designed so as to maximize the oil recovery and economic benefit of production. To estimate the drainage area of a horizontal well, first one must estimate the drainage area (or well spacing) of a vertical well.

PSEUDOSTEADY STATE

Dimensionless time, tD , which is used to define various regions, is given as:

[SEE FORMULA (1)]

and area-based dimensionless time

[SEE FORMULA (2)]

Thus

[SEE FORMULA (3)]

where: k = permeability (md), t = time (hr), f = porosity (fraction), viscosity (cp), cti = initial total compressibility (psi-1), A = area sq ft, and r_w = well bore radius, ft

For a vertical well located at the center of a drainage circle or a square, the time to reach pseudosteady state is $t_{DA} = 0.1$. Substituting this in Equation 3, we have

[SEE FORMULA (4)]

[SEE FORMULA (5)]

t_{pss} = time to reach pseudosteady state in hours

[SEE FORMULA (6)]

t_{pdss} is the time to reach pseudosteady state in days.

Generally, oil wells are developed on 40-acre spacing and gas wells are developed on 160-acre spacing. Hence 40 acres $40 \times 43,560$ sq ft/acre 1.7424×10^6 sq ft (7)

160 acres = $160 \times 43,560$ sq ft/acre = 6.9696×10^6 sq ft (8)

Substituting these areas into Equation 6 gives for a 40 acre well:

[SEE FORMULA (9)]

and for a 160 acre well:

[SEE FORMULA (10)]

Equations 4 and 5 show that transient time depends on the basic reservoir properties, such as permeability, porosity, and compressibility. Time to reach pseudosteady state does not depend on well stimulation.

In the case of oil wells, normally, the time to reach pseudosteady state is of the order of a few days to months.

In contrast, for gas wells in low-permeability reservoirs, the time to reach pseudosteady state could be very long; in some cases as long as a few years.

OIL WELL EXAMPLE

For an oil well drilled on 40-acre spacing, calculate the time to reach pseudosteady state given $f = 10\%$, $cti = 0.00005$ psi, $k = 35$ md, and $m = 4.2$ cp (shallow well-dead oil). Using Equation 5, $t_{pss} = 0.0002274 A = 396$ hr = 16.5 days.

GAS WELL EXAMPLE

Calculate the time required to reach pseudosteady state for a gas well drilled at either 20 or 160-acre spacing in a reservoir with an initial pressure (p_i) of 1,450 psi and the reservoir properties of $f = 7\%$, $k = 0.03$ md, $m = 0.015$ cp, and $cti = 0.000690$ psi-1.

Again using Equation 5 $t_{pss} = 0.00915A$. For 20 acres, $t_{pss} = 7,974$ hr = 332 days 0.91 years.

For 160 acres, $t_{pss} = 63,772$ hr 2,657 days 7.3 years of infinite-acting period.

As noted in the previous example, gas wells (or oil wells) drilled in a very tight reservoir, especially gas wells in reservoirs with permeability less than 0.1 md, can take years for the transient state to end. In such tight reservoirs, it is very difficult to drain the reservoir economically. In these cases, methods are needed to accelerate reservoir drainage.

Infill drilling and horizontal drilling provide alternatives to drain the reservoir effectively.

The dimensionless time to reach pseudosteady state is $t_{DA} = 0.1$, as long as the well is centrally located in a drainage plane, i.e., when the well is at the center of a circle or a square ($x_e/y_e = 1$).

When the drainage area becomes rectangular, the time to reach pseudosteady state increases. For example, when one side of a drainage rectangle is five times larger than the other side ($x_e/y_e = 5$) the dimensionless time to reach pseudosteady state is $t_{DA} = 1.0$, i.e., ten times longer than a vertical well located centrally in the drainage plane.

Thus, vertical wells are unable to drain effectively rectangular drainage areas in uniform permeability reservoirs.

As shown in Fig. 1a, a long horizontal well in a given time can drain a larger area than a vertical well.

A 40-acre spacing vertical well reaches pseudosteady state in 16 days. By the same principle (Fig. 1) a 2,000 ft long well would reach pseudosteady state in a 101-acre area in 16 days.

Table 1 tells us that the time to reach pseudosteady state using vertical well draining a rectangle with dimensions $x_e/y_e = 2.5$ would be 2.5 times longer than that for a 2,000 ft long horizontal well (assumes L is 1 - the quantity y_e/x_e).

Thus, horizontal wells can be utilized to drain a larger reservoir volume than vertical wells in a given time period. This becomes very important in tight reservoirs when close vertical well spacing is required to drain the reservoir effectively.

Therefore, in a tight reservoir, horizontal wells can be used to enhance drainage volume per well in a given time period.

AREAL ANISOTROPY

The discussion so far has been restricted to reservoirs with homogeneous areal permeability, namely $k_x = k_y$ (Fig. 1b). In naturally fractured reservoirs, the permeability along the fracture trend is larger than in a direction perpendicular to fractures. In such cases, a vertical well would drain more length along the fracture trend.

The derivation starting with Equation 11 can be used to estimate each side of a drainage area in an areally anisotropic reservoir. The equation assumes a single phase, steady-state (time independent) flow through an homogeneous formation.

[SEE FORMULA (11)]

Assuming constant values of k_x and k_y in x and y directions, respectively, Equation 11 is rewritten as

[SEE FORMULA (12)]

Multiplying and dividing throughout by $k_x k_y$, Equation 12 becomes

[SEE FORMULA (13)]

This can be transformed into

[SEE FORMULA (14)]

where

[SEE FORMULA (15)]

and

[SEE FORMULA (16)]

Thus, an areally anisotropic reservoir would be equivalent to a reservoir with effective permeability of $k_x k_y$. The drainage

length along the high-permeability side is larger by a factor of k_y/k_x than the drainage length along a low-permeability side.

Thus, if permeability along the fracture trend is 16 times larger than perpendicular to it, then drainage length along the fracture is four times larger than the length perpendicular to the fracture (Fig 1b).

In such areally anisotropy reservoirs, using vertical wells, it is difficult to drain the larger reservoir lengths in the low-permeability direction.

A horizontal well drilled along the low-permeability direction has a potential to drain a significantly larger area than a vertical well and therefore recover more reserves than vertical wells.

Thus, horizontal wells are highly beneficial in areally anisotropic reservoirs.

It is obvious that in naturally fractured formations, horizontal wells drilled in a direction perpendicular to the natural fractures are highly beneficial (Fig 1c). The success of horizontal wells in naturally fractured reservoirs, such as Austin chalk formation in Texas and Bakken formation in North Dakota, illustrates the advantage of horizontal drilling in areally anisotropic formations.

For fractured vertical wells, limited results are available to calculate the time to reach pseudosteady state in square drainage boundaries.^{1 2} Khan has obtained results for fractured vertical wells in rectangular areas.³

Recently, similar results were also available for horizontal wells.⁴⁻⁶ Mutalik, et al.,⁴ calculated the time to reach the pseudosteady state for fractured vertical wells and horizontal wells in rectangular drainage areas (Tables 1 and 2).

It is important to note that there is some discrepancy in calculating the time to start pseudosteady state. For a single-phase flow in a homogeneous reservoir, the relationship between the dimensionless pressure and the dimensionless time for a well producing at a constant rate in a bounded reservoir (i.e., reservoir with a fixed drainage area) is a given, as

[SEE FORMULA (17)]

where A' is a constant.

Taking derivative of Equation 17 gives

[SEE FORMULA (18)]

Thus, in a single-phase flow calculation, pseudosteady begins when slope, m , becomes $2p$.

Some engineers assume that when m reaches within 10% of $2p$ value, pseudosteady begins. Others use 5% criteria and a few use 1% criterion.

Depending upon the criterion used, one can estimate different values for the beginning of pseudosteady state. Different criterion can give significantly different values for the beginning of pseudosteady state.^{7 8}

At present, there is no consensus about the criterion, but most engineers accept $t_{DA} = 0.1$ as a dimensionless time to start a pseudosteady state for a vertical well located centrally in either a circular or square drainage area.

Reference 1 does not include information about criterion that were used to calculate $t_{DA} = 0.1$, probably because these results were obtained using a numerical simulator.

The results by Mutalik, et al.⁴ for calculation of pseudosteady state for horizontal wells are probably conservative because they used a slope requirement of 5% within the value of $2p$.

The above discussion indicates that before using any dimensionless time to reach pseudosteady state, it is important to critically review the criterion that has been used. This is especially important in determining well spacing in leases that last only for a short time, say less than 10 years.

In these reservoirs, knowing the beginning of pseudosteady state becomes important to drain a reservoir effectively in a

limited time period.

DRAINAGE

Due to longer well length, in a given time period under similar operating conditions, a horizontal well will drain a larger reservoir area than a vertical well. If a vertical well drains a certain reservoir volume of area in a given time, then this information can be used to calculate a horizontal well drainage area.

A horizontal well can be looked upon as a number of vertical wells drilled next to each other and completed in a limited pay-zone thickness. Then as shown in Fig. 1d, each end of a horizontal well would drain half a circular area, with a rectangular drainage area at the center.

This concept implicitly assumes that the reservoir thickness is considerably smaller than the sides of the drainage area. It is possible to calculate the drainage area of a horizontal well by assuming an elliptical drainage area in the horizontal plane, with each end of a well as a foci of drainage ellipse.

The methods to estimate drainage areas of horizontal wells generally give fairly similar results. As a rule of thumb, a 1,000 ft long horizontal well can drain twice the area of a vertical well, while a 2,000 ft long well will drain three times a vertical well, in a given time.

Thus, it is important to use larger well spacing for a horizontal well development than that used for a vertical well development.

The following examples for drainage area calculations are for reservoirs with uniform permeability in the areal plane. In a fractured reservoir, where permeability in one direction is higher than the other, then the well would accordingly drain a larger length in a high-permeability direction by a factor of k_y/k_x . The k_y represents higher permeability and k_x represents lower permeability in the horizontal plane (Fig. 1c).

HORIZONTAL WELLS NEEDED

A 400-acre lease is to be developed using 10 vertical wells. An engineer suggested drilling either 1,000 or 2,000 ft long horizontal wells. Calculate the possible number of horizontal wells that will drain the lease effectively. Assume that a single vertical well effectively drains 40 acres.

If r_{ev} is a drainage radius of a vertical well, then a 40 acre vertical well drains an area of a circle = $\pi r_{ev}^2 = 40 \text{ acres} \times 43,560 \text{ sq ft/acre}$, $r_{ev} = 745 \text{ ft}$.

Two methods can be employed to calculate horizontal well drainage area on the basis of 40 acre drainage area of a vertical well.

In Method 1 (Fig. 1d), a 1,000 ft long well will drain 74 acres. The drainage area is presented as two half circles at each end and a rectangle in the center. Similarly (Fig. 1d) a 2,000 ft long well will drain 108 acres.

In Method 2, if we assume that the horizontal well drainage area is an ellipse in a horizontal plane, then for a 1,000 ft long well:

$$a = \text{half major axis of an ellipse} = (L/2) + r_{ev} = (1,000/2) + 745 = 1,245 \text{ ft}$$

$$b = \text{half minor axis of an ellipse} = r_{ev} = 745 \text{ ft}$$

$$\text{Drainage area} = \pi ab / 43,560 = 67 \text{ acres}$$

$$\text{Similarly for a 2,000 ft long well, } a = (L/2) + r_{ev} = 1,745 \text{ ft}$$

$$b = 745 \text{ ft, and drainage area} = \pi ab / 43,560 = 94 \text{ acres.}$$

The two methods give different answers for drainage area. If average areas are used the 1,000 ft well will drain 71 acres, and a 2,000 ft well will drain 101 acres. Thus, a 400-acre field can be drained by ten vertical wells, six 1,000 ft long wells, or four 2,000 ft long wells.

Horizontal wells are very appropriate for offshore and hostile environment applications where a substantial upfront savings can be obtained by drilling long horizontal wells. Because a large area can be drained with less wells, fewer slots are required on offshore platforms, and therefore, costs are significantly reduced.

ALTERNATIVE WELL LENGTHS

A 600-acre lease is to be developed with ten vertical wells. Another alternative is to drill 500, 1,000, or 2,000 ft long horizontal wells. Table 3 shows the possible number of horizontal wells that will drain the leases effectively. A 60 acre vertical well would drain a circle of radius, r_w , of 912 ft. Area of a circle = $\pi r_w^2 = 60 \text{ acres} \times 43,560 \text{ sq ft/acre}$, $r_w = 912 \text{ ft}$.

Again using the two methods described in the previous example, Table 3 shows that a 600-acre field can be effectively drained either by ten vertical wells, eight 500 ft long horizontal wells, six 1,000 ft long wells, or five 2,000 ft long wells.

DEVELOPMENT PATTERNS

A 360 acre lease (Fig. 2) is to be developed using nine vertical wells. How many 1,000 ft long horizontal wells could drain this reservoir effectively? How many 2,000 ft long horizontal wells could drain this effectively? What is the suggested development pattern.

As shown in one of the previous examples, if a vertical well drains 40 acres effectively, 1,000 ft and 2,000 ft long horizontal wells would drain 80 and 120 acres, respectively.

With 1,000 ft long wells, the 360 acre lease could be developed using either four horizontal wells and one vertical well or three horizontal wells and three vertical wells. The possible configurations are shown in Fig. 2.

Because a 2,000 ft long horizontal well could drain 120 acres. A 360 acre lease also can be developed using three 2,000 ft long horizontal wells.

ANISOTROPIC DEVELOPMENT

A well, Harris-1, drains approximately 40 acres in a 35 ft thick naturally fractured reservoir.

Pressure tests conducted between the Harris-1 and the well to the east between Harris-1 and the well to the north, indicate permeability differences along the two directions. The permeability along the east-west, k_x , is 0.5 md, while the permeability along the north-south direction, k_y , is 4.5 md. An engineer proposed to drill a 2,000 ft long horizontal well along the east-west direction. Estimate the drainage area and dimensions of each drainage area side.

Let us assume that the vertical well, Harris-1, drains a rectangle area due to anisotropy.

If the reservoir has a uniform permeability, then the well would drain a 40 acre square with each side being

[SEE FORMULA]

The reservoir has nonuniform permeability in the areal plane with $k_x = 0.5 \text{ md}$ and $k_y = 4.5 \text{ md}$. Hence, $k_y/k_x = 4.5/0.5 = 9$ and $k_y/k_x = 3$

If the drainage rectangle has sides $2x_e$ and $2y_e$, and if we assume that Harris-1 drains only 40 acres (Equations 15 and 16):

$$(2x_e) \times (2y_e) = 40 \times 43,560$$

additionally due to anisotropy, $2y_e/2x_e = 3$.

Solving the above two equations simultaneously,

$$2x_e = 762 \text{ ft and } 2y_e = 2,286 \text{ ft}$$

Thus, for a vertical well, the drainage length along the north-south direction, which is a high permeability direction is 2,286 ft.

Hence, vertical well spacing along the north-south direction, $2y_e$, should be three times as large as along the east-west direction, $2x_e$.

Assuming that each well tip of a horizontal well drains half of a vertical well, for a 2,000 ft long horizontal well drilled along the east-west direction, the drainage length along this direction is $2x_e = 2,000 + 762 = 2,762$ ft.

Similarly, drainage length along the north-south direction will be the same as that for a vertical well which is $2y_e = 2,286$ ft.

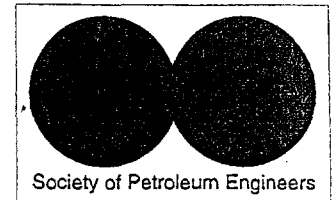
Therefore, well spacing should be at least 2,286 ft along the north-south direction and the horizontal well tips should be spaced at least 762 ft apart.

Thus, well spacing requirements for vertical, as well as horizontal wells, are different in isotropic and anisotropic reservoirs.

REFERENCES

1. Earlougher, R.C. Jr., "Advances in Well Test Analysis," Soc. of Petrol. Eng., 1977.
 2. Gringarten, A.C., Ramey, H.J., Jr., and Raghavan, R., "Unsteady-State Pressure Distribution Created by a Well with a Single Infinite-Conductivity Vertical Fracture," Soc. of Petrol. Eng. Journal, pp. 347-60, August 1974.
 3. Khan, A., "Pressure Behavior of a Vertically Fractured Well Located at the Center of a Rectangular Drainage Region," MS Thesis, The University of Tulsa, 1978.
- Mutalik, P.M., Godbole, S.P., and Joshi, S.D., "Effect of Drainage Area Shapes on the Productivity of Horizontal Wells," paper 18301, SPE 63rd Annual Technical Conference Houston, Oct. 2-5, 1988.
 - Daviau, F., Mouronval, G., Bourdarot, G., and Crutcher, P., "Pressure Analysis for Horizontal Wells." SPE Formation Evaluation, December 1988, pp. 716-24.
 - Goode, P.A., and Thambyanyagam, R.K.M., "Pressure Drawdown and Buildup Analysis of Horizontal Wells in Anisotropic Media," SPE Formation Evaluation, December 1987, pp. 683-97.
 - Onur, M. and Reynolds, A.C., "A New Approach for Constructing Derivative Type Curves for Well Test Analysis," SPE Formation Evaluation, March 1988, pp. 197-206.
 - Vongvuthipornchai, S., and Raghavan, R., "A Note on the Duration of the Transitional Period of Responses Influenced by Wellbore Storage and Skin," SPE Formation Evaluation, March 1988, pp. 207-14.
 - Dake, L.P., "Fundamentals of Reservoir Engineering," Elsevier Scientific Publishing Co., New York, 1978.

Copyright 1990 Oil & Gas Journal. All Rights Reserved.



SPE 64436

A Method to Estimate the Drainage Area of a Horizontal Well

P. Permadi, SPE, E. Putra, SPE, and M. E. Butarbutar, Institut Teknologi Bandung

Copyright 2000, Society of Petroleum Engineers Inc.

This paper was prepared for presentation at the SPE Asia Pacific Oil and Gas Conference and Exhibition held in Brisbane, Australia, 16–18 October 2000.

This paper was selected for presentation by an SPE Program Committee following review of information contained in an abstract submitted by the author(s). Contents of the paper, as presented, have not been reviewed by the Society of Petroleum Engineers and are subject to correction by the author(s). The material, as presented, does not necessarily reflect any position of the Society of Petroleum Engineers, its officers, or members. Papers presented at SPE meetings are subject to publication review by Editorial Committees of the Society of Petroleum Engineers. Electronic reproduction, distribution, or storage of any part of this paper for commercial purposes without the written consent of the Society of Petroleum Engineers is prohibited. Permission to reproduce in print is restricted to an abstract of not more than 300 words; illustrations may not be copied. The abstract must contain conspicuous acknowledgment of where and by whom the paper was presented. Write Librarian, SPE, P.O. Box 833836, Richardson, TX 75083-3836, U.S.A., fax 01-972-952-9435.

Abstract

Evaluation of the production performance of a horizontal well is an effort to justify both the technical and economic successes of the project, particularly in an area of horizontal well development. When this implementation shows a good promise for the plan of reservoir management, the engineers involved should be able to estimate the drainage area of the horizontal well. This is of importance in optimizing well spacing for the development.

This paper presents a method to estimate the drainage area of a producing horizontal well. The method was developed by combining an equation of production decline introduced by Shirman (1998) with an equation of material balance. The advantages of the method presented here over the existing ones available in the literature are simple and no requirement of ultimate recovery data.

Field data of four producing horizontal wells were used to evaluate the proposed method. Having the production performance and the rock and fluids properties data, calculation was performed to determine the drainage area of each well under the study. The validation was done by (1) comparing our results with that of a previous study and (2) calculating the productivity index (PI) using a horizontal well inflow equation and then compared with that measured in the field. The comparisons show a very good agreement for all the cases considered, revealing that the method is successfully applied.

In addition, the paper also discusses the strategy of orienting a horizontal wellbore to maximize the benefit of horizontal well application.

Introduction

The main objectives of the use of horizontal wells are to increase and accelerate the rate of oil production and to ultimately recover more oil from underground. These objectives can be accomplished because, compared with conventional vertical wells, for the same drawdown horizontal wells can produce higher volume of fluids daily and can drain larger reservoir area. Considering the latter advantage, the spacing employed for horizontal well should therefore be larger than that used for a vertical well. However, an optimum condition must be evaluated because both the reservoir characteristic and economic criteria dictate the well spacing.

Particularly, in the area of horizontal well development, the real challenge is to make accurate evaluation of the drainage area. Results of the evaluation are then considered in the development program for maximizing the oil recovery and economic benefit of production.

Several methods, such as pressure transient analysis,¹ decline curve analysis,^{2,3} and most recently inverted decline analysis,⁴ are commonly used for determining the drainage area of a vertical well. Principally, such approaches may also be employed for horizontal well cases.

In 1990, Joshi⁵ introduced methods to calculate drainage area of a horizontal well in isotropic and anisotropic reservoirs. He explained the relation between drainage area of a vertical well and that of a horizontal well. He suggested that one must estimate the drainage area of a vertical well in order to estimate the drainage area of a horizontal well. He also described the effect of lateral anisotropy on the drainage area. The drainage length along the high-permeability side is longer than the drainage length along a low-permeability side.

Later Reisz⁶ presented a method to estimate drainage area of a horizontal well in an effort to evaluating the reservoir performance of Bakken formation. The method is based on material balance and decline curve analysis for single phase flow. The derived equation for calculating the drainage area contains Recovery Factor, which is not always available for many cases.

Vo and Madden⁷ recently conducted an analysis study, which couples pressure transient test data and rate-time data of horizontal wells in an attempt to characterizing the reservoir and analyzing the performance of horizontal wells. The methodology is basically generic and could be applied to horizontal or vertical wells.

The objective of this paper is to provide an alternative method to estimate the drainage area of a horizontal well. The method was derived by employing equations of material balance and decline curve. Combining these two equations results in an equation from which a drainage area can then be calculated. Field data are used to validate the method. The results are compared with those obtained by previous study.

Since the lateral anisotropy affects the shape and size of a drainage area, some numerical examples are presented to highlight the importance of orienting a horizontal wellbore correctly in order to maximize the benefit of horizontal well technology.

Method of Approach

Decline curve analysis is a method that is widely used for predicting future production rate and for estimating the drainage area of a producing well. For a well producing oil from a bounded homogeneous reservoir holding incompressible fluid and a single phase flow at a constant well pressure, the following equation, which is derived from material balance and inflow performance equations is useful to be used for predicting production rate versus time.⁸

$$q(t) = \frac{P_i - P_{wf}}{\frac{1}{J} + \frac{5.615 B_o t}{A h \phi C_t}} \quad (1)$$

At a pseudo steady-state condition, productivity index of horizontal well, J_h , can be estimated using the equation below, neglecting wellbore frictional losses.⁸

$$J_h = \frac{0.00708 k_h h L}{\mu B \left[0.523 \left(X_e - Y_e \sqrt{\frac{h}{L}} \right) + \beta h \left\{ \ln \left(\frac{Y_e}{2r_w} \sqrt{\frac{h}{L}} \right) - 0.75 \right\} \right]} \quad (2)$$

When production data and all parameters in Eq. (1), except the drainage area, A , are available for a given producing well then A can be determined, as long as all the reservoir boundaries have been felt and single phase flow holds. This situation must yield a constant value of A at all time, assuming no interference caused by any new wells in the same reservoir.

In many cases, however, production data are erratic. To handle cases of this kind, a method that is capable of predicting the decline trend is required. There are type curve matching techniques that can be used to derive decline equation. Most recently, Shirman⁹ proposed a universal approach to the decline curve analysis. This method can be

employed to obtain the best trend line. His decline curve equation is written as follows:

$$q(t) = q_i (1 + b a q_i^b t)^{-1/b} \quad (3)$$

The procedure to use this approach is described in detail in Ref 9. Substituting Eq. (3) into Eq. (1) results in the equation below:

$$A = \frac{1.289 \times 10^{-4} B_o t}{h \phi C_t \left(\frac{P_i - P_{wf}}{q_i (1 + b a q_i^b t)^{-1/b}} - \frac{1}{J} \right)} \quad (4)$$

When the requirements in the assumption stated above are met, drainage area A should then be a constant. In reality physical properties of reservoir rocks and the residing fluids change with producing time, raising a difficulty in evaluating a constant value of A through Eq. (4). However, if we know the time for pseudosteady-state flow to start occurring in the reservoir, we may estimate the drainage area of the well. But this is not always the case.

To solve the problem, we offer two ways of solution for estimating drainage area of a well employing the equation above. The first way is to have the derivative $dA/dt = 0$, which is

$$\frac{J(P_i - P_{wf}) a q_i^b t}{(1 + b a q_i^b t)} - \left(J(P_i - P_{wf}) - q_i (1 + b a q_i^b t)^{-1/b} \right) = 0 \quad (5)$$

and solve for t . The time t obtained is then used for calculating the drainage area with the use of Eq. (4). The second way is to plot A versus t and then take the slope of zero on the curve, resulting in a constant A .

In this work, the later was used and the time t obtained at the slope equals to zero was compared with the time to start pseudosteady-state flow, t_{pss} . For the case of a horizontal well, the equation¹⁰ below can be used to estimate t_{pss} although t_{eprf} is not equal to but should be lower than t_{pss} because a pseudosteady-state flow occurs when the pressure transient has reached the farthest boundaries and the pressure disturbance in all directions has reached equilibrium.

$$t_{eprf} = \frac{1,650 \phi \mu C_t X_e^2}{k_h} \quad (6)$$

The method proposed here for estimating a drainage area is an alternative technique and will be demonstrated by employing field data to show its applicability.

Data and Decline Analysis

Data required for applying the method presented in this paper include daily production data versus time, flow test data, and reservoir rock and fluid properties data of the productive zone of interest. In this study, complete data sets available have been obtained from Ref. 7.

The reservoir and well data are shown here in Tables 1 and 2. The production data of each well under the study were digitized from the corresponding figure showing the actual daily rate versus time as presented in Ref. 7.

Application of the Shirman method to obtaining the best match of production data was carried out for each of the horizontal wells. Figs. 1 to 4 show results of the rate decline matched for the actual data of wells C-50, C-48, C-35, and C-29, respectively. Parameters a , b , and initial rate q_i obtained for each well are presented in Table 3. These parameters will then be used for the purpose of estimating the drainage area as required for the use of Eq. (4).

Results and Discussion

Drainage Area – Field Examples

In calculating a drainage area using Eq. (4), the most difficult data to measure with reasonable accuracy is an average thickness within a large area drained by the well. The data of thickness reported (see Table 1) and used in this work ranges from 20 to 50 ft. In this context, therefore, we have put some efforts to analyzing all the data available in estimating the average reservoir thickness for each horizontal well under this study.

The information that is helpful in the analysis is the flow capacity of each well and the productivity ratio of horizontal-to-vertical wells (J_h/J_v) for the field. The related information is presented in Table 2. With these data, we can determine productivity index of the corresponding vertical well in the similar conditions, i.e. $J_v = J_h/(J_h/J_v)$. Furthermore, we may say that for a given two vertical wells producing oil from similar reservoirs, $J_{v1}/J_{v2} \approx k_1 h_1/k_2 h_2$. The following is a description to estimate reservoir thickness from the available information.

On the basis of the flow capacity of all the wells, it appears that the highest flow capacity is provided by well C-29, i.e. $J_h = 2.43$ STB/day/psi, and thus the corresponding vertical well has $J_v = 2.43/1.8 = 1.35$ STB/day/psi. In the same way we can calculate J_v for the other wells, giving J_v 's significantly lower than 1.35 STB/d/psi. We might speculate therefore that the well C-29 drains the thickest zone in the field, i.e. 50 ft. Finally, using the approach of $J_{v1}/J_{v2} \approx k_1 h_1/k_2 h_2$, we can estimate average thickness for the other wells. The results are summarized in Table 4.

Based on the analysis just described above and the results obtained, we continue the work in estimating the drainage areas using Eq. (4). As has been explained in the section of method of approach above, the drainage area is determined at zero slope on the curve of A vs. time, as shown in Figs. 5 to 8 for our cases herein. Table 5 summarizes and compares the results with those of a previous study. Results of the two different studies are in good agreement.

It is clearly observed in Figs. 5 to 8 that A varies with producing time. Certainly, A for a given well should be constant when all the reservoir boundaries have been reached and an equilibrium condition has been achieved. This variation of A with time is merely due to inability of the analytical method to account for fluid and rock property changes, as implied by all restrictions born in the assumption used. However, the calculated drainage area should represent the area when the equilibrium conditions for pseudosteady-state flow has been achieved. The period of time required to achieve the equilibrium may be roughly estimated using Eq. (6) for a horizontal well case. It should be noted in this context that boundary affected flow will start after pseudo-radial flow ends. Therefore, we can check whether time t to obtain the zero slope is about close to t_{epf} estimated using Eq. (6), or not.

Table 6 presents results of t_{epf} calculations as compared with $t_{zero\ slope}$ for each horizontal well. In general, we obtain that they are in fair agreement, indicating that pseudosteady-state flow was established for most the cases at the respective $t_{zero\ slope}$.

At the end, we try also to calculate the productivity index employing Eq. (2) for each horizontal well under the study based on the drainage area obtained and then the results are compared with those observed in the field. Table 7 demonstrates the results and the comparison shows excellent agreement.

Effects of Lateral Anisotropy

All we have discussed above were focused on laterally isotropic cases. Probably, many reservoirs are laterally anisotropic, where permeability in x-direction is considerably different from that in y-direction. At present it is difficult to find any complete field data set in the pertinent literature representing the anisotropic cases.

Knowing detailed characteristics of a reservoir is very important because inflow performance of horizontal well is significantly influenced by the directional permeability. Knowledge of regional or local stresses distribution within a geological structure and the depositional history of the formation is also very useful in predicting the largest directional permeability. We believed that a horizontal well should be oriented such a way that the expected flow capacity is maximized. However, the objective of reservoir management must be achieved.

We now look insight about the effect of lateral anisotropy on the reservoir area drained by and the flow capacity expected from a well. To facilitate discussion, we have two sets of hypothetical reservoir data as presented in Table 8. For Case-1, a vertical well will drain an area comprising of a width $X_e = 1180$ ft and a length $Y_e = 2066$ ft. If, instead of a vertical well, a 1700-ft horizontal well is drilled in y-direction in this reservoir then the drainage area components will be $X_e = 1180$

ft and $Y_e = (1700+2066)$ ft = 3766 ft, or $A = 102$ acres. At this condition, productivity index of the horizontal well will be 1.76 STB/d/psi. But if the well is drilled in x-direction then the drainage sides will be $X_e \times Y_e = 2880$ ft x 2066 ft and thus the area will be 137 acres with the productivity index of 1.85 STB/d/psi. It is obvious for Case-1 that a horizontal well should be drilled with wellbore axis perpendicular to the largest directional permeability.

Example of Case-2, which is a kind of fracture reservoir, will give a more clearer picture when the degree of lateral anisotropy becomes higher (see Table 8). For this case, a vertical well will drain an area with $X_e = 843$ ft and $Y_e = 2893$ ft. Substituting for the vertical well, the 1700-ft horizontal well drilled along y-direction will have a drainage area of 843 ft x 4593 ft or $A = 89$ acres and a productivity index of 3.3 STB/d/psi. Whilst, the horizontal well drilled along the x-direction will drain 2543 ft x 2893 ft or $A = 169$ acres, resulting in a productivity index of 5.52 STB/d/psi.

From the two examples described above, one can realize the importance of detailed characteristics of a reservoir before the implementation. Benefits obtained by orienting a horizontal wellbore axis perpendicular to the highest directional permeability are two folds, which are larger drainage area and higher productivity index.

Conclusions

1. An alternative method to estimate the drainage area of a horizontal well has been presented. Applicability of the method has been demonstrated by using field data.

2. The degree of uncertainty of the average reservoir thickness within the drainage area may be reduced by analyzing all the data available that relate to the flow capacity.

3. Detailed characteristics of the reservoir is absolutely important to maximize the benefits offered by horizontal well technology. Orienting the wellbore axis requires knowledge of the reservoir permeability distribution and direction.

Nomenclature

a = production decline at unit rate

A = drainage area, acre

A_v = vertical well drainage area, acre

b = decline exponent

B_o = oil formation factor, rb/STB

C_t = total compressibility, psi⁻¹

h = reservoir thickness, ft

J = productivity index, STB/d/psi

J_h = productivity index of horizontal well, STB/d/psi

J_v = productivity index of vertical well, STB/d/psi

k_h = horizontal permeability, md

k_v = vertical permeability, md

k_x = permeability in x-direction, md

k_y = permeability in y-direction, md

k_z = permeability in z-direction, md

L = horizontal well length, ft

P_i = initial pressure, psi

P_{wf} = bottom hole flowing pressure, psi

q = production rate, STB/d

q_i = initial production rate, STB/d

r_w = wellbore radius, ft

t = time, day

t_{epf} = end of pseudoradial flow, hrs

X_e = reservoir width, ft

Y_e = reservoir length, ft

β = vertical anisotropy factor, dimensionless

μ = viscosity, cp

ϕ = porosity of reservoir rock, fraction

References

1. Earlougher, R.C., Jr.: "Estimating Drainage Shapes from Reservoir Limit Tests," *JPT* (October, 1971), 1266-1268.
2. Arps, J.J.: "Analysis of Decline Curves," *Trans., AIME* (1945), 228-247.
3. Fetcovich, M.J.: "Decline Curve Analysis Using Type Curves," paper SPE 4629 presented at the 1973 Annual Fall Meeting, Las Vegas, Sept. 30-Oct. 3.
4. Rietman, N.D.: "Determining Permeability, Skin Effect and Drainage Area from the Inverted Decline Curve (IDC)," paper SPE 29464 presented at the 1995 Production Operations Symposium, Oklahoma City, OK, April 2-4.
5. Joshi, S.D.: "Methods Calculate Area Drained by Horizontal Wells," *OGJ* (Sept 17, 1990), 77-82.
6. Reisz, M.R.: "Reservoir Evaluation of Horizontal Bakken Well Performance on the Southwestern Flank of the Williston Basin," paper SPE 22389 presented at the 1992 International Meeting on Petroleum Engineering, Beijing, Cina, March 24-27.
7. Vo, D.T. and Madden, M.V.: "Coupling Pressure and Rate-Time Data in Performance Analysis of Horizontal Wells: Field Examples," paper SPE 26445 presented at the 1993 Annual Technical Conference and Exhibition, Oct. 3-6.
8. Permadi, P.: "Practical Methods to Forecast Production Performance of Horizontal Wells," paper SPE 29310 presented at the 1995 Asia Pacific & Gas Conference, Kuala Lumpur Malaysia, March 20-22.
9. Shirman, E.: "Universal Approach to Decline Curve Analysis," paper CIM 98-50 presented at the 1998 Annual Technical Meeting of the Petroleum Society, Calgary, Canada, June 8-10.
10. Lichtenberger, G.J.: "Data Acquisition and Interpretation of Horizontal Well Pressure-Transient Tests," *JPT* (Feb., 1994), 157-162.

Reservoir pressure, psi	350
Reservoir temperature, °F	85
Porosity, fraction	0.30
Reservoir thickness, ft	20-50
Oil gravity, °API	22
Oil Formation Volume Factor, rb/STB	1.03
Oil viscosity, cp	43
Borehole diameter, ft	0.66

Well	L_{eff} (ft)	k_h (md)	k_v (md)	P_i (psi)	P_{wf} (psi)	C_i (psi ⁻¹)	Observed PI (STB/d/psi)	J_h/J_v
C-50	1166	832	83.2	136.8	21.5	1.5×10^{-5}	1.21	1.4
C-48	1047	272	22.3	210.3	33.4	1.5×10^{-5}	0.73	2.2
C-35	730	372	43.6	159.8	15	1.0×10^{-5}	0.56	1.5
C-29	1246	950	24.5	275.7	76.2	2.2×10^{-5}	2.43	1.8

Well	a	b	q_i STB/month
C-50	1.03e-8	1.82	21340.06
C-48	3.69e-8	1.76	7777.25
C-35	2.73e-9	2.12	9354.25
C-29	1.5e-11	2.38	32366.4

Well	k_h (md)	J_h (STB/d/psi)	J_h/J_v	J_v (STB/d/psi)	h (ft)
C-50	832	1.21	1.4	0.86	35
C-48	272	0.73	2.2	0.33	43
C-35	372	0.56	1.5	0.37	40
C-29	950	2.43	1.8	1.35	50

Well	Time to obtain Zero Slope (days)	Drainage Area (Acres)	
		Present Study	Previous Study ⁷
C-50	1680	1445	1119
C-48	756	346	367
C-35	1272	908	574
C-29	338	492	694

TABLE 6 – COMPARISON OF TIME PERIOD FOR ZERO SLOPE AND t_{epf}

<u>Well</u>	<u>Drainage Area</u> (Acres)	<u>X_e</u> (ft)	<u>t_{epf}</u> (days)	<u>$t_{zero\ slope}$</u> (days)
C-50	1445	7900	1000	1680
C-48	346	3800	737	756
C-35	908	6300	942	1272
C-29	492	4600	440	338

TABLE 7 – CALCULATED PRODUCTIVITY INDEX AND THE COMPARISON WITH FIELD DATA

<u>Well</u>	<u>Productivity Index (STB/d/psi)</u>	
	<u>Calculated</u>	<u>Field Data⁷</u>
C-50	1.29	1.21
C-48	0.77	0.73
C-35	0.52	0.56
C-29	2.40	2.43

TABLE 8 – HYPOTHETICAL DATA OF RESERVOIR AND WELL DESCRIPTION

<u>Parameters</u>	<u>Case-1</u>	<u>Case-2</u>
h_{net} , ft	39	39
k_z , md	13	150
k_x , md	17	17
k_y , md	52	200
μ_o , cp	7.1	7.1
B_o , rb/STB	1.10	1.10
r_w , ft	0.38	0.38
A_w , acres	56	56

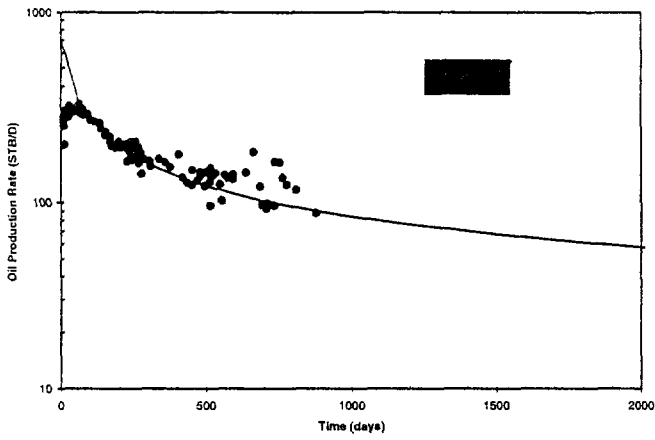


Fig. 1—Production decline of well C-50.

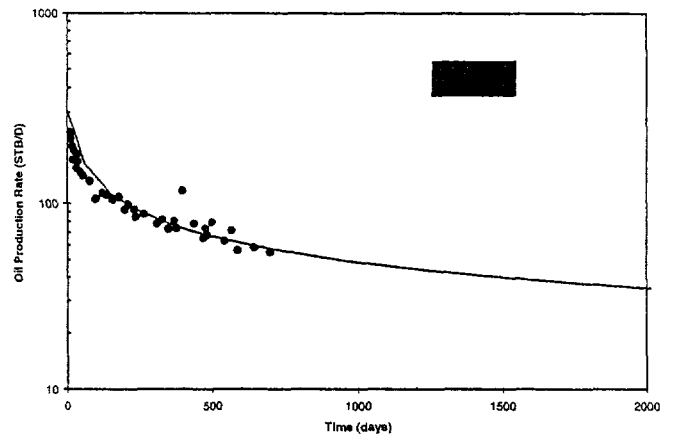


Fig. 3—Production decline of well C-35.

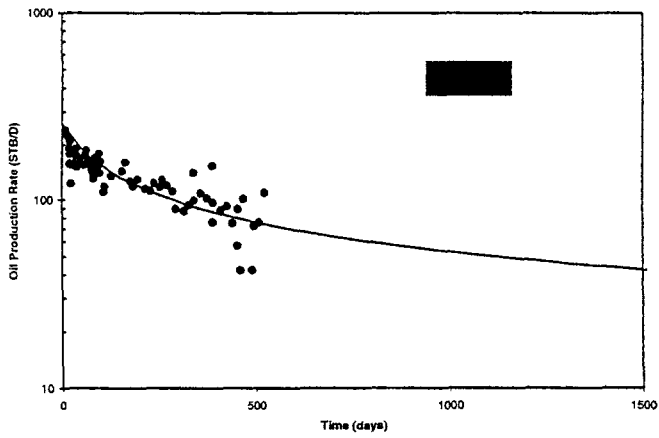


Fig. 2—Production decline of well C-48.

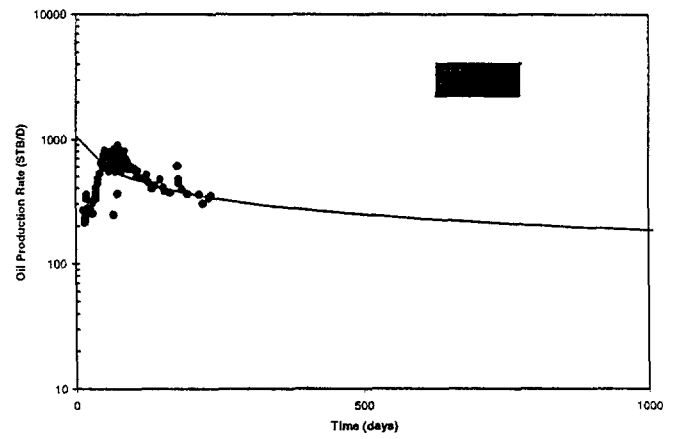


Fig. 4—Production decline of well C-29.

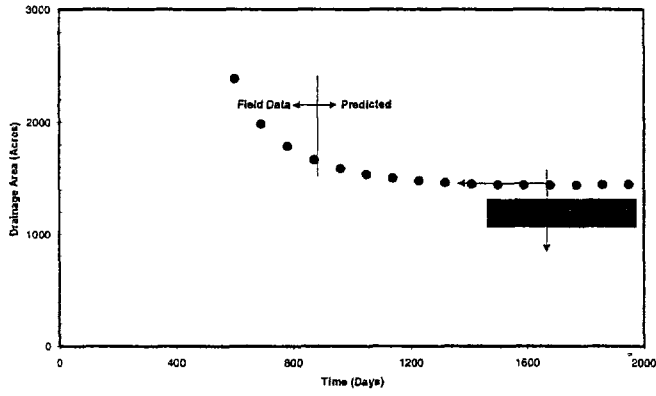


Fig. 5- Determination of drainage area for well C-50.

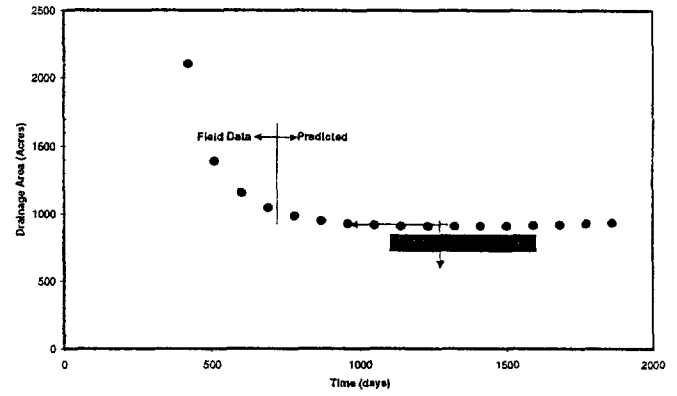


Fig. 7- Determination of drainage area for well C-35.

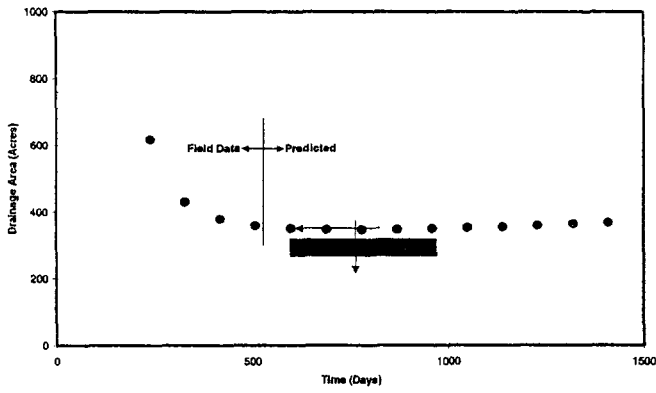


Fig. 6- Determination of drainage area for well C-48.

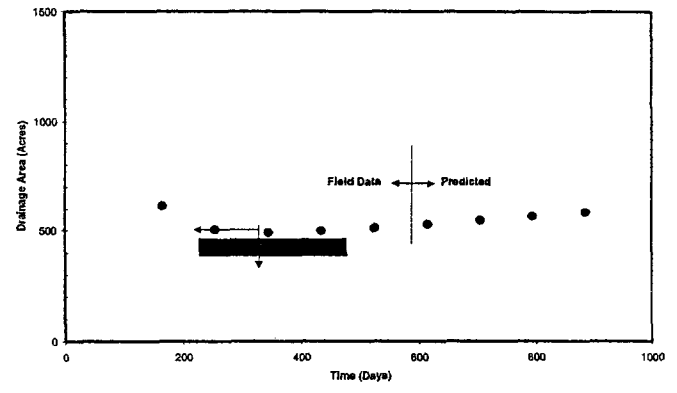


Fig. 8- Determination of drainage area for well C-29.

A Parametric Comparison of Horizontal and Vertical Well Performance

Hemanta Mukherjee, SPE, and Michael J. Economides,* SPE, Dowell Schlumberger

SPE 18303

Summary. This paper presents screening criteria for vertical and horizontal wells with or without induced fractures. The parametric basis of such screening makes the decision on either type of well more objective. A simple procedure to calculate the optimum number of orthogonal transverse fractures in horizontal wells and their sizes is also presented. Two important comparisons have not appeared in the literature: (1) the performance of a fully completed horizontal well with that of a hydraulically fractured well and (2) the performance of a hydraulically fractured horizontal well with that of a hydraulically fractured vertical well. In addition, previous work does not take into account the effect of the plumbing system on well performance. This paper is intended to fill these gaps.

Introduction

In the early 1980's, major production successes through horizontal wells were reported at the Prudhoe Bay field and the Rospo Mare field, offshore Italy. The reported increase in production was on the order of at least two to three times the equivalent production of vertical wells. The Rospo Mare field happens to be the ideal application of horizontal wells because of its producing formation type. Giger *et al.*¹ reported that the Rospo Mare pay consists of karsts that are very-low-permeability, compact carbonates. The oil resides mainly in the fractures and vugs of the karstic matrix system. A horizontal well is more apt to intersect many of these discrete natural fractures or vugular systems in such formations.

Recently, with the improvement in horizontal well drilling and completion technology, the feasibility of horizontal wells is seriously considered for such different reservoirs as the naturally fractured Austin chalk formations, the low-permeability Spraberry formations in west Texas, the Hugoton formations in the Kansas/Oklahoma region, and the naturally fractured Bakken formation in the Williston basin. Improvements in technology and operating procedures have also resulted in a substantial cost reduction. Wilkerson *et al.*² reported a reduction in cost per foot of horizontal wells on the order of 40% over the average cost per foot of the original three horizontal wells drilled at the Prudhoe Bay field. Drilling costs, however, are still reported to be 1.3 to 2 times higher than for comparable vertical wells.

Attempts have also been made to induce hydraulic fractures in horizontal wells of low-permeability reservoirs. Unlike vertical wells, more than one fracture can be induced in a horizontal well. These fractures should be parallel to each other and can be orthogonal to the horizontal well, depending on its inclination with the in-situ principal stress directions.³

In general, horizontal wells are believed to perform better than their vertical counterparts in thin reservoirs, naturally fractured reservoirs (dual-porosity and discretely fractured), reservoirs with water- and gas-coning problems, and reservoirs with favorable vertical permeability anisotropy. Naturally fractured reservoirs normally have favorable vertical permeability anisotropy largely as a result of vertical fractures. In this case, the anisotropy (ratio of horizontal/vertical permeability) is almost unity. In reservoirs where the drive mechanism is bottomwater, gas cap, or a combination, a horizontal well can be placed strategically and can be produced with significantly lower drawdown, resulting in increased production and ultimate recovery.⁴

This study presents the effects of permeability anisotropy, net pay thickness, and horizontal permeability on the productivity of horizontal wells on the basis of the inflow-performance relationship suggested by Joshi.⁵ The performance of fractured vertical and fractured horizontal wells is compared. The fractured horizontal well is treated as a choked vertical fracture because of the limited contact between the well and the fracture. Well performance, calculated by the optimum number of induced hydraulic fractures in

a horizontal well compared with those in a hydraulically fractured vertical well, is evaluated with net-present-value (NPV) considerations.

Inflow Performance of Horizontal Wells

Giger *et al.*¹ reported the productivity of horizontal wells using the steady-state equations for flow into horizontal wells presented by Merkulov⁶ and Borisov.⁷ They used (in Darcy units)

$$q_H = \frac{2\pi k_H h \Delta p}{\mu B \left[\ln \frac{1 + \sqrt{1 - (L/2r_{DH})^2}}{(L/2r_{DH})} + \frac{h}{L} \ln \left(\frac{h}{2\pi r_w} \right) \right]} \dots (1)$$

The derivation of Eq. 1 was not published in Ref. 1.

The flow of a single-phase fluid through a homogeneous porous medium of uniform net thickness and produced through a horizontal well can be described by a 3D Laplace equation ($\nabla^2 p = 0$). The pressure distribution around the horizontal wellbore in the reservoir drainage area can be calculated by the solution of the 3D equation, with appropriate inner and outer boundary conditions. Joshi⁵ simplified the 3D problem by coupling two 2D problems on the premise that a horizontal well drains an ellipsoidal volume around the wellbore of length L , as shown in Fig. 1. A conventional vertical well, on the other hand, drains a right circular cylindrical volume symmetrical around the vertical well axis. Fig. 2 shows the configuration of the two 2D problems solved by Joshi. Immediately around the wellbore, the flow is studied in a plane orthogonal to the wellbore axis—radial flow is basically assumed in this region (Cross Section BB). The other flow component into the horizontal wellbore is considered to be in a horizontal plane (Cross Section AA). The radial-flow problem is solved with Darcy's law, where the drainage radius is assumed to be one-half the net pay thickness, the well is in the middle of the pay thickness, and the medium is isotropic. Thus, radial flow into the wellbore in an orthogonal vertical plane is

$$q_r = \frac{2\pi k_H L \Delta p}{\mu B (\ln h/2r_w)} = \frac{2\pi k_H h \Delta p}{\mu B (h/L) [\ln(h/2r_w)]} \dots (2)$$

and gravity effects are neglected.

Note that the factor π in the second term of the denominator of Eq. 1, presented by Giger *et al.*, does not occur in Eq. 2.

The other flow component into the horizontal well in the horizontal plane, as solved by Muskat⁸ using potential theory, was presented by Joshi as

$$q_H = \frac{2\pi k_H h \Delta p}{\mu B \{ \ln [a + \sqrt{a^2 - (L/2)^2}] / (L/2) \}} \dots (3)$$

*Now at Leeban Mining U.

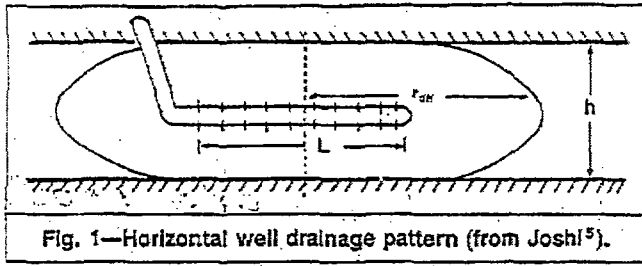


Fig. 1—Horizontal well drainage pattern (from Joshi⁵).

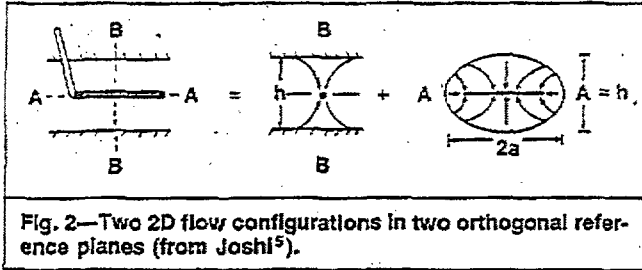


Fig. 2—Two 2D flow configurations in two orthogonal reference planes (from Joshi⁵).

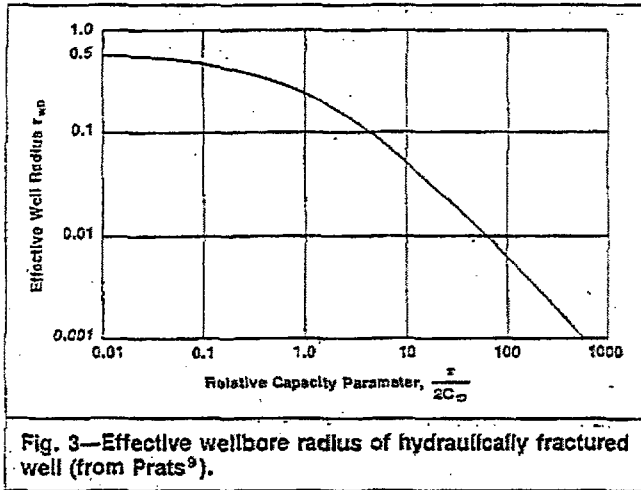


Fig. 3—Effective wellbore radius of hydraulically fractured well (from Prats⁶).

Total production of the horizontal well resulting from these two flow components is obtained by adding the respective flow resistances, or pressure drawdown per unit volumetric flow rate:

$$\Delta p/q = (\Delta p/q_r) + (\Delta p/q_H), \dots (4)$$

$$\text{and thus } q = \frac{2\pi k_H h \Delta p}{\mu B \left[\ln \frac{a + \sqrt{a^2 - (L/2)^2}}{(L/2)} + \frac{h}{L} \ln \left(\frac{h}{2r_w} \right) \right]} \dots (5)$$

for \$L > h\$ and \$L/2 < 0.9r_{DH}\$, \$a\$, one-half the major axis of the drainage ellipse shown in Fig. 2 and given by Joshi, is

$$a = L/2 \left(0.5 + \{ 0.25 + [r_{DH}/(L/2)]^4 \}^{0.5} \right)^{0.5} \dots (6)$$

The derivation of Eq. 5 assumes complete isotropy in both the horizontal and vertical planes and that permeability is \$k_H\$ in all directions.

The assumption of isotropy in the horizontal plane is very common in radial-flow calculations for vertical wells. The radial flow component in the vertical plane, however, cannot be assumed to be isotropic. In such sedimentary rock as sandstone, the horizontal/vertical permeability ratio is commonly assumed to be 10:1. Consequently, Eq. 2 for radial flow in a vertical plane to a horizontal well should be modified to account for any vertical anisotropy. Muskat⁸ accounted for such effects in the vertical plane by modifying the vertical axis. The simple transformation to account for permeability anisotropy is done by multiplying the net pay thickness

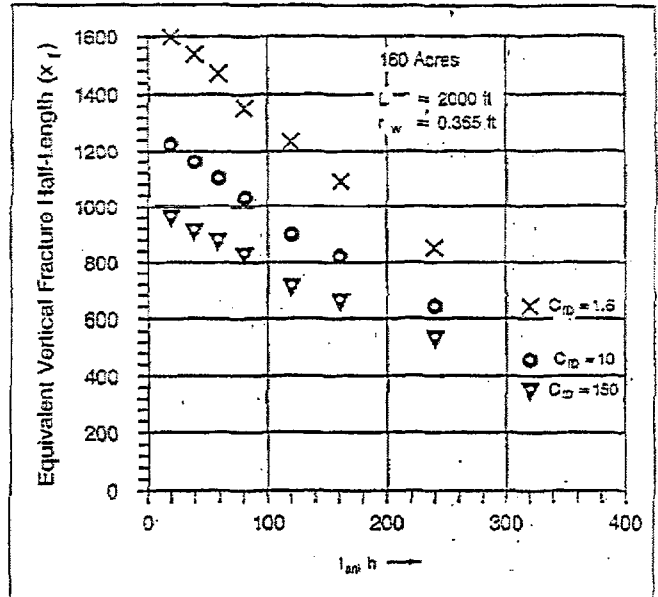


Fig. 4—Equivalent fracture half-length in vertical well to match production from horizontal well.

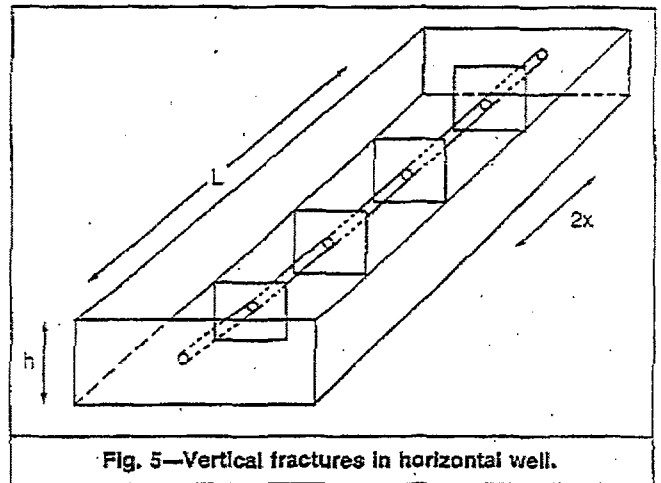


Fig. 5—Vertical fractures in horizontal well.

by \$I_{ani} = (k_H/k_V)^{1/2}\$ and replacing permeability in the vertical plane by a geometric average permeability, \$(k_H k_V)^{1/2}\$. Thus, the transformed horizontal well productivity equation for a homogeneous reservoir with vertical anisotropy is

$$q = \frac{2\pi k_H h \Delta p}{\mu B \left\{ \ln \left[\frac{a + \sqrt{a^2 - (L/2)^2}}{(L/2)} \right] + \frac{I_{ani} h}{L} \ln \left(\frac{I_{ani} h}{2r_w} \right) \right\}} \dots (7)$$

where \$I_{ani} = \sqrt{k_H/k_V}\$, \$L > I_{ani} h\$, and \$L/2 < 0.9r_{DH}\$. Eq. 7 (which is in Darcy units) is used extensively in the parametric study of the effects of anisotropy presented later. Note that \$r_w\$ is actual, not effective, wellbore radius.

Economides *et al.*⁹ later found that Eq. 7 requires an augmentation. The term \$2r_w\$ in the second logarithmic expression in the denominator must be replaced by \$(I_{ani} + 1)r_w\$. For large permeability anisotropies, this discrepancy can lead to errors.

Comparison of Horizontal Wells With Hydraulically Fractured Vertical Wells

In low-permeability reservoirs where vertical wells are almost always hydraulically fractured, the engineering feasibility of unfractured horizontal wells should always be based on comparison with equivalent vertical wells with hydraulic fractures. An easy way to

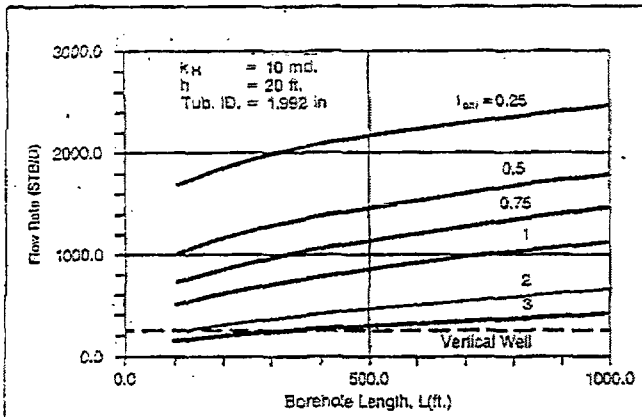


Fig. 6—Anisotropy effect on performance of horizontal oil well and comparison with vertical well performance.

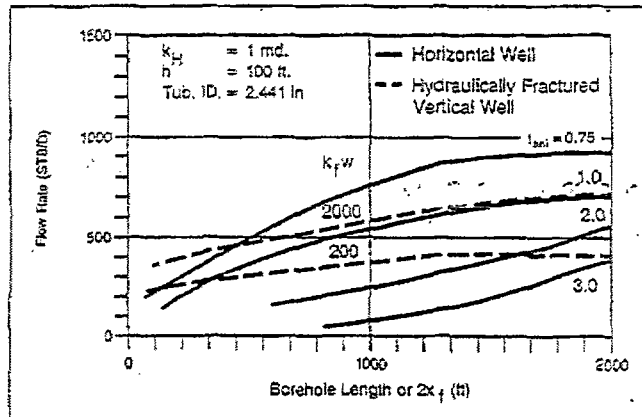


Fig. 7—Anisotropy effect on performance of horizontal oil well and comparison with hydraulically fractured vertical well in thick, low-permeability formation.

do such a comparison is to use the concept of equivalent or effective wellbore radius. Equivalent wellbore radius is the extended wellbore radius (underreamed well) that results in an equivalent PI of a well with a fixed fracture half-length and conductivity. Fig. 3 shows Prats' correlation of dimensionless wellbore radius, r_{wD} , with dimensionless fracture conductivity, C_{fD} , given by

$$r_{wD} = r_{wa}/x_f \quad (8)$$

where r_{wa} is the effective wellbore radius resulting from a fracture half-length, x_f , and

$$C_{fD} = k_{fw}/k_H x_f \quad (9)$$

where k_{fw} = proppant-pack conductivity. Assume that

$$r_{wD} = m = r_{wa}/x_f \quad (10)$$

where $m=0.5$ for an infinite-conductivity vertical fracture ($C_{fD} \geq 30$) and $m < 0.5$ for a finite-conductivity vertical fracture. In other words, for infinite-conductivity vertical fractures, a fracture half-length of 1,000 ft is equivalent to an unfractured well with a wellbore radius of 500 ft as far as productivity is concerned. For finite conductivity, this number can be calculated from Fig. 3.

When Prats' correlation is applied, an equivalent fracture half-length in a vertical well can be calculated to match the production from a horizontal well of any fixed length. In this case, it may not be unreasonable to assume equal drainage volumes, $r_{aH} = r_{aV}$. If the hydraulically fractured vertical well is assumed to have an equivalent wellbore radius, r_{wa} , then equating its PI with that of a horizontal well results in

$$\frac{2\pi k_H h}{\mu B \ln(r_{aV}/r_{wa})} \Big|_V = \frac{2\pi k_H h}{\mu B \left[\ln \frac{a + \sqrt{a^2 - (L/2)^2}}{L/2} + \frac{I_{ani} h}{L} \ln \left(\frac{I_{ani} h}{2r_w} \right) \right]} \Big|_H \quad (11)$$

$$\text{and thus } r_{wa} = \frac{r_{aV}(L/2)}{\left\{ [a + \sqrt{a^2 - (L/2)^2}] \left(\frac{I_{ani} h}{2r_w} \right)^{I_{ani} h/L} \right\}} = mx_f \quad (12)$$

where $m=0.5$ for an infinite-conductivity vertical fracture. Eq. 12 shows that in low-permeability formations, the economic feasibility of horizontal wells depends strongly on the permeability anisotropy I_{ani} . The higher the value of I_{ani} , the lower the fracture half-length required in the vertical well will be to match the productivity of a horizontal well. In fact, the product $I_{ani} h$ forms a better correlating parameter with equivalent fracture half-length, x_f . Fig. 4 presents this correlation of x_f vs. $I_{ani} h$ for the assumed fracture

conductivities of 1.6, 10, and 150, respectively; and $r_{aH} = r_{aV} = 1,490$ ft, $r_w = 0.365$ ft, and $L = 2,000$ ft. Fig. 4 leads to the following important observations: (1) for $I_{ani} h \geq 100$, a vertical well with an $x_f < 1,000$ ft and a $C_{fD} = 10$ can replace a 2,000-ft horizontal well; and (2) increasing I_{ani} for a fixed h requires a lower fracture conductivity, a lower fracture half-length, or both to replace a 2,000-ft horizontal well. Note that Fig. 4 presents an example for a 2,000-ft horizontal well. Increasing the well length would make the horizontal well compare better with the hydraulically fractured vertical well.

Infinite-Conductivity Vertical Fractures in Horizontal Wells

To induce multiple transverse vertical fractures in horizontal wells, the horizontal section must be cased, selectively perforated, and fractured starting at the end of the horizontal section. If the non-fractured casing interval is not perforated, then a minimum number, n , of vertical fractures is required just to attain the productivity of the open hole (uncased horizontal completion). This analogy is also applicable when massive natural fractures in a tight formation are penetrated by the well. n can be calculated by assuming infinite-conductivity vertical fractures with fracture half-length x_f . For an openhole completion, horizontal well productivity is given by Eq. 7.

If n orthogonal hydraulic fractures of half-length x_f are required to match the openhole production, then each fracture must produce with a rate q_{fH} , where

$$q/\Delta p = n q_{fH}/\Delta p \quad (13)$$

Assuming that the distance between two fractures is $2x$ (Fig. 5) and that only linear flow occurs in the formation to produce into the fractures, then

$$q_{fH}/\Delta p = [2k_H(2x_f h)]/\mu B x \quad (14)$$

Combining Eqs. 7, 13, and 14 yields

$$\frac{2\pi k_H h}{\mu B \left\{ \ln \left[\frac{a + \sqrt{a^2 - (L/2)^2}}{(L/2)} \right] + \frac{I_{ani} h}{L} \ln \left(\frac{I_{ani} h}{2r_w} \right) \right\}} = \frac{[2nk_H(2x_f h)]/\mu B x}{\mu B} \quad (15)$$

$$\text{or } \pi/C = (2x_f n)/x \quad (16)$$

$$\text{where } C = \ln \left[\frac{a + \sqrt{a^2 - (L/2)^2}}{L/2} \right] + \frac{I_{ani} h}{L} \ln \left(\frac{I_{ani} h}{2r_w} \right) \quad (17)$$

$$\text{and } x = L/[2(n-1)] \quad (18)$$

Substituting the x value from Eq. 18 into Eq. 16 gives

$$\pi/C = [4x_f n(n-1)]/L \quad (19)$$

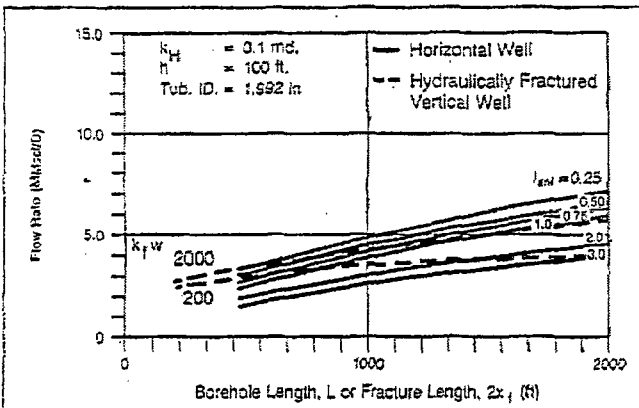


Fig. 8—Anisotropy effect on performance of horizontal gas well and comparison with hydraulically fractured vertical well in thick, low-permeability formation.

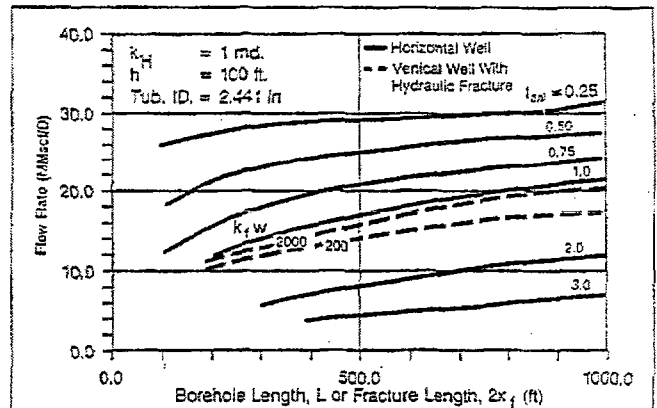


Fig. 9—Anisotropy effect on performance of horizontal gas well and comparison with hydraulically fractured vertical well in thick, higher-permeability formation.

$$\text{i.e., } n(n-1) = (L\pi/4Cx_f) = D \quad (20)$$

$$\text{and } n = (1 + \sqrt{1 + 4D})/2 \quad (21)$$

Eq. 21 shows that a minimum n of infinite-conductivity vertical fractures are needed, when the cased horizontal section is not perforated outside the fractured regions, to match the production from the unfractured openhole horizontal completion.

Example Application: Given $L=2,000$ ft, $h=100$ ft, $I_{ani}=3$, $r_{dH}=1,490$ ft (160-acre spacing), and $r_w=0.365$ ft, calculate the minimum number of infinite-conductivity vertical fractures of $x_f=100$ ft to match the unfractured openhole production. Calculations are shown below.

$$\begin{aligned} \text{From Eq. 6: } a &= \frac{L}{2} \left[0.5 + \sqrt{0.25 + \left(\frac{r_{dH}}{L/2} \right)^4} \right]^{0.5} \\ &= \frac{2,000}{2} \left[0.5 + \sqrt{0.25 + \left(\frac{1,490}{1,000} \right)^4} \right]^{0.5} = 1,666. \end{aligned}$$

From Eq. 17:

$$\begin{aligned} C &= \ln \left(\frac{1,666 + \sqrt{1,666^2 - 1,000^2}}{1,000} \right) + \frac{300}{2,000} \ln \left(\frac{300}{2 \times 0.365} \right) \\ &= 1.10 + 0.90 = 2.0. \end{aligned}$$

From Eq. 20: $D = (2,000 \times \pi) / (4 \times 2 \times 100) = 7.85$.

From Eq. 21: $n = (1 + \sqrt{1 + 4 \times 7.85}) / 2 = 3.35 \approx 4$.

In this case, at least four infinite-conductivity fractures are needed to produce the equivalent of an openhole horizontal completion. Consequently, if horizontal wells need fracturing, the economics may favor a vertical well with vertical fracture, unless the formation is very thin.

TABLE 1—INPUT DATA FOR PROBLEMS USED IN FIGS. 6 THROUGH 9

	Oil Well	Gas Well
p_g , psia	200	600
Gravity, °API	30	—
GLR, scf/STB	400	—
γ_g	0.65	0.65
\bar{p} , psia	3,500	4,000
r_w , ft	0.25	0.25
A, acres	160	160
T, °F	200	200
D, ft	8,000	8,000
Surface temperature, °F	80	80

GLR = gas/liquid ratio.

Anisotropy Effects

Productivity of horizontal wells determined from Eq. 7 shows its dependence on anisotropy. Joshi⁵ presented these effects by comparing productivity ratios of horizontal wells with those of vertical wells for different horizontal well lengths and permeability anisotropies. These productivity ratios actually compare the absolute open-flow potentials (OFF's) without considering the effects of the tubing, flowline, etc. Depending on the nature of the tubing intake curves, the effect of the plumbing system on well production may obscure the well performance predicted by productivity ratios. In the present study, anisotropy effects on actual oil and gas production are shown in Figs. 6 through 9. These figures present flow rates vs. horizontal wellbore lengths for a range of I_{ani} that represents the anisotropy. If $k_H > k_V$, then $I_{ani} > 1$. $I_{ani} = 1$ for the case of vertical isotropy, whereas $I_{ani} < 1$ when $k_V > k_H$. In sedimentary formations with primary porosity and permeability, the I_{ani} value should always be greater than unity. Normally, it is assumed to equal 3. In naturally fractured formations, I_{ani} can be very close to or less than unity. By inducing clean, transverse-propped hydraulic fractures in horizontal wells, especially in very-low-permeability formations, one may create an effective $I_{ani} \leq 1$.

Figs. 7 through 9 also compare the performance of horizontal wells with that of vertical wells with induced hydraulic fractures for two different fracture conductivities, $k_f w$ (200 and 2,000 md-ft). Figs. 6 and 7 are for oil wells, and Figs. 8 and 9 are for gas wells. Table 1 presents the data used to generate these figures.

Horizontal well flow rates for an oil well with good permeability are compared with the vertical well productivity for the same reservoir. Fig. 6 presents this comparison for a number of I_{ani} values between 0.25 and 3. The formation thickness in this case is 20 ft. Because this is a thin formation, a 400-ft-long horizontal well completion produces more than its vertical counterpart, even for very unfavorable anisotropy ($I_{ani}=3$). For $I_{ani} < 3$, any horizontal well with more than about 100-ft horizontal openhole-completion length yields more production than the vertical well.

Fig. 7 compares the horizontal well performance for several anisotropy values and horizontal completion lengths with a hydraulically fractured vertical well in a thick, low-permeability oil formation. It is very clear from Fig. 7 that, except for very low I_{ani} (< 1), an induced vertical fracture in a vertical well in the formation produces more fluids to the surface. For a fracture conductivity of 200 md-ft (which is low) and vertical isotropy, a horizontal well exceeding 300 ft will produce better than the hydraulically fractured vertical well with the same fracture length as the horizontal completion length. For a better-conductivity (2,000 md-ft) vertical fracture in a vertical well, however, the I_{ani} value must be < 1.0 for the horizontal well even to compare in productivity.

Effects of anisotropy and length of horizontal completion are also studied for low-permeability gas formations. Fig. 8 describes a low-permeability gas well ($k=0.1$ md). For a good fracture conductivity (2,000 md-ft), the only way that a horizontal well of reasonable

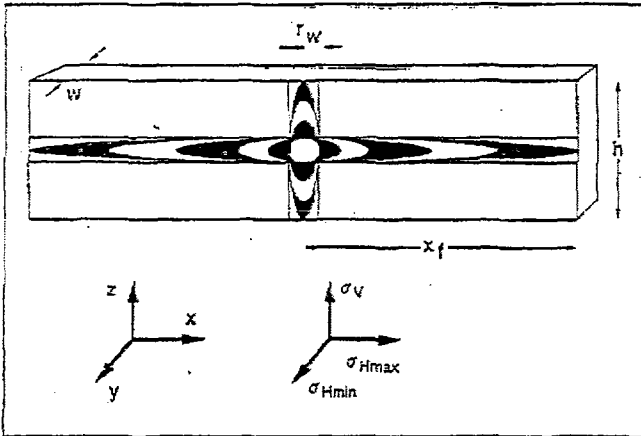


Fig. 10—Vertical fracture with all possible well configurations. Each ellipse corresponds to different angles of contact between well and fracture.

length ($\leq 2,000$ ft) could perform better than the vertical well/vertical fracture is if $I_{ani} \leq 1$. For a low-conductivity fracture (200 md-ft), a horizontal well would generally perform better than the fractured vertical well if length is not a constraint. Fig. 9 describes a higher-permeability gas well ($k=1$ md). Here there is a clear-cut distinction: horizontal wells are better when $I_{ani} \leq 1$ and worse when $I_{ani} \geq 2$ when they are compared to fractured vertical wells. This clearly suggests that naturally fissured gas reservoirs are good candidates for horizontal wells.

Fractured Horizontal vs. Fractured Vertical Wells

In this section, the performance of a horizontal well with an induced vertical fracture is compared with that of a fractured vertical well. As in all hydraulically fractured wells, flow is assumed to be from the reservoir into the fracture and then from the fracture into the wellbore. The remaining part of the well, perforated or not, is assumed to contribute negligible flow. In other words, this comparison is for reasonably tight wells, which, if left unfractured, would have virtually no production. Note that, for hydraulically fractured horizontal wells in tight formations, most of the benefits resulting from the extended reach are not similar to those in higher-permeability reservoirs. Hence, fractures in a horizontal well should be perceived more as means to improve and extend drainage patterns rather than just to increase the flow when compared with a vertical well completion. With the exception of the limiting and unlikely case from an execution point of view, where the fracture direction coincides perfectly with the well direction, the actual contact between fracture and well is very small. For the comparison presented here, an analogy between a vertical well with a vertical fracture and a horizontal well with a vertical fracture will be used. The produced fluid is assumed to enter the wellbore only through the fractures.

The impact of the inefficient contact between the well and fracture can be quantified with a skin effect, s_c , resulting from the choke of the limited contact. Fig. 10 contains all possible configurations of the contact between the well and the fracture. The fracture direction, away from the well, is always normal to the minimum stress. With the rare exception of very shallow wells, where the fracture is horizontal, the direction is vertical and normal to the minimum horizontal stress. In Fig. 10, the minimum horizontal stress is in the y direction and the fracture is in the xz plane. For a perfectly vertical well, the fracture would have a full exposure to the well along the z axis. A similar configuration would result for a well drilled along the x axis. Any other angle results in a reduction in the contact between the well and the fracture. This can happen in deviated holes with an angle between the z axis and the xy plane or in a perfectly horizontal well with an angle between the y axis and the xz plane, which describes the fracture. The smallest contact between the well and the fracture is for a well drilled exactly in the y direction and thus normal to the xz plane. This con-

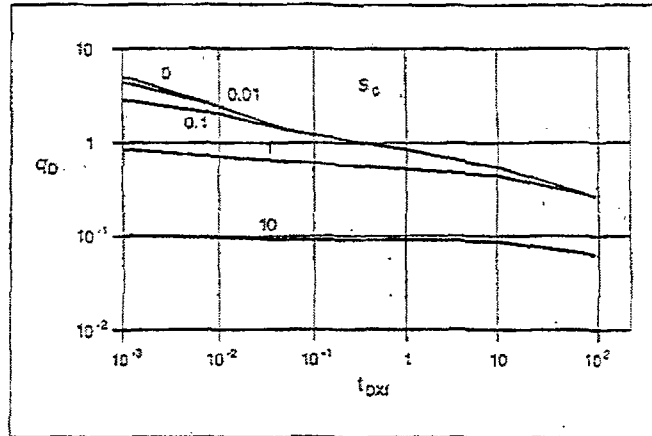


Fig. 11—Solution for finite-conductivity fracture ($C_{FD} = 10$) intercepted by horizontal well. Effect of choke skin resulting from limited contact between well and fracture.

figuration would result in the largest skin effect. On the other hand, multiple fractures generated with this geometry could aid in the best coverage of the drainage area.

The skin effect results in an additional pressure drop from the radial flow generated around the entry point. For a horizontal well, penetrating the fracture at its midpoint and normal to its plane, the radius of the radial flow is $h/2$, where h is the fracture height (assumed to coincide with the reservoir height.) The pressure drop within this radial zone is

$$(p - p_{wf})_r = [q\mu \ln(h/2r_w)] / 2\pi k_f w, \dots (22)$$

where p is the pressure at the outer boundary and k_f and w are permeability and fracture width, respectively. Eq. 22 assumes no gravity effects. It is simply the steady-state expression of Darcy's law for radial flow through a reservoir of extent $h/2$ and "height" w . This pressure drop must be adjusted by subtracting the pressure drop that would result from the linear flow within the fracture into a fully penetrating well:

$$(p - p_{wf})_L = [(1/2)q\mu(h/2)] / k_f wh, \dots (23)$$

where wh is the flow area. The factor $1/2$ accounts for flow from both wings of the fracture.

The pressure difference between radial and linear flow is then

$$\Delta p_s = (p - p_{wf})_r - (p - p_{wf})_L \dots (24)$$

$$\text{or } \Delta p_s = \frac{q\mu}{2\pi} \left[\frac{\ln(h/2r_w)}{k_f w} - \frac{\pi}{2k_f w} \right] \dots (25)$$

Multiplying and dividing the right side of Eq. 25 by kh results in

$$\Delta p_s = \frac{q\mu}{2\pi kh} \left\{ \frac{kh}{k_f w} [\ln(h/2r_w) - \pi/2] \right\} \dots (26)$$

The multiplier $q\mu / (2\pi kh)$, in Eq. 26 in Darcy units, is the standard multiplier of the dimensionless pressure for finite-conductivity fractured wells that accounts for the pressure drop at the well. Hence, Eq. 26 describes a steady-state pressure drop to be added to the fracture pressure drop. We define the bracketed quantity as s_c for the choke from the well and fracture contact:

$$s_c = (kh/k_f w) [\ln(h/2r_w) - \pi/2] \dots (27)$$

This is the maximum value of s_c that occurs when the well is normal to the fracture plane. When the well is vertical or along the fracture direction, then $s_c = 0$. Except in rare cases, a longitudinal fracture would not improve the production over a vertically fractured well appreciably. Hence, this observation generally nullifies the need to drill a horizontal well exactly in the expected direction of the induced fracture—i.e., along the maximum horizontal stress direction. An exception to this rule, however, is the case of carbonate reservoirs requiring acid fractures. In these cases, it is

TABLE 2—DATA FOR COMPARISON OF VERTICAL vs. HORIZONTAL FRACTURED-WELL PERFORMANCE EXAMPLE

ϕ , fraction	0.1
μ , cp	0.7
c_r , psi ⁻¹	10^{-5}
k , md	1
t , days	30
x_f , ft	500
w , in.	0.25
k_f , md	24,000
h , ft	100
B , res bbl/STB	1.1
p_i , psia	6,500
p_{wf} , psia	4,500
r_w , ft	0.408

difficult to obtain enough fracture half-length from the vertical well. A horizontal well drilled in the direction of the maximum horizontal principal stress may lead to the inducement of a long, vertical, longitudinal fracture along the horizontal wellbore.

Note that a vertical well in a formation to be fractured should be drilled with as little deviation from the z axis as possible. Hence, if a deviated hole is necessary (offshore, pad drilling, etc.), a well to be fractured should be completed vertically within the reservoir to minimize the contact skin effect.

On the other hand, horizontal well performance can substantially benefit from a completion with multiple fractures. Each vertical fracture penetrating a horizontal well is penalized with a skin of the form given by Eq. 27. The total dimensionless pressure for a horizontal well penetrating a vertical fracture at 90° is then given in oilfield units for oil as

$$(p_D)_T = p_D + s_c = kh\Delta p / (141.2qB\mu) \dots (28)$$

$$\text{and for gas as } (p_D)_T = p_D + s_c = kh\Delta p_p / (1,424qT) \dots (29)$$

The value of this skin effect can be substantial and can have a major effect on the production behavior of a hydraulic fracture. For $C_{FD} = 10$, a graph of q_D vs. t_{FD} for various s_c values is shown

TABLE 3—WELL AND RESERVOIR DATA FOR OPTIMIZATION OF FRACTURES IN VERTICAL AND HORIZONTAL GAS WELLS

k , md	0.8
p_i , psia	4,200
r_w , ft	0.333
T , °F	230
h , ft	103
A_v , acres	160
A_H , [*] acres	40
ϕ , fraction	0.1
Model	PKN
Fluid, ^{**} lbm/1,000 gal	40
Proppant, [†] mesh	16/30
p_H , psia	2,000
d_{gr} , in.	27/8
D , ft	8,159 to 8,262
E , psia	3.8×10^6
ν	0.25
σ_{Hmin} , psia	6,980
Δp_{10} , [‡] psia	1,000
l , [§] bbl/min	20
C_{M1} , [§] lbm/gal	10

*Four orthogonal fractures.

**Crosslinked gel.

†Prepacked sand.

‡Maximum.

§At end of job.

PKN = Perkins-Kern-Nordgren model.

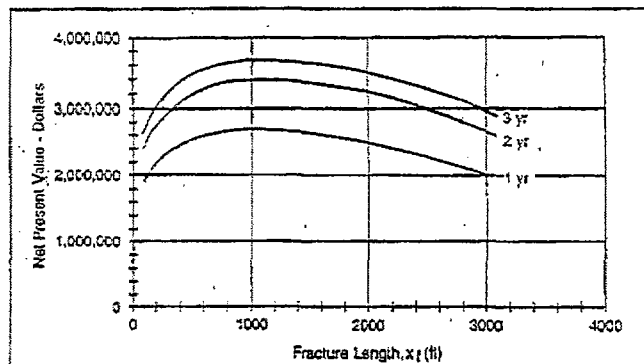


Fig. 12—NPV calculation for vertical fracture intercepted by vertical well.

in Fig. 11. An example solution is presented below, for the well described in Table 2, to calculate the 30-day production rate,

$$C_{FD} = \frac{k_f w}{k x_f} = \frac{(24,000)(0.25/12)}{(1)(500)} = 1 \dots (30)$$

$$\text{and } t_{xFD} = \frac{0.0063kt}{\phi\mu c_r x_f^2} = \frac{(0.0063)(1)(30)}{(0.1)(0.7)(10^{-5})(500)^2} = 1.08 \dots (31)$$

Then from Cinco-Ley and Samaniego-V.'s¹¹ solution, $p_D = 2.2$. In a vertical hole $s_c = 0$, and from Eq. 28, $q = 836$ STB/D.

In a horizontal hole (Eq. 27) $s_c = 0.65$, resulting in a $(p_D)_T = 2.85$. The flow rate through this well is then (Eq. 28) $q = 645$ STB/D, a 200-STB/D drop. As can be seen from Eq. 27, the skin effect from the contact is proportional to the kh product. As a result, its relative impact on the reduction in the well flow rate is greater. In general, the type of calculation shown above can allow estimation of the number of fractures required to match the well performance of a vertical well penetrated by a vertical fracture. A simulator^{12,13} can be used to optimize the number and size of hydraulic fractures with the NPV concept.

At first, a simulation is done for a vertical well with vertical fracture configuration. This results in an optimum fracture size corresponding to the maximum NPV. This simulation is done for the total drainage area described by the length of the horizontal reach of the well and the parallel no-flow boundaries. The minimum number of orthogonal vertical fractures is calculated with Eq. 21. Then, for each number of contemplated hydraulic fractures, the drainage area is divided equally, and the performance of these fractures over time is corrected with the choke skin, as shown by Eqs. 28 and 29. The corresponding NPV is calculated. The number of fractures is increased to optimize the NPV and to exceed the NPV of the induced-fractured vertical well. To calculate the skin effect, some value of the $k_f w$ product must be assumed ahead of time. Following the optimization, this assumption may be readjusted as a minor trial-and-error calculation. In general, this product does not change

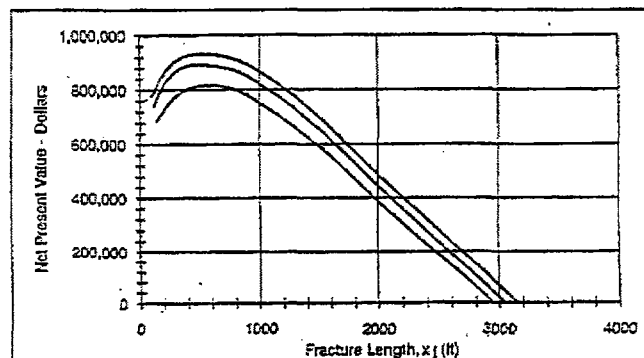


Fig. 13—NPV calculation for vertical fracture intercepted by horizontal well.

greatly. An optimization of the number of fractures vs. the total NPV may then be done. Each of these fractures has a corresponding optimum size that is always smaller than that in the vertical well case.

Fig. 12 plots NPV vs. fracture half-length of a fractured vertical well. Table 3 contains the important parameters used in this simulation. Fig. 13 is the NPV vs. fracture half-length of a fractured horizontal well that was "choked" with the skin effect described by Eq. 27. Two things are important here: the optimum fracture length dropped from 1,100 to 500 ft, and the maximum NPV dropped from \$3.6 million to \$0.9 million. Hence, at least four fractures are needed in the horizontal well to equal the NPV of a single fracture in the vertical hole. This does not include the additional cost of drilling the horizontal well, which can be incorporated as fixed costs in the NPV calculations and allocated equally to each fracture to be completed in the horizontal well.

This calculation generally depends heavily on the kh product and the fracture permeability. If kh is large or k_f is small (damaged), then s_c is large, resulting in a disproportionate penalty on the hydraulically fractured horizontal well. Most 2,000-ft horizontal wells that are candidates for fracturing need from two to eight orthogonal fractures to equal the NPV of a vertical fractured well. As the horizontal well length changes, the optimum number of fractures also changes.

Conclusions

While horizontal wells are viable alternatives to vertical wells, they are not a panacea. Their choice over a vertical well must be decided on the basis of careful engineering evaluation. Applications where horizontal wells are preferable are listed below.

1. For $I_{ani}h < 100$, a horizontal well performs better than a vertical well with induced hydraulic fractures of reasonable length (2,000 ft). Eq. 12 can be used to generate this criterion for any other well lengths, drainage radii, and dimensionless fracture conductivities.

2. For an idealized vertical isotropic medium, horizontal wells may appear to be preferable to vertical wells in almost all cases. For reasonable vertical anisotropy ($I_{ani} > 1.5$) and low permeability (≤ 0.1 md), however, even an extended-reach horizontal well ($L=2,000$ ft) does not perform better than a vertical well with a hydraulic fracture.

3. Horizontal wells are particularly useful when $I_{ani} \leq 1$, which may be the case in massively, naturally fractured formations. In this case, a horizontal well can intercept a number of discrete natural fractures and have a significant improvement in production.

4. For reservoirs that are obvious candidates for hydraulic fracturing, it is reasonable to compare a vertical well with a vertical fracture to a horizontal well with a number of orthogonal vertical fractures. The number and size of these fractures are calculated on the basis of their performance. This performance is penalized by a skin effect resulting from the limited contact between the well and the fracture.

The NPV concept has been used to compare the optimum fracture size in a vertical well with the number of optimum fractures in a horizontal well. Note that in all cases the productivity increase, if any, must take into account the additional costs incurred by the drilling of the horizontal well.

Nomenclature

- a = half-axis of drainage ellipse (Eq. 6), ft
 A = drainage area, acres
 B = FVF, res bbl/STB
 c_t = total system compressibility, psi^{-1}
 C_{fD} = dimensionless fracture conductivity
 C_M = slurry concentration, lbm/gal
 d_{wg} = tubing diameter, in.
 D = well depth, ft
 E = Young's modulus, psi
 h = reservoir height, ft
 i = injection rate, bbl/min
 I_{ani} = anisotropy index $= (k_H/k_V)^{1/2}$

- k = formation permeability, md
 k_f = fracture permeability, md
 k_H = horizontal permeability, md
 k_V = vertical permeability, md
 L = horizontal length, ft
 m = slope, psi/cycle
 n_f = number of fractures
 p = pressure, psia
 \bar{p} = average reservoir pressure, psia
 p_D = dimensionless pressure
 p_i = initial reservoir pressure, psia
 p_p = real gas pseudopressure, psi^2/cp
 p_r = treatment pressure, psia
 p_{if} = flowing tubing pressure, psia
 p_{wf} = flowing bottomhole pressure, psia
 Δp = pressure drop, psia
 q = flow rate, STB/D and Mscf/D
 q_{fH} = flow rate from fractured horizontal well
 q_H = horizontal well flow rate
 q_r = radial flow rate
 r_{dH} = horizontal drainage radius, ft
 r_{dV} = vertical drainage radius, ft
 r_w = wellbore radius, ft
 r_{wa} = effective wellbore radius, ft
 r_{wD} = dimensionless effective wellbore radius
 s_c = skin effect from limited fracture/well contact
 t = time, days
 t_{fD} = fracture dimensionless time
 T = absolute temperature, °R
 w = fracture width, ft
 x = horizontal distance, ft
 x_f = fracture half-length in x direction, ft
 y = horizontal distance, ft
 z = vertical distance, ft
 γ_g = gas specific gravity (air=1)
 μ = viscosity, cp
 ν = Poisson's ratio
 σ_{Hmax} = maximum horizontal stress, psia
 σ_{Hmin} = minimum horizontal stress, psia
 σ_V = vertical stress, psia
 ϕ = porosity, fraction

Subscripts

- H = horizontal
 L = linear
 r = radial
 s = skin
 T = total
 V = vertical

Acknowledgments

We express our appreciation to Dowell Schlumberger for permission to publish this work. We also thank Joe Mach and Christine Ehlig-Economides for their valuable input. Wanda Reid did an excellent job in the preparation of this manuscript.

References

- Giger, F., Reiss, L.H., and Jourdan, A.: "The Reservoir Engineering Aspects of Horizontal Drilling," paper SPE 13024 presented at the 1984 SPE Annual Technical Conference and Exhibition, Houston, Sept. 16-19.
- Wilkinson, J.P. et al.: "Horizontal Drilling Techniques at Prudhoe Bay, Alaska," *JPT* (Nov. 1988) 1445-51.
- Roegiers, J.C. and Detournay, E.: "Considerations on Failure Initiation in Inclined Boreholes," paper presented at the 1988 U.S. Symposium Rock Mechanics, U. of Minnesota, Minneapolis, June.
- Sherrard, D.W., Brice, B.W., and MacDonald, D.G.: "Application of Horizontal Wells at Prudhoe Bay," *JPT* (Nov. 1987) 1417-25.
- Joshi, S.D.: "Augmentation of Well Productivity With Slant and Horizontal Wells," *JPT* (June 1988) 729-39; *Trans., AIME*, 285.

Authors



Economides



Mukherjee

Hemanta Mukherjee is a senior staff engineer at Dowell Schlumberger Inc.'s Western Division in Denver. Presently working on the design and evaluation of well stimulation, he has worked at other Schlumberger affiliates in the areas

of well testing, nodal analysis, gas-lift analysis and design, and pipe-flow modeling. Previously, he worked on the development of a coupled well management and wellbore hydraulics program in black-oil reservoir simulators at Gulf Science and Technology Co. Mukherjee holds MS and PhD degrees in petroleum engineering from the U. of Tulsa. He serves on the Production Operations Technical Committee and served on the Editorial Review Committee during 1982-87. **Michael J. Economides** is a professor of petroleum engineering and director of the Inst. of Drilling & Production at Leoben Mining U. in Austria, where he has worked since Nov. 1989. Previously, Economides worked at Dowell Schlumberger in Houston and London, the U. of Alaska in Fairbanks, Shell Oil Co., and Celanese Chemical Co. He holds BS and MS degrees in chemical engineering from the U. of Kansas and a PhD degree in petroleum engineering from Stanford U. A 1991-92 SPE Distinguished Lecturer, Economides served on SPE's 1988-89 Forum Series Committee, 1987 Technology Today Series Committee, which he chaired during 1987-88, and the 1982-86 Editorial Review Committees. He also chaired (1986-87) and served on (1985-87) the Reservoir Engineering Technical Committee.

6. Merkulov, V.P.: "Le débit des puits déviés et horizontaux," *Nefi. Khoz.* (1958) 6, 51-56.
7. Borisov, Yu.P.: *Oil Production Using Horizontal and Multiple Deviation Wells*, Nedra, Moscow (1964) (Translated into English by J. Straus, Phillips Petroleum Co., Bartlesville, OK).

8. Muskat, M.: *The Flow of Homogeneous Fluids Through Porous Media*, reprint, Intl. Human Resource Development Corp., Boston (1982).
9. Economides, M.J. et al.: "Comprehensive Simulation of Horizontal Well Performance," paper SPE 20717 presented at the 1990 SPE Annual Technical Conference and Exhibition, New Orleans, Sept. 23-26.
10. Prats, M.: "Effect of Vertical Fractures on Reservoir Behavior—Incompressible Fluid Case," *SPEJ* (June 1961) 105-16; *Trans.*, AIME, 222.
11. Cinco-Ley, H. and Sarmiento-V., F.: "Transient Pressure Analysis for Fractured Wells," *JPT* (Sept. 1981) 1749-66.
12. Meng, H.-Z. and Brown, K.E.: "Coupling of Production Forecasting, Fracture Geometry Requirements, and Treatment Scheduling in the Optimum Hydraulic Fracture Design," paper SPE 16435 presented at the 1987 SPE Low Permeability Reservoirs Symposium, Denver, May 18-20.
13. Balen, R.M., Meng, H.-Z., and Economides, M.J.: "Applications of the Net Present Value in the Optimization of Hydraulic Fractures," paper SPE 18541 presented at the 1988 SPE Eastern Regional Meeting, Charleston, WV, Nov. 1-4.

SI Metric Conversion Factors

acres	× 4.046 873	E+03	= m ²
°API	141.5/(131.5+°API)		= g/cm ³
bbl	× 1.589 873	E-01	= m ³
cp	× 1.0*	E-03	= Pa·s
ft	× 3.048*	E-01	= m
ft ³	× 2.831 685	E-02	= m ³
°F	(°F-32)/1.8		= °C
in.	× 2.54*	E+00	= cm
lbm/1,000 gal	× 1.198 264	E+02	= g/m ³
md	× 9.869 233	E-04	= μm ²
psi	× 6.894 757	E+00	= kPa
psi ⁻¹	× 1.450 377	E-01	= kPa ⁻¹

*Conversion factor is exact.

SPEFE

Original SPE manuscript received for review Oct. 2, 1988. Paper accepted for publication Dec. 10, 1990. Revised manuscript received Nov. 16, 1990. Paper (SPE 18303) first presented at the 1988 SPE Annual Technical Conference and Exhibition held in Houston, Oct. 2-5.

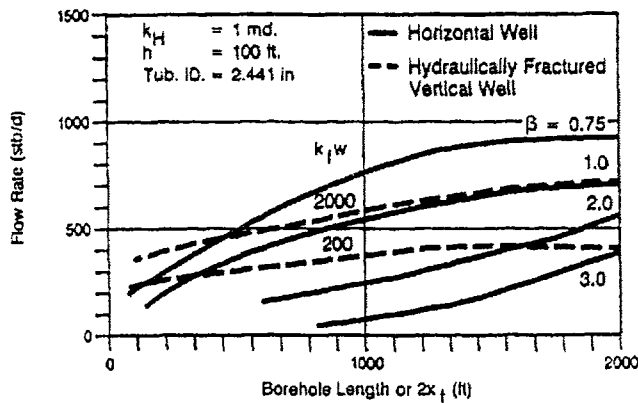


Fig. 7—Effect of anisotropy on the performance of a horizontal oil well and its comparison with a hydraulically fractured vertical well in a thick, low permeability formation.

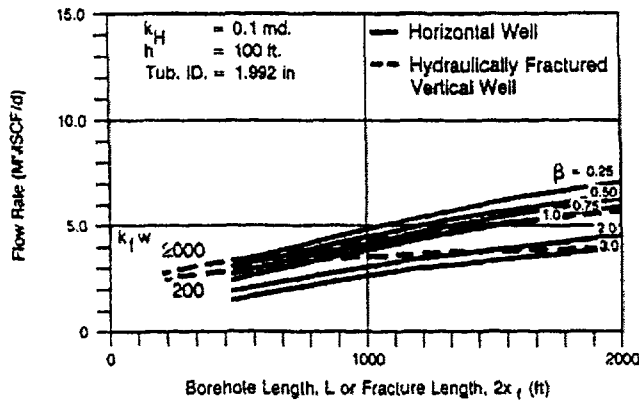


Fig. 8—Effect of anisotropy on the performance of a horizontal gas well and its comparison with a hydraulically fractured vertical well in a thick, low permeability formation.

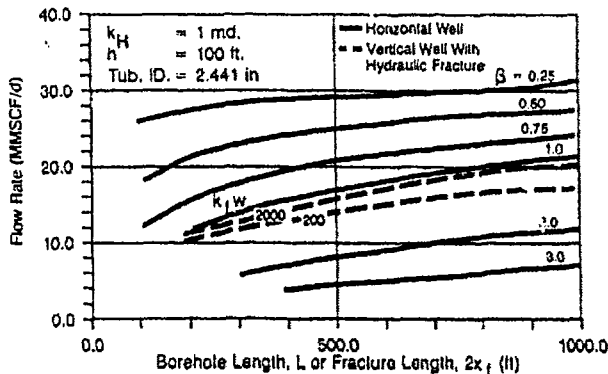


Fig. 9—Effect of anisotropy on the performance of a horizontal gas well and its comparison with a hydraulically fractured vertical well in a thick, higher permeability formation.

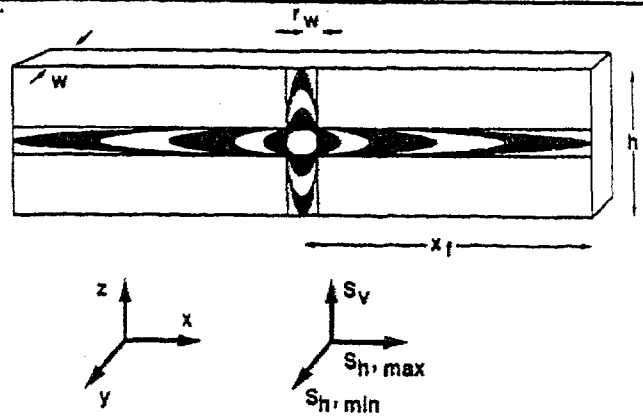


Fig. 10—Vertical fracture with all possible well configurations. Each ellipse corresponds to different angles of contact between the well and the fracture.

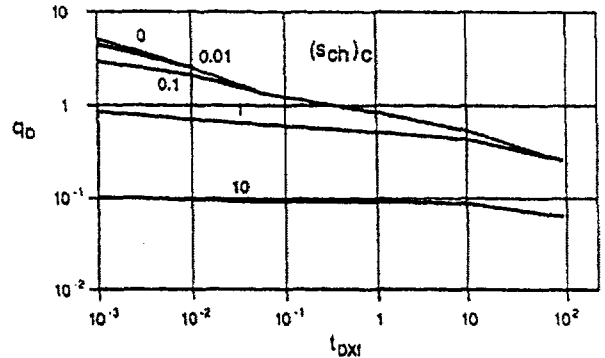


Fig. 11—Solution for a finite conductivity fracture ($F_{CD} = 10$) intercepted by a horizontal well. Effect of the choke skin resulting from the limited contact between well and fracture.

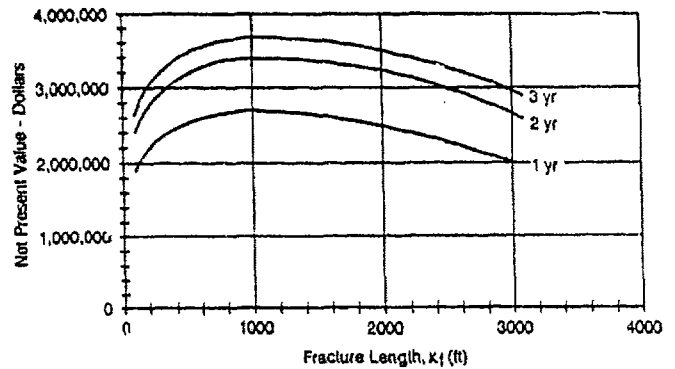


Fig. 12—Net present value (NPV) calculation for a vertical fracture intercepted by a vertical well.

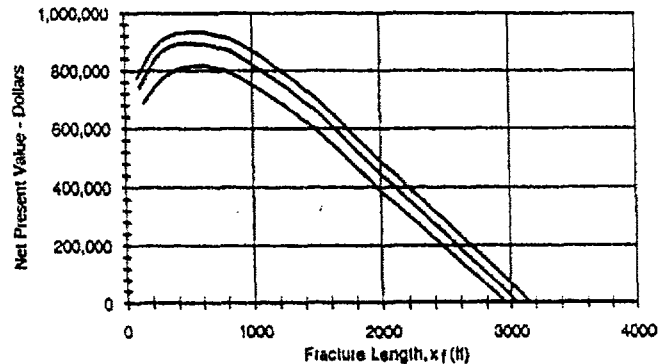
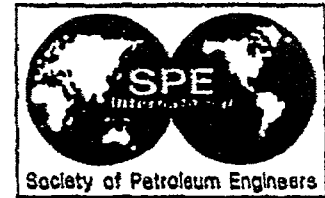


Fig. 13—Net present value (NPV) calculation for a vertical fracture intercepted by a horizontal well.



SPE 26445

Coupling Pressure and Rate-Time Data in Performance Analysis of Horizontal Wells: Field Examples

D.T. Vo and M.V. Madden, Unocal Corp.

SPE Members



Copyright 1993, Society of Petroleum Engineers, Inc.

This paper was prepared for presentation at the 68th Annual Technical Conference and Exhibition of the Society of Petroleum Engineers held in Houston, Texas, 3-8 October 1993.

This paper was selected for presentation by an SPE Program Committee following review of information contained in an abstract submitted by the author(s). Contents of the paper, as presented, have not been reviewed by the Society of Petroleum Engineers and are subject to correction by the author(s). The material, as presented, does not necessarily reflect any position of the Society of Petroleum Engineers, its officers, or members. Papers presented at SPE meetings are subject to publication review by Editorial Committees of the Society of Petroleum Engineers. Permission to copy is restricted to an abstract of not more than 300 words. Illustrations may not be copied. The abstract should contain conspicuous acknowledgment of where and by whom the paper is presented. Write Librarian, SPE, P.O. Box 833836, Richardson, TX 75083-3836, U.S.A. Telex, 163245 SPEUT.

ABSTRACT

Horizontal well performance analysis can be difficult. Pressure transient interpretation on horizontal wells is complicated by the possibility of a multiple-flow-regime appearing during testing, and even by the non-appearance of a particular flow regime due to wellbore storage and testing time limitations. As a result, interpretation of horizontal well pressure transient data alone may be ambiguous and unreliable for performance predictions. Rate-time data is frequently available and can be used to improve the analysis, but is often overlooked in horizontal well evaluation.

This paper presents a practical procedure to evaluate and predict performance of horizontal wells. The procedure couples the analysis of pressure transient and rate-time data to enhance the reservoir-well description and accurately predict long-term performance of horizontal wells. The applicability of the procedure is demonstrated by several field examples.

Results from the field tests illustrate that inclusion of the rate-time data in pressure transient testing can be valuable to the design of a successful pressure test. Field examples of the design, planning, and tools used in the pressure tests are discussed. Rate-time data can also help improve the pressure match resulting in a comprehensive set of reservoir and well properties (vertical and horizontal permeabilities, well skin condition, effective well length, reservoir pressure, boundary effect, etc.) which enhances the reservoir-well description. This enhanced description can be used to realistically predict a

well's long-term performance. Results indicate analytical solutions available in the literature can be used with care to perform the analysis. The application and limitations of the use of these models are discussed. Good agreement between model prediction and actual long-term well performance is shown.

INTRODUCTION

Horizontal and extended reach drilling has been increasing in the last ten years. Several field applications have demonstrated the benefit of horizontal wells.¹⁻³ Increasing in drilling activity has led to the emergence of horizontal well drilling⁴ and other related technologies. Included in these technologies is a large volume of publications devoted to the understanding of fluid flow mechanism towards horizontal wellbores, interpreting pressure transient tests and predicting horizontal well performance.⁵⁻³² This related technology is also the focal point of discussion in this paper.

The objective of this paper is to provide a practical procedure to evaluate and predict horizontal well performance. Although the methodology is generic and could be applied to horizontal or vertical wells, it is more important for horizontal wells because of the peculiar interaction between the horizontal wellbore and the reservoir. The procedure, based on pressure transient testing, utilizes the available rate-time performance data to enhance the reservoir-well description from pressure transient test interpretation. The enhanced reservoir-well description can then be used to predict well performance. The

References and figures at end of paper.

paper also shows that analytical models proposed in the literature can be used with care to perform the task effectively. The applicability of the suggested procedure is demonstrated by several field examples encompassing a wide range of reservoir-well conditions. Field experience with pressure test design, tools used, and relevant engineering and geological aspects of the wells and reservoirs under study is also provided.

HORIZONTAL WELL PRESSURE TRANSIENT TESTING

The goal of pressure transient testing is to determine reservoir and well properties in the well drainage area so that the well performance can be predicted. Because of the horizontal well geometry, the flow regimes are different than those of a vertical well. The pressure transient response can take on several particular flow regimes: early radial flow, early linear flow, late radial flow and boundary-affected flow. Figure 1 depicts each flow regime geometry²⁹ and shows how to identify each on a log-log diagnostic plot of pressure and pressure derivative.

Depending on which flow period affects the well test data, a horizontal well test can allow the analyst to compute: horizontal permeability, vertical permeability, effective well length, well skin factor, reservoir pressure and reservoir size or limits. Conventional techniques based on segmental analysis of each flow regime identified may be convenient, however its applicability often fails because of the obscured flow regimes encountered. Type curve matching based on modeling may be the only recourse to completely define those test parameter objectives mentioned.

A typical horizontal well type curve analysis procedure would be

- From pressure match compute horizontal permeability
- From time match compute effective well length
- From dimensionless well length compute vertical permeability
- Skin effect, reservoir pressure, and reservoir size obtained directly from modeling

In practice, many have reported difficulties with horizontal well test interpretation using type curves, especially due to the non-uniqueness problem.²⁶⁻³² Our experience with numerous horizontal well tests has shown wellbore storage effect often distorts the early time radial flow and possibly the early time linear flow data and thus prohibits the direct calculation of vertical permeability and skin factor. Horizontal permeability has been obtainable with confidence in most tests given a fair permeability formation. However, effective well length computed is commonly shorter than the actual completed length. In many instances, the unknown estimate of actual pay thickness hinders the estimates of other parameters. Equally

important, testing time limitations can also prohibit the evaluation of those parameters, especially for low permeability formations. It is obvious that additional information is needed to enhance the model established from type curve match. Information such as core, well logs, mud logs, and production data, is often available prior to a pressure test and should be used to enhance the pressure test interpretation. This paper focuses on using production data to assist the pressure test design and enhance the pressure test interpretation.

HORIZONTAL WELL PERFORMANCE PREDICTION

Many authors have presented methods to predict horizontal well rate behavior in the recent past.¹²⁻²⁰ Some methods are based on analytical solutions¹²⁻¹⁸ and others are based on numerical simulation.¹⁹⁻²⁰ In this work, we mainly focus our discussion on the analytical approaches¹⁴⁻¹⁵ to predict horizontal well rates. This choice was made for consistent and interchangeable usage of the same model employed in pressure test interpretation as well as rate prediction. One can also use numerical simulation to predict rates after the well test interpretation. However this is not the scope of this paper.

The model established from pressure interpretation is also used to predict well performance. The analytical model, based on the constant pressure solution, is found applicable for most of the wells tested because these wells are on pumps with constant producing bottomhole pressure. Essentially, all parameters computed from well tests are kept the same when the model is turned to constant pressure production mode. Sometimes, adjustments need to be made for better match on the cumulative production curve to compensate for the initial unstabilized rate before the well is pumped off. For the most part, the effective well length, horizontal and vertical permeabilities computed from well test interpretation remain the same in the rate-time performance prediction.

PERFORMANCE ANALYSIS PROCEDURE

The following generic analysis procedure was used to test and evaluate wells after completion:

1. Stabilize the well's rate for some time after well completion and estimate the well productivity index²¹⁻²⁴ based on estimates of reservoir parameters
2. Establish a well-reservoir model¹²⁻¹⁸ for rate-time prediction (based on Step 1) and tune the model by history matching the observed data
3. Design and conduct a pressure buildup test based on the parameters estimated from the previous two steps
4. Interpret the pressure test data⁵⁻¹⁶ and confirm the model established with the available rate-time data via an iterative

process

5. Predict well rate based on the enhanced model established from both rate-time and pressure-time interpretation
6. Periodically repeat Steps 3-5 to update the model prediction

In the following, horizontal well test examples from two fields are presented. The contrast in permeability of the two reservoirs under study demonstrates a wide spectrum of application for the suggested procedure. In each example, the reason for the horizontal well application, relevant geological, drilling, completion and production data are given. The well test design, conduct and analysis are then discussed. Next, the enhancement of the pressure test interpretation using available production data to predict rates is presented. Comparison of the observed and predicted well performance is then shown.

FIELD EXAMPLES

The Dos Cuadras Field - High Permeability

Background

The Dos Cuadras field, located offshore of Ventura in the Santa Barbara channel, has been exploited with horizontal drilling since 1990. The primary reason for drilling horizontal wells in this field is to reach extremely shallow and widespread sands which were previously unreachable, even with slanted drilling rigs that started drilling at 30°. Secondary benefits include increasing well productivity and accelerating production.

Since the first Well C-50 was completed in November of 1990, a total of eight horizontal wells have been completed in this field. The main target of the horizontal wells is a high permeability, shallow and unconsolidated sand reservoir that contains fairly viscous fluid at low pressure. Table 1 provides reservoir data and a description of the first four horizontal wells. Figure 2 shows their locations in the field. All of these wells have been drilled with waterbase mud and completed with wire-wrapped screens for sand control. Detailed description on the drilling and completion of these horizontal wells can be found in Ref. 33.

A systematic well performance evaluation program was carried out following the procedure presented above to evaluate the performance of the first four wells. Correlation of results obtained from the data analysis would be of value for planning additional wells for further field development.

Pressure test design and conduct

The primary goal here is to predict time required for the late-time radial flow to develop. First, well productivity index (PI) estimate²³ and rate-time performance analysis¹⁴⁻¹⁵ were carried out to match the observed data. This sensitivity analysis was done using a range of the reservoir-well parameters. Although determining the reservoir and well condition from such an analysis is difficult, it is helpful for a pressure test design.

Based on the above analysis and a pressure test design, the late-time radial flow was anticipated to develop within a couple of days. Due to the well mechanical condition and cost considerations, surface shut-in and fluid level measurement were used in the buildup tests for Wells C-50, C-35, and C-48. The buildup data on Well C-29 were acquired using capillary tubing installed downhole. Overall, the quality of all test data were good. The late-time radial flow periods showed up within a reasonably short-time after shutin (one to two days). This is mainly dictated by the fairly high permeability of the reservoir (> 200 md). During testing, periodic data collection and analysis allowed the tests to be terminated at the optimal time.

Pressure test interpretation and well performance prediction

For each well test, the type curve match of the measured and modeled data are presented. The pressure integral technique³⁴⁻³⁵ was utilized to eliminate scattering and facilitate the type curve matching. The method was found to work well with the data. For each test, plots showing type curve matches of pressure, pressure integral and a Horner analysis are shown. It should be noted that the type curve match is based on the pressure integral function, and the non-smoothed plot of the pressure match is presented for reference purposes. Plots presenting the well performance prediction are also shown including both rate-time and cumulative production data for each well. The reservoir and well parameters computed from well tests and used in rate prediction are summarized in Tables 2 and 3. Figures 3-7, 8-12, 13-17, and 18-22, present data of Wells C-50, C-48, C-35 and C-29, respectively.

As observed in some of these figures, particularly for Well C-29, the early-time shutin data show some behavior typical of wellbore compressibility changes. This is not unexpected because of a significantly long wellbore which allows phase segregation during production and gas returning to solution during the pressure buildup. Also note that in all the tests, the producing times are relatively long compared to the shutin times. As a result, the drawdown type curves presented appear to be adequate to match the test data.

From the analysis, determining vertical permeability is uncertain because wellbore storage effect masked the early radial and linear flow data. However, from type curve matching, k_z can be inferred in the range of 0.005 to 0.11 of k_h using a thickness of 50 ft for all wells.

In general, the effective well length, L_{eff} , computed from the time match, can be used as a qualitative measurement, in conjunction with other parameters (L_D , skin), to evaluate the efficiency of a horizontal well. For Wells C-50 and C-48, the computed effective well lengths, L_{eff} , are close to the actual well lengths, L . On the other hand, L_{eff} computed for Wells C-35 and C-29 are only a half and a third of the actual length, L , respectively. It should be noted that, the actual well length of each well is determined from the MWD gamma-ray data and confirmed with the mud log data.

The dimensionless well length, L_D , is a measurement of how effectively a horizontal well drains the vertical direction. The larger the value of L_D the more predominant the linear flow is and thus more fluid can be withdrawn for the same drawdown. As shown in Ref. 7, a horizontal well with a $L_D > 25$ would behave similarly to that of a fractured well ($t_D > 10$). On the other hand, as shown by Ref. 25, a horizontal well with L_D of 0.5 would behave similarly to that of a vertical well. For our wells tested, the computed L_D values vary from 0.8 (C-50) to as high as 3 (C-48). The L_D values computed suggest these wells perform as well as expected from a horizontal well standpoint. Although having similar actual lengths, Well C-50 shows a low L_D value compared to that of C-48 or even C-35. Assuming k_f/k_h is similar throughout, this possibly means Well C-50 actually drains a thicker sand than that associated with C-48 or C-35. This speculation seems in agreement with the larger flow capacity value of Well C-50 compared to those of C-35 and C-48. Similarly, the longer actual length and large flow capacity computed for C-29 could mean its effective well length would be short and/or the well drains a thicker sand.

Strictly speaking, mechanical skin effect to horizontal wells can only be obtained with high confidence from analyzing the early radial flow data. Because wellbore storage effect masked these data in all tests analyzed, the model match and a comparison of the magnitude of the pseudoskin value obtained from the late-time radial flow semilog analysis are relied on to identify damage. In the modeling type curve match for all tests, zero skin damage was used. From the semilog analysis for the late-time radial flow, all wells exhibited large negative values for pseudoskin factor computed from the late-time semilog analysis. This leads to the conclusion that formation damage to the wells was unlikely. From these well tests, no boundary effect nor depletion was observed. Average pressure in each well drainage area was obtained by extrapolating the semilog straight line of the late-time radial flow to infinite shutin time.

Once the pressure transient data were analyzed, the same parameters were used to make rate-time performance predictions. For the most part, all parameters from well tests were kept the same, especially the horizontal effective permeabilities and well lengths. Table 3 presents the parameters used in the rate prediction for all wells. The

drainage areas shown in this table are large compared to the actual physical reservoir limits. This is believed to be the result of the inability of analytical models to account for fluid property changes and the non-uniqueness problem in general. While it is impossible to attach any physical meaning to the drainage areas shown, it is not so critical since good rate prediction still can be made. In addition to predicting well performance, theoretical PI's for all wells were computed using the parameters obtained from the well tests data, and compared to the observed PI's. This was done to further confirm the well test model interpretation and to compare the well performance to that of a vertical well under similar conditions. Table 4 presents the PI comparison for all wells.

Simply based on improving productivity over vertical wells, all cases show the use of horizontal wells is more favorable than that of vertical wells with productivity at least one and a half times better. A correlation of the actual well productivity index varying with the actual well length is presented in Figure 23. The solid line shown is the least-square fit straight line for the first four wells. Following the success of these wells, additional wells were drilled in the same zone of the field. The actual PI data of the two new wells C-30 and 40 are also shown in Fig. 23. As observed, the PI-well length correlation drawn from the first four wells also fit well with the additional wells. A correlation of cumulative oil recovery with well length for these wells is also presented in Figure 24. As expected, the longer the well length the more oil is recovered. It is also noted that the lengths of the first four wells were dictated by the reservoir limits and well control. Following these first four wells, additional wells are all longer, in excess of 3000-ft displacement.

Field X - Low Permeability

Background

The horizontal well application in this case is to improve reserves by increasing wellbore contact with the tight formation, by intersecting more fractures and by reducing water production. The well was completed with a slotted liner for about 2000-ft horizontal pay. The well was on production for about four months and made little water prior to the pressure test.

Pressure test design and conduct

Based on a modeling attempt, a test design was done to anticipate the sufficient shutin time for the buildup test. Unlike the previous example, little was known about this formation. For example, pay thickness is estimated to be in the range of 30-150 ft and permeability is guessed to be rather low. Figure 25 presents an attempt to match the well performance data to that predicted from the model assuming

certain reservoir properties. A low permeability of about 0.3 md and a thickness of 30 ft were used in the model. Based on the modeling results and the well mechanical condition, the test was planned for about a week and conducted by employing surface shutin and downhole capillary tubing for pressure recording. As before, data were periodically collected and reviewed during testing to allow the test to be terminated at the optimal time. The early-time radial flow period showed up after about ten days due to significant storage effect and low permeability. During the test, it was recognized that longer test time may be helpful to reduce the non-uniqueness problem, the test was terminated at about eleven days for cost saving, with the realization that good quality rate-time data was available for confirmation of the type curve match. This example clearly demonstrates the importance of using available horizontal well rate data in enhancing the pressure test analysis, especially for low permeability reservoirs.

Pressure test interpretation and well performance evaluation

Figure 26 presents the pressure match of the observed data onto the modeled results. Figure 27 shows a Horner plot of the pressure test. Figures 28 and 29 present the rate performance and cumulative oil recovery of the well with the modeled and actual data. Results obtained from well test and well performance analyses are summarized in Table 5.

Although the pressure buildup data did not reach the linear flow nor late-time radial flow data which could pose non-uniqueness problem for test interpretation, the uncertainty in analyzing the pressure test data is greatly reduced with the rate-time history matching. The rate-time performance analysis involves iteration varying horizontal and vertical permeability as well as thickness. Again, the use of horizontal well modeling is the only recourse to analyze the test data to achieve the test objectives. From modeling, the apparent radial flow period observed from the test is identified as the early-radial flow period rather than the late-time flow period. The Horner analysis on the early radial flow data provides an independent way to obtain vertical permeability and skin factor and confirm the model type curve match results. The final match presented is the best match confirmed using the three analysis techniques: modeling type curve match, semilog, and rate-time performance analyses.

From the combined analysis, horizontal effective oil permeability is 0.11 md assuming a 90-ft thick pay zone. The thickness used is confirmed by the rate-time analysis. Vertical permeability of nearly 0.01 md is determined. The effective well length, L_{eff} , is computed as 1759 ft, or about 87 per cent of the actual completed length of 2000 ft.

For horizontal wells, it is sometimes difficult to estimate how much the actual pay thickness the well drains. For this well, it

has been suggested that thickness can vary from 30 ft to 150 ft. One of the pressure test objective was to estimate the pay zone thickness. Although there is no clear evidence of the early-time linear flow in the pressure data that may help estimate thickness, the combined effort of buildup test analysis and rate-time performance evaluation used in this work, yields the thickness estimate of 90 ft with certainty.

As mentioned, mechanical skin damage to horizontal wells can only be obtained with high confidence from analyzing the early radial flow data. This test is one of a few horizontal well tests observed where the early radial flow is evident. Although wellbore storage effect partially masked the early-time radial data, results from both the model type curve match and Horner analyses indicate decisively the well is undamaged. No boundary effect nor depletion was observed from the well test data. Extrapolation of the early-time radial flow data in Fig. 27 to infinite shutin time yields a pressure of 3092 psia.

Based on parameters obtained from the well test and well performance analyses, rate prediction was made assuming a 101-acre square drainage area (2100ft x 2100ft). Results presented in Figs. 28-29 show good matches of the observed and modeled data for the time period following the buildup test. Even so, due to certain limitations of analytical modeling as noted above, periodic updating production data to observe the model match was exercised. As before, the theoretical well PI was also computed and compared to the actual PI to confirm the well test model data and compare the well performance to that of a vertical well. Results show the actual and computed PI are 0.053 and 0.04 stb/d/psi, respectively. Simply based on PI improvement, results also indicate the horizontal well PI would be about five times that of a vertical well. Based on this and other parameters computed ($L_D=3$; $L_{eff} = 0.87 L$; skin=0), this well is an effective horizontal well.

DISCUSSION

The methodology presented utilizes the analytical solutions to analyze pressure transient data and predict horizontal well performance accurately over several field examples. The success of the methodology in predicting rates is in part due to (i) the little production of water and (ii) the not so large changes in the effective oil permeability. In fact, three buildup tests were run on Well Dos Cuadras C-29 over the years. Results indicated some changes in the effective oil permeability and effective well length computed (Table 3). However, these changes are not significant enough to impact the long-term rate prediction (Figs. 22-23). In cases wherein significant changes in the system compressibility and/or large changes in relative permeability due to significant multiphase flow effects are expected, numerical simulation may be required. Even in these cases, the analytical approaches and the methodology proposed can still be used for shorter-term prediction by periodic testing.

CONCLUSIONS

The following generic conclusions are warranted:

1. A systematic procedure to evaluate horizontal well performance has been presented. The procedure coupling the use of pressure transient testing and rate-time data analysis is a practical and reliable method to predict long-term well rates.
2. Rate-time data analysis is helpful when coupling with pressure test interpretation for horizontal wells, especially for low permeability and unknown formation thickness. This is because (i) the many parameters involved in the pressure analysis may hinder the uniqueness of the pressure test interpretation alone and (ii) testing time limitations often prohibit a desired longer test.
3. Field test examples pertaining to a wide range of reservoir and well conditions are shown and discussed in detail. Results show that the procedure is effective and reliable to predict horizontal well performance.

On the particular tests considered, the following specific conclusions are drawn:

4. The efficiency of horizontal wells can be identified by evaluating parameters obtained from pressure and rate-time data analyses. Parameters such as effective permeability, well length, dimensionless well length, PI and PI ratio, and oil recovery can be identified from such an analysis.
5. For our test data, despite the magnitude of the formation permeability, a horizontal well with a dimensionless well length in the order of 2 to 3 is achievable and effective as a horizontal well application.
6. For the wells tested, the suggested procedure can be performed effectively using analytical approaches. Certain limitations on the use of these models are noted.

ACKNOWLEDGEMENT

We are indebted to Unocal Corporation for its permission to present this work.

REFERENCES

1. Reiss, L.H.: "Production From Horizontal Wells After 5 Years," JPT Nov. 87, 1411-1416.
2. Murphy, P.J.: "Performance of Horizontal Wells in the Helder Field," JPT Jun. 1990, 792-800.
3. Broman, W.H., Stagg, T.O. and Rosenzweig, J.J.: "Horizontal Well Performance at Prudhoe Bay," JPT Oct. 92, 1074-1080
4. Mueller, M.D., Quintana, J.M. and Bunyak, J.M.: "Extended-reach Drilling from Platform Irene," JPT Jun. 91, 138-44.
5. Clonts, M.D. and Ramey, H.J., Jr.: "Pressure Transient Analysis for Well with Horizontal Drain Holes," paper SPE 15116 presented at the 1986 California Regional Meeting, Oakland, April 2-4.
6. Goode, P.A. and Thambynayagam, R.K.M.: "Pressure Drawdown and Buildup for Horizontal Wells in Anisotropic Media," SPEFE Dec. 87, 683-97; Trans., AIME, 283.
7. Ozkan, E., Raghavan, R., and Joshi, S.D.: "Horizontal Well Pressure Analysis," SPEFE (Dec. 1989) 567-75; Trans., AIME, 287.
8. Rosa, A.J. and Carvalho, R. de S.: "A Mathematical Model for Pressure Evaluation of Infinite-Conductivity Horizontal Well," SPEFE Dec. 89, 559-566.
9. Daviau, F., Mouronval, G. and Bourdarot, G. and Curuchet, P.: "Pressure Analysis for Horizontal Wells," SPEFE Dec. 89, 716-24.
10. Odeh, A.S. and Babu, D.K.: "Transient Flow Behavior of Horizontal Wells: Pressure Drawdown and Buildup Analysis," SPEFE Mar. 90, 7-15.
11. Kuchuk, F.J., Goode, P.A. and Thambynayagam, R.K.M.: "Pressure Transient Behavior of Horizontal Wells with and without Gas Cap and Aquifer," SPEFE Mar. 91, 86-94.
12. Ozkan, E. and Raghavan, R.: "New Solutions for Well-Test-Analysis Problems: Part 1 - Analytical Considerations," SPEFE Sept. 91, 359-368.
13. Ozkan, E. and Raghavan, R.: "New Solutions for Well-Test-Analysis Problems: Part 2 - Computational Considerations and Applications," SPEFE Sept. 91, 369-378.
14. Ozkan, E.: "Performance of Horizontal Wells," PhD dissertation, U. of Tulsa, Tulsa, OK (1988).
15. Ohaeri, C.U. and Vo, D.T.: "Practical Solutions for Interactive Horizontal Well Test Analysis," paper SPE 22729 presented at the 1991 Annual Technical Conference

- and Exhibition in Dallas, Oct. 6-9.
16. Thompson, L.G., Manrique, J.L., and Jelmert, T.A.: "Efficient Algorithms for Computing the Bounded Reservoir Horizontal Well Pressure Response," paper SPE 21827, Rocky Mountain Meeting, 1991.
 17. Aminian, K. and Ameri, S.: "Predicting Horizontal Well Production Performance Using Type Curves," paper SPE 19342 presented at the 1989 Eastern Regional Meeting in Morgantown, WV, Oct. 24-27.
 18. Mutalik, P.N. and Joshi, S.D.: "Decline Curve Analysis Predicts Oil Recovery from Horizontal Wells," Oil & Gas Journal, Sept. 92, 42-48.
 19. Zagalai, B.M. and Murphy, P.J.: "Reservoir Simulation of Horizontal Wells in the Helder Field," JPT Aug. 1991, 906-913.
 20. Economides, M.J., Deimbacher, F.X., Brand, C.W., and Heinemann, Z.E.: "Comprehensive Simulation of Horizontal-Well Performance," SPEFE Dec. 91, 418-426.
 21. Giger, F.M., Reiss, L.H. and Jourdan, A.P.: "The Reservoir Engineering Aspect of Horizontal Drilling," paper SPE 13024 presented at the 1984 Annual Technical Conference and Exhibition, Houston, Sep. 16-19.
 22. Joshi, S.D.: Horizontal Well Technology, PennWell Books, Tulsa, Oklahoma.
 23. Babu, D.K. and Odeh, A.S.: "Productivity of a Horizontal Well," SPEFE Nov. 1989, 417-421.
 24. Kuchuk, F.J. and Goode, P.A.: "Inflow Performance of Horizontal Wells," SPEFE Aug. 91, 319-323.
 25. Gilman, J.R. and Jargon, J.R.: "Evaluating Horizontal vs. Vertical Well Performance," World Oil (April 1992) 67-72.
 26. Williams, E.T. and Kikani, J.: "Pressure Transient Analysis of Horizontal Wells in a Naturally Fractured Reservoirs," paper SPE 20612 presented at the 1990 Annual Technical Conference and Exhibition in New Orleans, LA, Sept. 23-26.
 27. Lichtenberger, G.J.: "Pressure Buildup Test Results from Horizontal Wells in the Pearsall Field of the Austin Chalk," paper SPE 20609 presented at the 1990 Annual Technical Conference and Exhibition in New Orleans, LA, Sept. 23-26.
 28. Zuber, M.D., Holditch, S.A., Deters, J.C. and Lee, W.J.: "A Practical Approach for Analysis of a Pressure Transient Test From a Horizontal Well in a Gas Storage Reservoir," paper SPE 22675 presented at the Annual Technical Conference and Exhibition in Dallas, TX, Oct. 6-9.
 29. Clark, G., Shah, P., Deruyck, B., Gupta, D.K. and Sharma, S.K.: "Horizontal Well Testing in India," Oilfield Review, Vol. 2, No. 3, 64-67.
 30. Domzalski, S. and Yver, J.-P.: "Horizontal Well Testing the Gulf of Guinea," Oilfield Review, April 1992, 42-45.
 31. Temeng, K.O.: "On the Interpretation of Horizontal Well Tests," paper SPE 21403 presented at the 1991 SPE Middle East Oil Show, Bahrain, Nov. 16-19.
 32. Sognesand, S.: "Testing of the Oseberg Gamma North Horizontal Well," paper SPE 25372 presented at the 1993 SPE Asia Pacific Oil & Gas Conference and Exhibition, Singapore, Feb. 8-10.
 33. Payne, J.D., Huston, C., and Bunyak, M.J.: "Field Results of Shallow Horizontal Drilling in Unconsolidated Sand, Offshore California," paper OTC 007020, presented at the 1992 Offshore Technology Meeting, Houston, May 4-7.
 34. Blasingame, T.A., Johnston, J.L. and Lee, W.J.: "Type Curve Analysis Using the Pressure Integral Method," paper SPE 18779 presented at the 1989 SPE California Regional Meeting, Bakersfield, April 5-7.
 35. Onur, M., Peres, A.M.M. and Reynolds, A.C.: "New Pressure Functions for Well Test Analysis," paper SPE 19819 presented at the Annual Technical Conference and Exhibition, San Antonio, Oct. 8-11.

NOMENCLATURE

B	= formation volume factor, rb/stb
c	= compressibility, 1/psi
C	= wellbore storage coefficient, bbl/psi
C_D	= dimensionless storage coefficient
h	= formation thickness, ft
k_h	= horizontal permeability, md
k_z	= vertical permeability, md
L	= actual well length (displacement), ft
L_{eff}	= effective well length (from well test), ft
L_D	= dimensionless well length
p	= pressure, psia
p_i	= initial pressure, psia
P_D	= dimensionless pressure
PI	= productivity index, stb/day/psi

**COUPLING PRESSURE AND RATE-TIME DATA IN PERFORMANCE ANALYSIS
OF HORIZONTAL WELLS: FIELD EXAMPLES**

8

SPE 26445

- PI(v) = vertical well productivity index, stb/day/psi
- PI(h) = horizontal well productivity index, stb/day/psi
- q = flow rate, stb/d
- r_w = wellbore radius, ft
- s = skin factor
- Δt = time, hrs
- t_p = producing time, hrs

DEFINITIONS

Dimensionless pressure, p_D

$$p_D = \frac{k_h}{141.2qB\mu} [p_i - p]$$

Dimensionless time, t_D

$$t_D = \frac{0.0002637kt}{\phi\mu c_v(L/2)^2}$$

Dimensionless well length, L_D

$$L_D = \frac{L}{2h} \sqrt{\frac{k_z}{k_h}}$$

Horizontal permeability, k_h

$$k_h = \sqrt{k_z k_v}$$

Vertical permeability, k_v

$$k_v = \sqrt{k_z k_h}$$

Dimensionless storage coefficient, C_D

$$C_D = \frac{5.615C}{2\pi\phi hc_v(L/2)^2}$$

APPENDIX

In this appendix, we present an example calculation for the well test presented. The data pertains to Field X.

From the model type curve matching,

$$\begin{aligned} [p_D/\Delta p]_M &= 3.5 \times 10^{-4} / \text{psi} \\ [t_D/\Delta t]_M &= 1.2 \times 10^5 / \text{hr} \\ L_D &= 2.7 \end{aligned}$$

From the pressure match,

$$kh = 141.2(162)(1.3)(0.96)3.5 \times 10^{-4} = 10 \text{ md-ft}$$

Using $h = 90$ ft from the rate-time analysis, $k_h = 0.11$ md.

From the time match,

$$L_{eff} = 2 \sqrt{\frac{0.0002637(0.11)}{0.249(0.96)1.32 \times 10^{-5}(1.2 \times 10^{-5})}} = 1759 \text{ ft}$$

From the L_D match,

$$\frac{k_z}{k_h} = \left(\frac{2hL_D}{L}\right)^2 = \left(\frac{2(90)(2.7)}{2000}\right)^2 = 0.06$$

This results in k_z of 0.007 md. If one uses L_{eff} instead of L in the above equation, one can obtain $k_z/k_h = 0.076$ and thus k_z of 0.008 md.

Using conventional Horner analysis for the early-radial flow period shown in Fig. 27, one can obtain vertical permeability.

$$k_v L = \sqrt{k_z k_h} L = \frac{162.6qB\mu}{m} = \frac{162.6(162)(1.3)(0.96)}{623.8} = 52.7 \text{ md-ft}$$

This results in $k_v L = 52.7$ md-ft. Using $L = 2000$ ft yields $k_v = 0.026$ md. Assuming k_v equal to k_h results in k_z of 0.006 md. [Using L_{eff} of 1759 ft and $k_h = 0.11$ md yields $k_v = 0.03$ md and $k_z = 0.008$ md.] In addition, using the conventional skin equation for Horner analysis yields skin estimate of -0.6.

Results obtained from the pressure type curve match, rate-time modeling and semilog analyses appear to be in agreement and complete the determination of the objective parameters to enhance the evaluation of the horizontal well under study. Without using one or the other, it would be difficult to obtain the full set of reservoir-well properties as such, especially for this low permeability reservoir encountered.

TABLE 1

DOS CUADRAS RESERVOIR & WELL DESCRIPTIONS

Reservoir pressure	=	350 psi
Reservoir temperature	=	85° F
Depth	=	850 ft
Porosity	=	0.3
Thickness	=	20-50 ft
Oil gravity	=	22° API
Oil FVF	=	1.03 rb/stb
Oil viscosity	=	43 cp
Compressibility	=	5×10^{-6} /psi
Wellbore radius	=	0.33 ft

Well	Completion Details			Data Before Shutting in			
	Date	Length ft	Zone	BU test	t_p hrs	Q_o stb/d	P_{wfs} psia
C-50	11/90	1223	C1P	1	7300	140	21.5
C-48	8/91	1047	CP	1	6200	130	33.4
C-35	5/91	730	C1P	1	8000	82	14.5
C-29	7/91	2900	C1P	1	192	200	272.6
				2	3720	400	117.7
				3	8760	330	76.2

TABLE 2

DOS CUADRAS HORIZONTAL WELL TEST RESULTS

Well	Test	Technique	k_{hh} md-ft	k_h md	k_z md	L_{eff} ft	L_D	C bbl/psi	s_t	p^* psia
C-50	1	Type Curve	41587	832	3.6	1166	0.8	0.29	---	---
		Semilog	43271	865	---	---	---	---	-4.3	136.8
C-48	1	Type Curve	13577	272	22.3	1047	3	0.23	---	---
		Semilog	18553	371	---	---	---	---	-5.5	210.3
C-35	1	Type Curve	18614	372	43.6	327	2.5	0.11	---	---
		Semilog	18570	371	---	---	---	---	-4.3	159.8
C-29	1	Type Curve	75045	1501	16	905	3	0.1	---	---
		Semilog	81400	1628	---	---	---	---	-5.5	320.7
C-29	2	Type Curve	67541	1350	6.4	783	2	0.12	---	---
		Semilog	69246	1385	---	---	---	---	-5.4	282.1
C-29	3	Type Curve	47466	949	4.5	1246	2	1.1	---	---
		Semilog	46416	928	---	---	---	---	-5.7	275.7

TABLE 3

DOS CUADRAS HORIZONTAL WELL PARAMETERS USED IN RATE-TIME PERFORMANCE PREDICTION

Well	L_{eff} ft	k_h md	k_z md	X_e ft	Y_e ft	P_i psia	P_{wf} psia	c_f $10^{-5}/psi$	skin
C-50	1166	832	83.2	6500	7500	136.8	21.5	1.5	0
C-48	1047	272	22.3	4000	4000	210.3	33.4	1.5	0
C-35	730	372	43.6	5000	5000	159.8	15	1	0
C-29	1246	950	24.5	5500	5500	275.7	76.2	2.2	0

TABLE 4

DOS CUADRAS HORIZONTAL WELL PI COMPARISON

Well	Computed		Observed	
	PI stb/d/psi	PI(h)/PI(v)	PI stb/d/psi	PI(h)/PI(v)
C-50	1.36	1.6	1.21	1.4
C-48	0.98	3.0	0.73	2.2
C-35	1.0	2.7	0.56	1.5
C-29	5.8	4.2	2.43	1.8

TABLE 5

RESERVOIR & WELL DESCRIPTION - FIELD X

Initial pressure	=	3000 psia
Depth	=	6000 ft
Porosity	=	0.249
Thickness	=	30-150 ft
Oil gravity	=	28° API
Oil FVF	=	1.3 rb/stb
Oil viscosity	=	0.96 cp
Total compressibility	=	$1.32 \times 10^{-5}/psi$
Wellbore radius	=	0.3 ft
Data before shutting in		
Producing time	=	3096 hrs
Oil rate	=	162 stb/day

WELL TEST AND RATE-TIME PERFORMANCE ANALYSIS RESULTS

Method/Technique	k_h md	k_z md	skin	P_i psia	L_{eff} ft	L_D	PI stb/d/psi	h ft
Well test analysis								
Type curve	0.11	0.008	0	3127	1760	2.7	0.054	---
Horner	---	0.006	-0.6	3092	---	---	---	---
Rate-time analysis	0.11	0.01	0	3127	2000	3.4	0.04	90

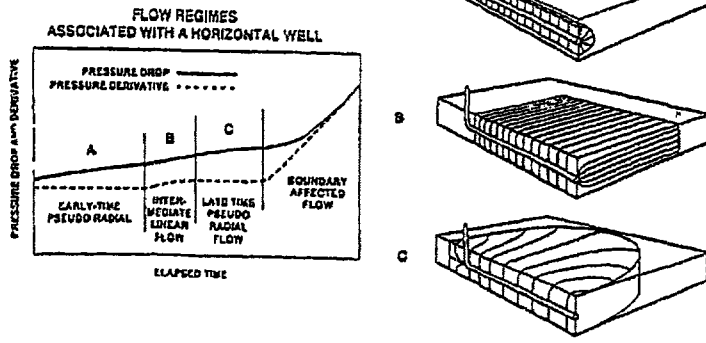
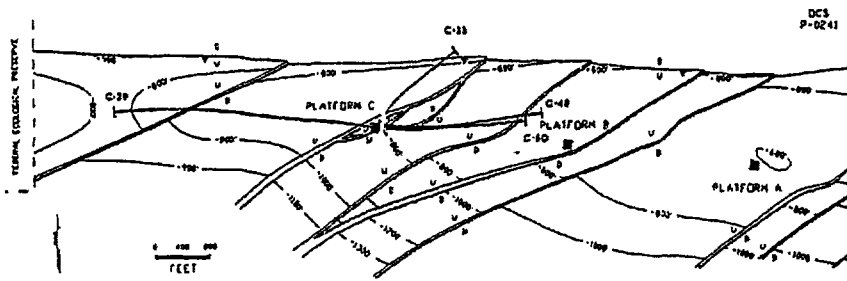


Figure 1 - Horizontal Well Flow Regime Identification



DOS CUADRAS FIELD ACTUAL WELL PATHS

Figure 2 - Map of Dos Cuadras Horizontal Wells

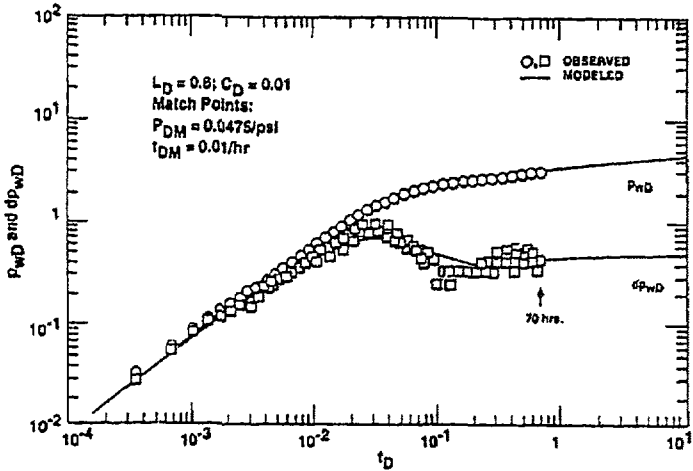


Figure 3 - Horizontal Well Pressure Buildup - Dos Cuadras C-50

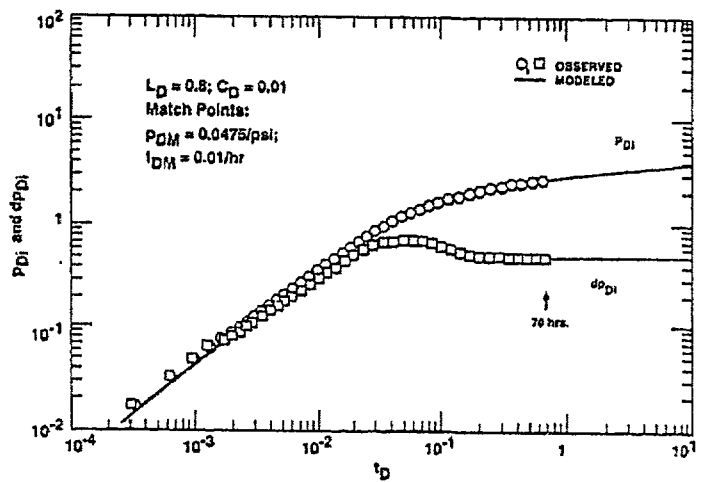


Figure 4 - Horizontal Well Pressure Buildup - Dos Cuadras C-50

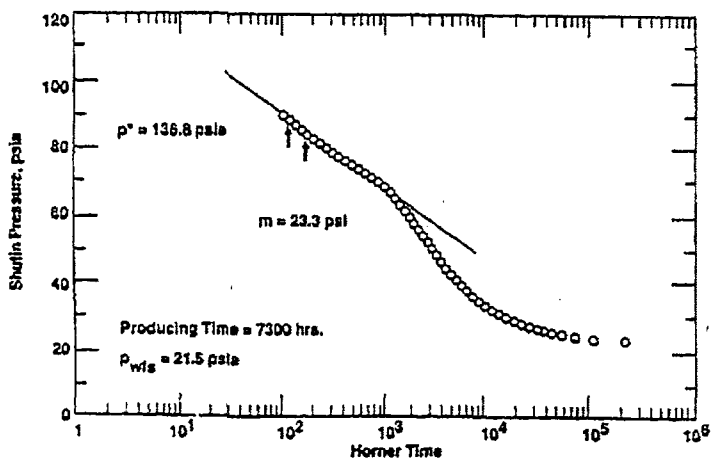


Figure 5 - Horizontal Well Pressure Buildup - Dos Cuadras C-50

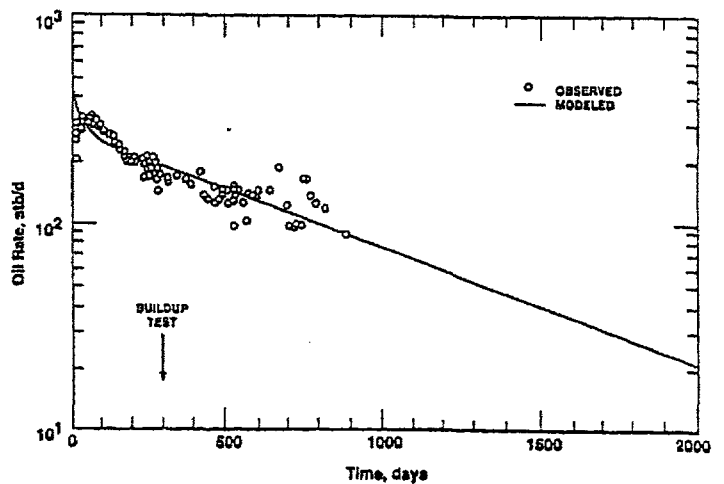


Figure 6 - Horizontal Well Performance - Dos Cuadras C-50

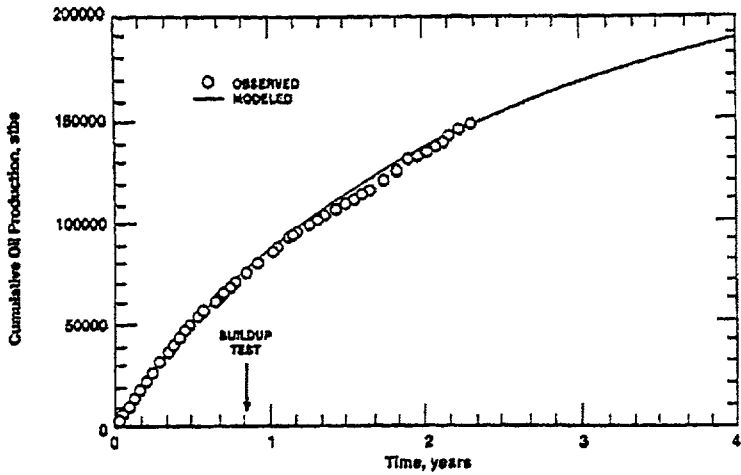


Figure 7 - Horizontal Well Performance - Dos Cuadras C-50

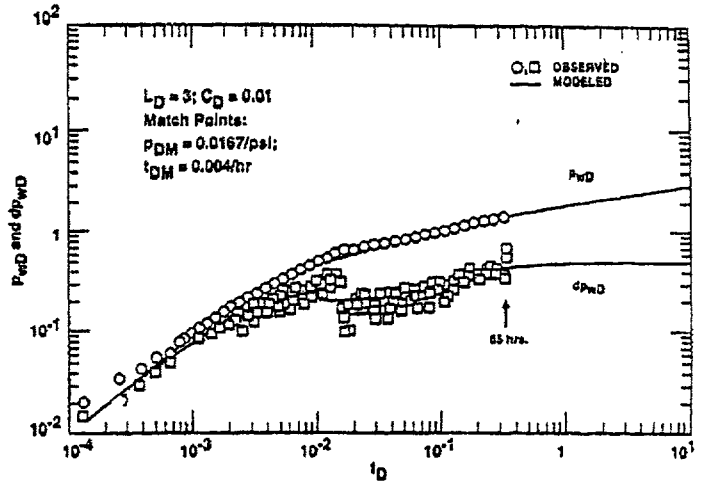


Figure 8 - Horizontal Well Pressure Buildup - Dos Cuadras C-48

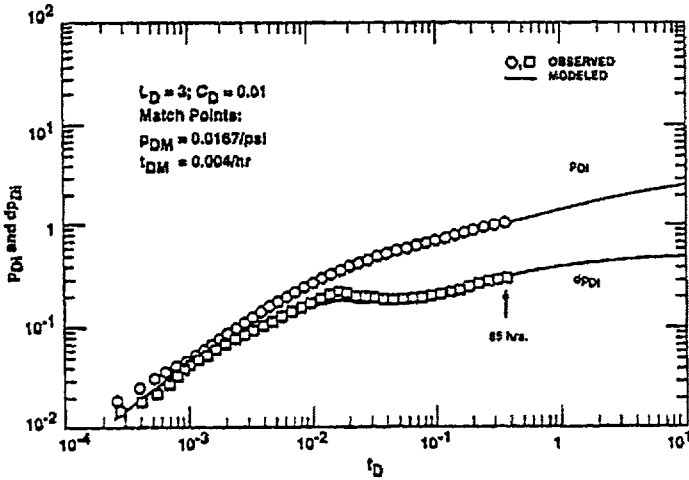


Figure 9 - Horizontal Well Pressure Buildup - Dos Cuadras C-48

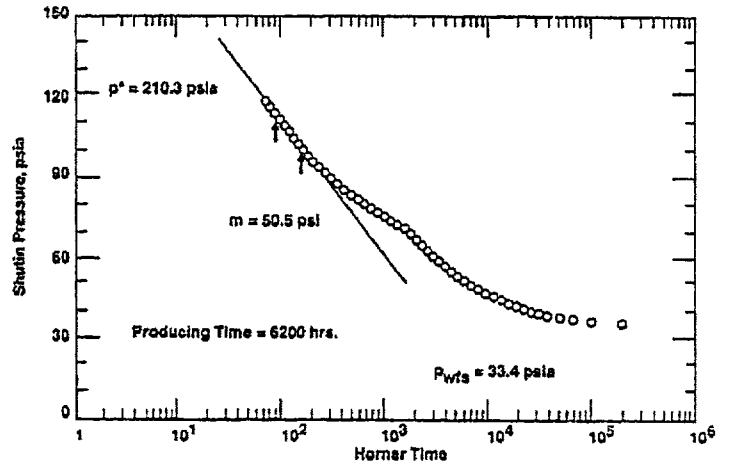


Figure 10 - Horizontal Well Pressure Buildup - Dos Cuadras C-48

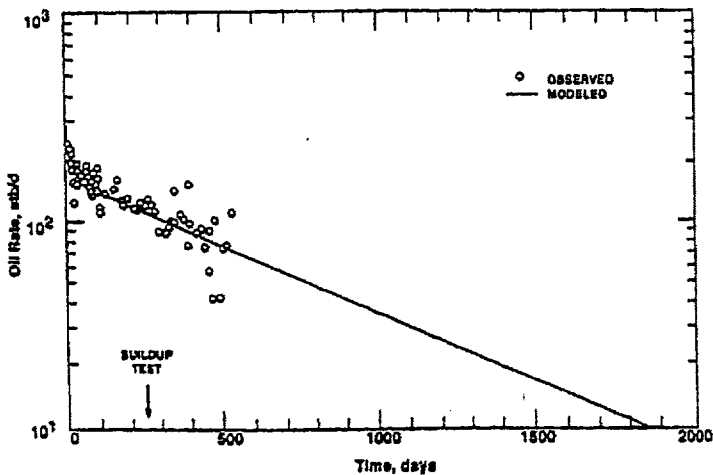


Figure 11 - Horizontal Well Performance - Dos Cuadras C-48

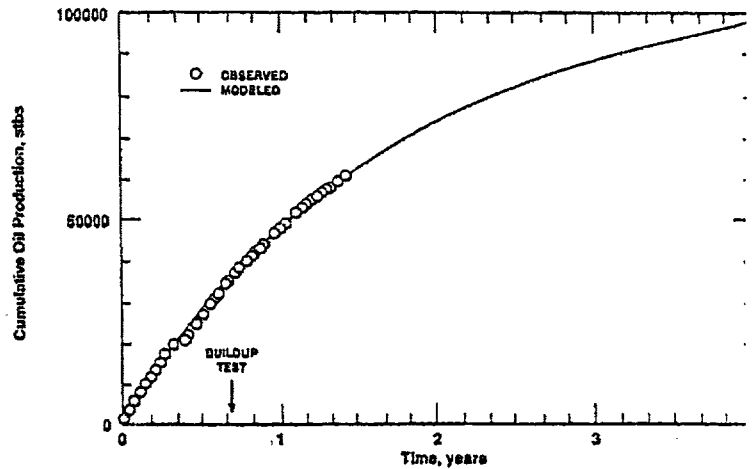


Figure 12 - Horizontal Well Performance - Dos Cuadras C-48

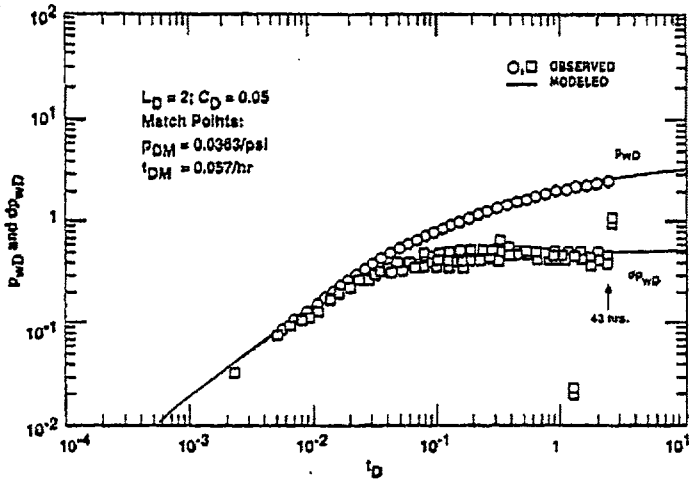


Figure 13 - Horizontal Well Pressure Buildup - Dos Cuadras C-35

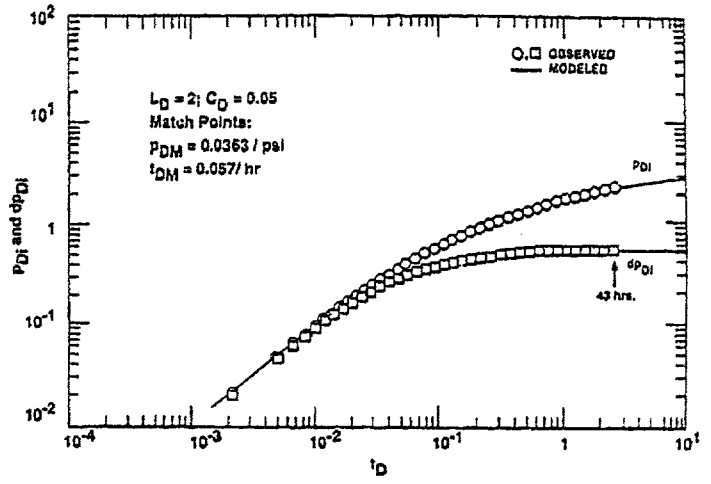


Figure 14 - Horizontal Well Pressure Buildup Test - Dos Cuadras C-35

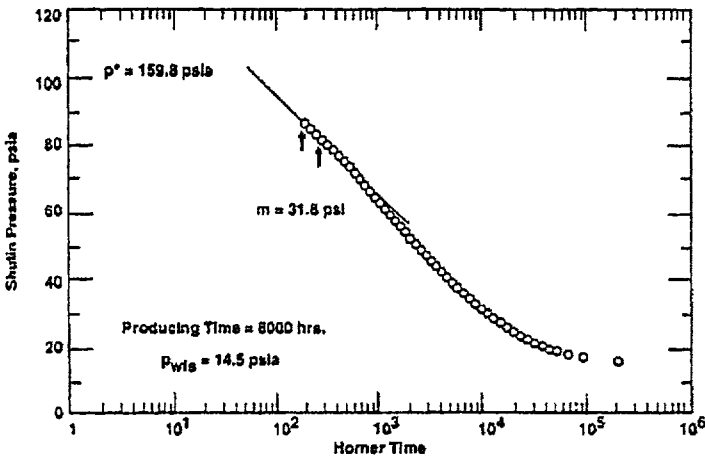


Figure 15 - Horizontal Well Pressure Buildup - Dos Cuadras C-35

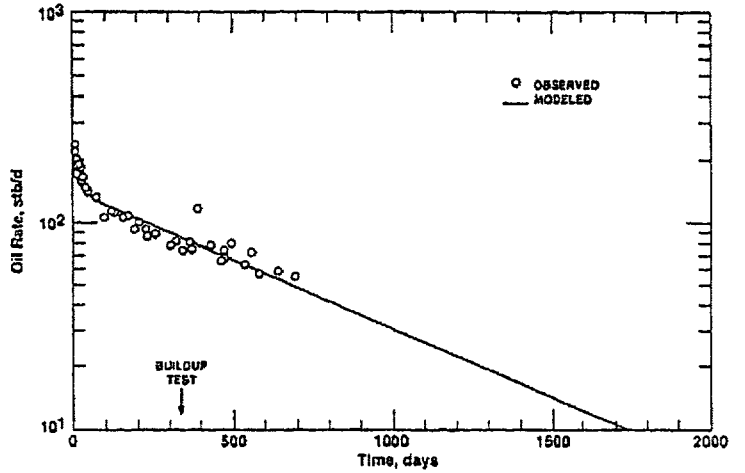


Figure 16 - Horizontal Well Performance - Dos Cuadras C-35

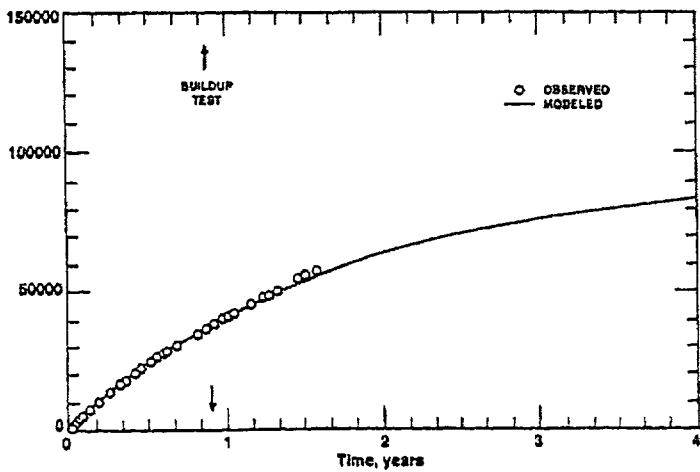


Figure 17 - Horizontal Well Performance - Dos Cuadras C-35

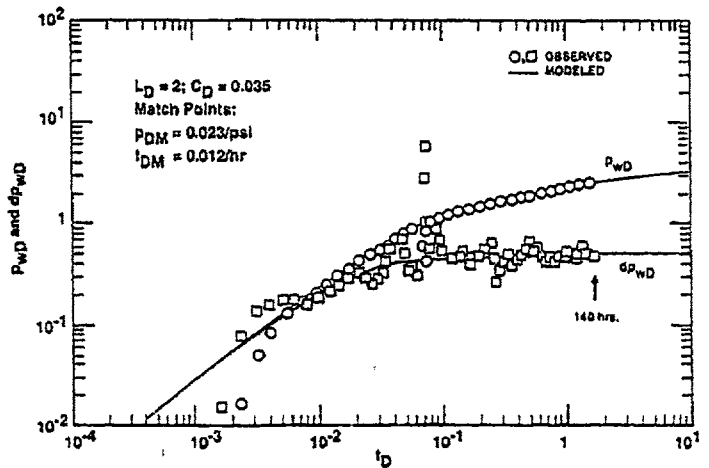


Figure 18 - Horizontal Well Pressure Buildup - Dos Cuadras C-29

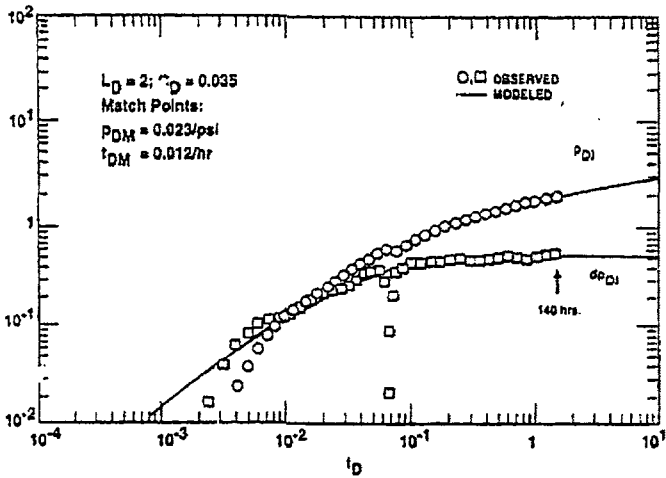


Figure 19 - Horizontal Well Pressure Buildup - Dos Cuadras C-29

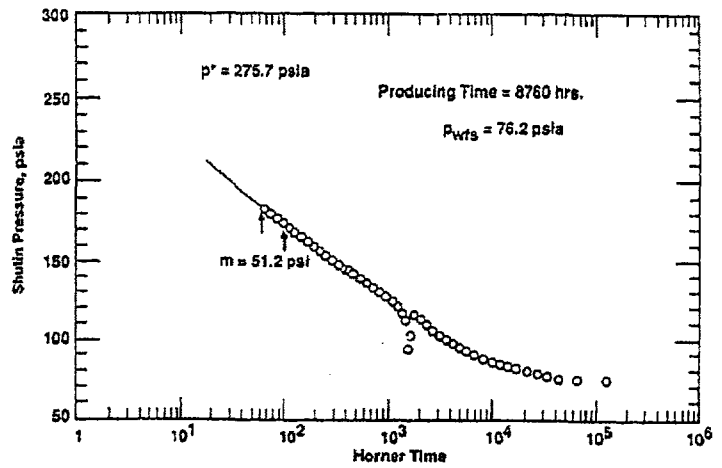


Figure 20 - Horizontal Well Pressure Buildup - Dos Cuadras C-29

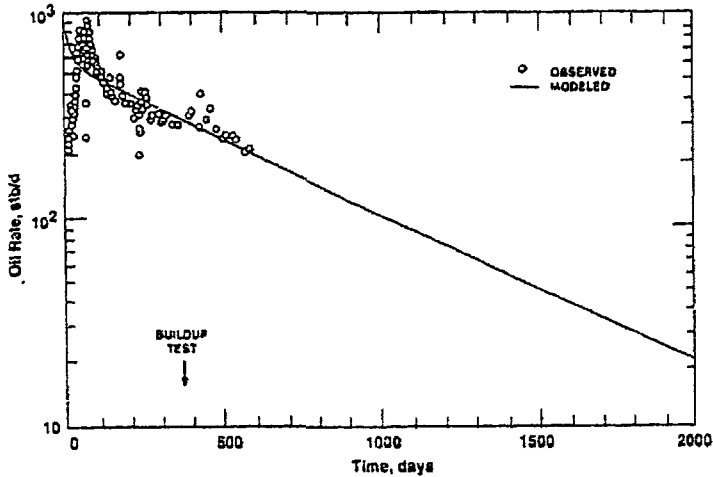


Figure 21 - Horizontal Well Performance - Dos Cuadras C-29

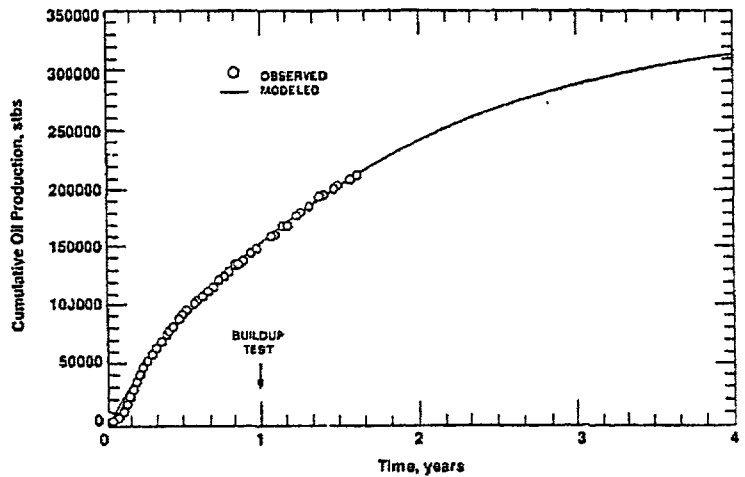


Figure 22 - Horizontal Well Performance - Dos Cuadras C-29

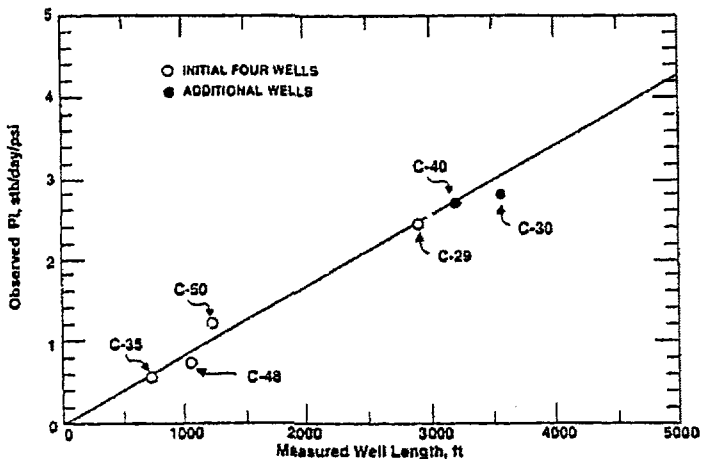


Figure 23 - PI Correlation of the Dos Cuadras Horizontal Wells

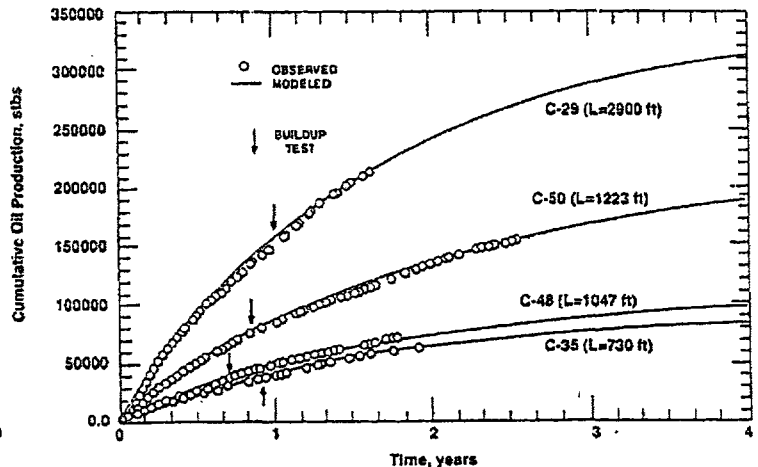


Figure 24 - Correlation of the Dos Cuadras Horizontal Well Performance with Well Lengths

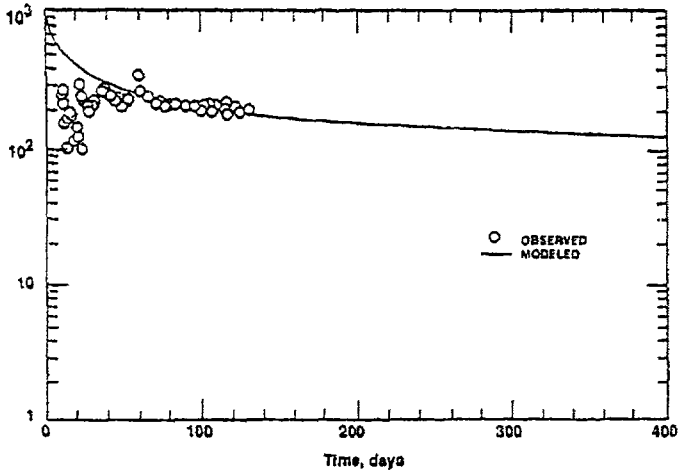


Figure 25 - Horizontal Well Performance - Field X

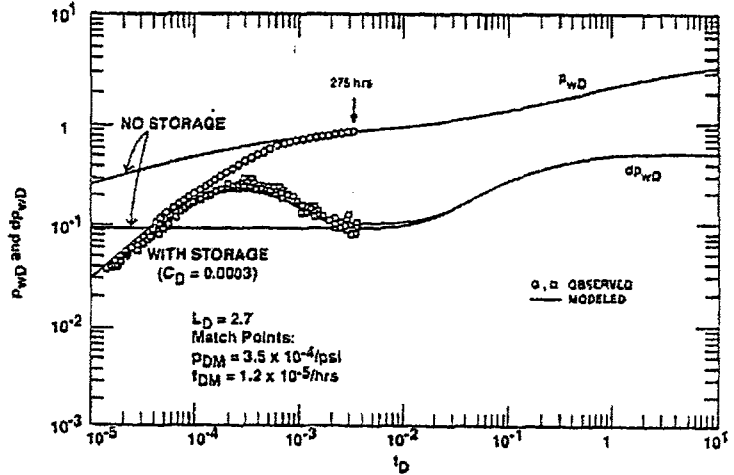


Figure 26 - Horizontal Well Pressure Buildup - Field X

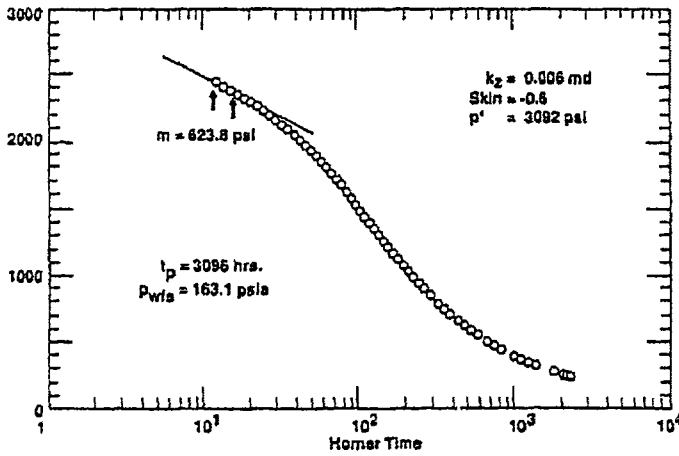


Figure 27 - Horizontal Well Pressure Buildup - Field X

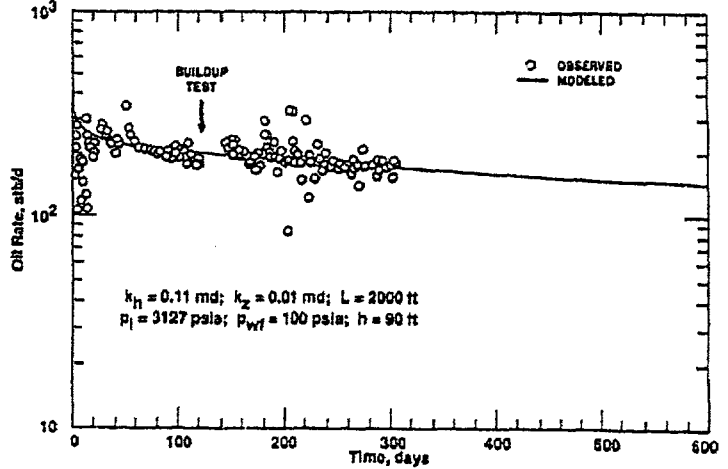


Figure 28 - Horizontal Well Performance - Field X

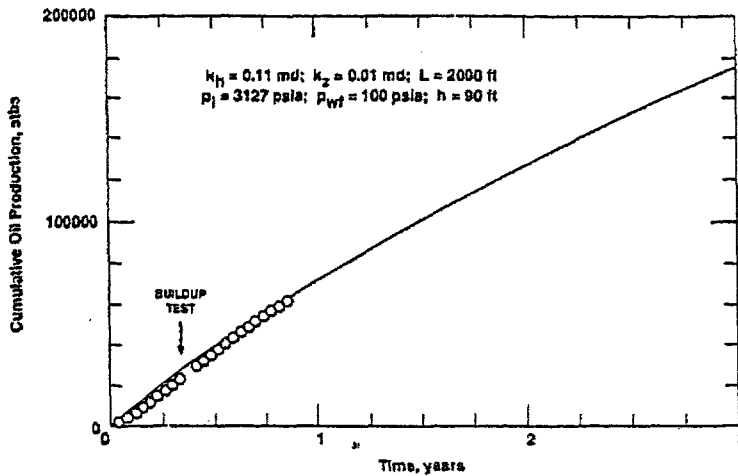
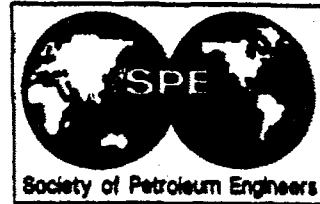


Figure 29 - Horizontal Well Performance - Field X



SPE 25567

Case Studies of Horizontal Well Design and Production Forecast

Ben Wang, B.N. Markitell, and W.S. Huang, Texaco Inc./EPTD

SPE Members

Copyright 1990, Society of Petroleum Engineers, Inc.

This paper was prepared for presentation at the SPE Middle East Oil Technical Conference & Exhibition held in Bahrain, 3-6 April 1993.

This paper was selected for presentation by an SPE Program Committee following review of information contained in an abstract submitted by the author(s). Contents of the paper, as presented, have not been reviewed by the Society of Petroleum Engineers and are subject to correction by the author(s). The material, as presented, does not necessarily reflect any position of the Society of Petroleum Engineers, its officers, or members. Papers presented at SPE meetings are subject to publication review by Editorial Committees of the Society of Petroleum Engineers. Permission to copy is restricted to an abstract of not more than 300 words. Illustrations may not be copied. The abstract should contain conspicuous acknowledgment of where and by whom the paper is presented. Write Librarian, SPE, P.O. Box 833636, Richardson, TX 75083-3636, U.S.A., Telex, 163246 SPEUT.

ABSTRACT

This paper presents the observed and predicted performance of horizontal wells in four fields: (1) heavy oil reservoir - to increase productivity and reduce gas coning, (2) thin oil column with gas cap and bottom water - to minimize gas and water coning, (3) waterflood in a tight oil sandstone reservoir - to increase injectivity/productivity, areal sweep efficiency, and improve pressure maintenance (4) gas reservoir with bottom water - to increase productivity and minimize water coning.

A special program, named "HVVWELL", was used in these studies to predict horizontal and vertical well production performance. HVVWELL requires minimal reservoir and fluid information to create a complete input dataset for running a finite difference simulator. It is equipped with a unique automatic grid set-up option to create correct grid geometry to model various horizontal well lengths and well locations. The geometries relate to GOC/WOC, and hydraulic fractures perpendicular to the horizontal wellbore. The options can greatly minimize the input errors and reduce grid requirements by simulating a symmetrical element instead of a full pattern. HVVWELL not only calculates well productivities, but also predicts 3-D, 3-P coning behavior for either vertical or horizontal wells. Short summary and graphical outputs are automatically generated for each run.

The horizontal well design and production predictions using HVVWELL will be discussed in detail, and compared to field data for each case.

INTRODUCTION

In the last few years, the number of horizontal wells drilled has substantially increased worldwide. Very encouraging field results are revealed and published in many papers.¹⁻⁴ The major

advantages of using horizontal wells are increasing productivities, minimizing gas and water coning, extending areal sweep, and connecting vertical fractures. To drill a successful and economical horizontal well for a specific reservoir requires state-of-the-art drilling/completion techniques, a detailed geologic/reservoir description study, and an optimal well design. The horizontal well design involves many aspects such as well length, location relating to GOC/WOC, spacing, and performance prediction compared to a vertical well.

In this paper, we exhibit the tool used within Texaco to design and evaluate horizontal wells. The applications for four field cases: (1) heavy oil, (2) severe gas and water coning reservoir, (3) oil reservoir with water injection, and (4) gas reservoir, are illustrated.

HVVWELL: A Tool For Horizontal Well Evaluations

The best tool to evaluate a vertical or horizontal well performance is a numerical simulator. Only the three-phase, three-dimensional, finite difference models can accurately model the sophisticated multiple-phase fluid flow around the wellbore. However, to setup a model for a reservoir simulation requires many input data including gas/oil and oil/water relative permeabilities, gas and oil PVT tables, grid dimensions for x, y, and z directions, well index, etc. The grid setup for a horizontal well is much more complicated than a vertical well. Using very fine grids to simulate horizontal well performance can be costly and time consuming, but using coarse grids may result in erroneous predictions. In addition, constantly changing the grid setup for various horizontal well lengths and vertical locations requires substantial manhours to optimize the horizontal well design.

A special program was generated to solve the simulator input problems for single well (vertical or horizontal) performance

predictions. This program, so-called "HVWELL", consists of three modules; a pre-processor (input panels), a single/dual porosity model, and a post-processor. The pre-processor requires minimum reservoir and fluid information to create a complete input dataset, with PVT and rock correlations, for running a single porosity (or dual porosity) simulator. An automatic grid set-up option is also built into HVWELL to create correct grid geometry for modeling various vertical and horizontal well length and well location relating to GOC/WOC, and hydraulic fractures perpendicular to the horizontal wellbore. Well block productivity indices for both vertical and horizontal wells are automatically calculated using the method of Peaceman⁵. These features greatly save man-time and cpu-time for the data preparation in reservoir simulation.

The simulator used in HVWELL is the VIP-ENCORE simulator developed by Western Atlas International. VIP-ENCORE is a three-phase, three-dimensional, single/dual porosity, fully-implicit (or IMPES) simulator. Results reported in this work were calculated using the fully implicit reservoir and wellbore pressure options. The pressure drop in the wellbore was assumed to be negligible in this study. The post-processor generates short summary and graphical outputs for each run.

HVWELL not only calculates well productivities in single or dual porosity reservoirs, but also predicts coning behavior for either vertical or horizontal wells. This program has been used within Texaco for horizontal well design and production forecast.

Figure 1 illustrates the 3-D cartesian grids generated by HVWELL for a 2,000 ft horizontal well in a 4,000 ft X 4,000 ft pattern. The 50-ft oil column is underlain by a 300 ft bottom water and overlain by a 50-ft gas cap. Due to the symmetry of the flow pattern, only one quarter (2,000 ft X 2,000 ft) of the drainage volume and one half of the horizontal well (1,000 ft) were simulated and shown in the figure. A total of 11 logarithmically spaced grid blocks are used in the x-direction, and 21 grid blocks are used in the z-direction. Constant Δz of 5 and 10 ft are assigned to the oil column and the gas cap, and Δz gradually increases in the aquifer region. The horizontal well is placed in parallel to the y axis, 35 ft below the original GOC. A total of 15 grid blocks are used in the y direction. The fine grid blocks used around the tip of the horizontal well are necessary to better define the gas/water cones and to monitor the fast pressure drop in the region. The well is located at $I=1$, $J=1-8$, $K=13$. A total of 3,150 grid blocks was used for this example.

In some reservoirs, the horizontal well penetrates the whole y-direction (horizontal well length would be equal to 4,000 ft in Figure 1). The ideal symmetrical shape of the cresting along the y axis simplifies the 3-D model to a 2-D xz model, which greatly reduces the computer time. In addition, HVWELL also generates cylindrical (r-z) grids for vertical well predictions if needed.

FIELD CASE STUDIES

Case 1: Heavy Oil Reservoir

The reservoir is an unconsolidated sandstone fault block in offshore shallow (200 ft) water. Average reservoir properties are shown in Table 1, and the structure map of the reservoir fault block is shown in Figure 2. Note that the reservoir is very shallow (700 ft subsea) and the total drainage area is about 30 acres. Vertical wells had been drilled in this fault block with commingled production from other zones. By the time the horizontal well was planned, the reservoir pressure had been depleted from the original of 369 psia to 280 psia. Since the oil viscosity is very high (39.8 cp), drilling a horizontal well was suggested to increase productivity.

HVWELL was used in this case for the purpose of (1) to compare the differences between a vertical well and a horizontal well, and (2) to conduct a history match with available horizontal well data and provide a production forecast.

Figure 3 illustrates a comparison of two horizontal well lengths (1270-ft and 635-ft) as well as a vertical well projection. The initial total (oil and gas) production rate of 1,200 RB/D and the bottomhole pressure limit of 50 psia were assumed for the horizontal wells, and the initial total production rate of 300 RB/D and the same bottomhole pressure limit of 50 psia were assumed for the vertical well. The vertical well projection rate was estimated by means of calculating the productivity improvement ratio.⁶ In this case, the horizontal well (1270-ft) was expected to increase productivity by a factor of 4.52 (a conservative factor of 4 was used in this study). The productivity improvement theory is discussed in Appendix.

The results reveal that higher and faster oil recovery can be obtained from drilling horizontal wells. This happens because pressure drawdown for horizontal wells is in general much lower than that of the vertical wells even though the production rates for the horizontal wells are higher. Therefore, for a unconsolidated formation, horizontal wells are more advantageous in that a small pressure drawdown can be utilized to produce a higher rate without the jeopardy of risking large amount of sand production. In addition, the longer horizontal well would have a much higher oil production rate.

A 1270-ft horizontal well was drilled and the production history was available. A production history match was made using HVWELL. After the model was set up, the oil production rates were used as input, and the gas-oil ratio and the calculated bottomhole flowing pressures were plotted against the observed data. Since water cut was less than one percent, the water production history match was neglected.

At the time the history match was made, only 300 days of production data was available. Figure 4 shows the oil history match. Excellent bottomhole flowing pressure history match

can also be observed in Figure 5. Note that high bottomhole flowing pressures were calculated as were observed. This indicated that very small pressure drawdown was required in the beginning of the horizontal well operation. The bottomhole flowing pressure was gradually reduced as can be seen in Figure 5. The gas-oil ratio history match is shown in Figure 6. Although the history match is not exact, it is believed that the model describes the production trend of this reservoir.

A production forecast was run using the last bottomhole flowing pressure of 50 psig after 300 days. Result of the oil production curve after 300 days was plotted in Figure 4 with additional production data. It can be seen that the production forecast matched with the field data closely. With this close history match and prediction, production potential of the fault block can be confidently established.

We may summarize the observations below:

- a) Horizontal wells can greatly improve productivity in a heavy oil reservoir. Longer horizontal well lengths result in higher oil production rates.
- b) The low pressure drawdown between a horizontal well and unconsolidated formations minimizes sand production problems.

Case 2: Thin Oil Column With Gas Cap And Bottom Water

This reservoir is located offshore in approximately 280 ft of water. The field is mature and has been on production since 1974. By the time the horizontal well was drilled, the reservoir pressure had been depleted from 2418 psia to 1800 psia. The reservoir properties are shown in Table I. A limited surface map, denoting the area of evaluation and relative position of the gas cap and the horizontal well, is shown in Figure 7.

The horizontal well technology was suggested as a means to improve oil recovery by increasing productivity and minimizing the severe gas and water coning in this area. Three concerns were raised in designing the horizontal well; (1) the optimum horizontal well length, (2) within the provided drilling window, what is the best vertical level for the well, and (3) what distance should the well be placed from the edge of the gas cap.

All sensitivities were run using the model as shown in Figure 8. Since the extent of the gas cap was limited, a half of the pattern (instead of a quarter of the pattern used in the other cases) was simulated. The gas cap is 60 ft thick and 1960 ft in length. The oil column is 100 ft gross and 35 ft net with varying sand/shale layers. The water column is 600 ft thick and provides the aquifer support which is evident from the field history.

A history match was done based on the performance of nearby wells (V1 and V2 in Figure 7) in order to verify the reservoir parameters to be used in the horizontal well projection cases. An 18 year history match was established which noted increasing gas-oil ratios and water cuts with time.

Various horizontal well lengths and vertical positions were evaluated to test the gas and water coning sensitivity. Well lengths of 500, 1400, and 2000 ft were positioned at the center of the oil column and 20 ft above/below the center for production comparisons. Additionally, the lateral position of the horizontal well with respect to the gas cap was reviewed.

Figure 9 shows a comparison case of various horizontal well lengths as well as a vertical well projection. These cases are for the horizontal well positioned at the center of the oil column. The maximum total (gas, oil and water) production rate of the horizontal wells was assumed to be 1,638 RB/D, which is three times that of the vertical well (Joshi's⁶ productivity ratio is 2.87). The results clearly show that all of the horizontal wells have higher, but faster declining oil rates compared to the vertical well. The longer the well, the longer the high oil production rate can be maintained. The oil rate of a 500-ft horizontal well drops below that of the vertical well after 1.5 years of production.

The results of the vertical position runs recommend that the horizontal well be located at or below the center of the oil column in order to maximize the oil rate and recovery. The model indicated that gas coning tendencies were more prevalent than water coning. The lateral position of the well did not, however, greatly affect the productivity. Figures 10-12 show a comparison case of a 1400-ft horizontal well located at the center and 20 ft below the center of the oil column.

A 1414 foot horizontal well was successfully drilled and completed slightly below the center of the oil column. The field results and projections are shown graphically by oil rate, gas-oil ratio, and water cut vs. time. Most notable are the greatly improved oil rates of the horizontal well cases over that of the vertical well as shown in Figure 10. The vertical and horizontal well performance data has been superimposed on the plot to assess the accuracy of the model. Production rates are 3 times that of the vertical wells.

The gas coning problems realized in the vertical wells can be seen in Figure 11 which shows the gas-oil ratio versus time. The projected GOR's of the vertical wells continue to increase with time and range from 5 to 7 times that of the horizontal well cases. The reduced pressure drop in the horizontal well in addition to the optimum placement helps to stabilize the gas cone and minimize gas production. As shown in Figure 11, the horizontal well placed 20 ft below the center of the oil column has a lower GOR than the one placed at the center.

The water coning problem realized in the vertical wells can be seen in Figure 12 which shows the water cut versus time. Water cut plots show an improvement in water production for horizontal wells. As can be seen in Figure 12, horizontal wells at the lower vertical position have a higher water cut than the case at the center of the oil column. Actual water production has been dropping even though one of the sand members penetrated was wet.

Several observations can be summarized below:

- a) Horizontal wells greatly reduce the gas and water coning problems seen in vertical wells.
- b) Horizontal wells outproduce conventional wells by a factor of 3 in this reservoir.
- c) Horizontal wells will increase recovery and reduce the number of development wells needed to effectively deplete this reservoir.
- d) Vertical position of the horizontal well had a greater influence on the well performance (especially coning) than the lateral distance away from the gas cap.

Case 3: Tight Oil Reservoir With Water Injection

The reservoir is a relatively tight (2 md) sandstone reservoir undergoing a waterflood expansion. It has a 45-year production history and is located at a depth of about 8000 ft. Average reservoir properties are shown in Table 1 and the structure map is shown in Figure 13. The production mechanism is natural water drive. However, water also has been injected into the reservoir to maintain the reservoir above its bubble point pressure. After 45 years of production and 40 years of water injection, the reservoir pressure has declined from 3560 psig to 2000 psig. Prior to 1991, the reservoir had two active vertical water injectors and six vertical oil producers which produced approximately 250 BOPD. The proposed horizontal wells are shown in the middle (producer) and the west side of the reservoir (injector). The objective of the horizontal oil producer was to accelerate oil production and to reduce the number of wells drilled. The objective of the horizontal water injector was to effectively maintain the reservoir pressure near 2000 psig.

In late 1990, a vertical producer, V-1 was drilled. The production data on V-1 was used for a history match study to properly tune the reservoir parameters. When the study was made in mid 1991, six months of the vertical well production data was available. A vertical well history match and prediction curve was established as shown in Figure 14. Subsequently, as more data became available, they were plotted on the same prediction curve. It can be seen that an excellent history match and production forecast for the vertical well was obtained.

Based on Joshi's productivity improvement equation, a 7.25-fold production rate increase should be observed in a 1500-ft horizontal well. Using a 6-fold maximum production rate limitation for a horizontal well, HVWELL was set up to run the horizontal well production forecast. The predicted oil production curve is shown in Figure 14 with the actual production data. Note that the actual oil rate is lower than predicted but the total fluid production matches the prediction reasonably well. Since no water production was expected, the total fluids establish the production potential of the horizontal well. In this prediction, water injection was not used and in reality the water injection in the horizontal injector was limited due to mechanical problems.

Several remedial actions were taken to restore water injection in this fast pressure decline reservoir. Figure 15 shows predicted oil production rate for some higher water injection to fluid production ratios. The total fluids production data are plotted with the prediction curve where no additional water injection was assumed. Water injection rates set to both one-half of the production value and the production value are also shown. Results indicate that with successful water injection the reservoir pressure is maintained, and high oil production rates of 450 BOPD can be expected from the horizontal well.

Several observations are summarized for this case:

- a) Productivity can be greatly increased (more than 6 fold) by drilling a horizontal well in a tight oil reservoir.
- b) Pressure maintenance is very important to keep the high production rate for the horizontal well.

Case 4: High Permeability Gas Reservoir With Bottom Water

The following example is located offshore. The proposed well was to be drilled in 250 ft of water for shallow (1700 ft TVD) gas bearing formations. Normal development would require extended-reach directional wells.

The sand is a high permeability, unconsolidated, middle Pleistocene sandstone. Logs showed 40 ft of gas on 110 ft of water in a nearby well. Depositional environment suggests that the sand is a bifurcating channel deposit. Figure 16 shows the structure map and position of the horizontal well.

A number of deeper horizons have been produced to depletion in the area which set up the opportunity to develop the shallow gas zones. High angle wells were drilled and successfully completed in intermediate levels. Due to the nature of the objective sand being thin with a water column, horizontal wells were considered a viable option to efficiently and effectively produce the gas reserves. Water coning had been a problem in other horizons and presented an interesting drilling and completion challenge.

In order to determine the appropriate recommendation for developing the gas reserves, several runs were made to investigate (1) horizontal well length effect on gas productivity, and (2) gas rate effect on water coning.

Figure 17 is a projection of various horizontal well lengths compared to that of a vertical well, all producing at a constant rate of 15 MMCF/D. The plot suggests that increasing horizontal well length improves the production capability to maintain higher rates for longer periods. Based on Joshi's equation, the productivity improvement ratio of the 300-ft horizontal well to the vertical well is 1.48, which is relatively less than those of the three previous oil reservoirs.

We must, however, look at water breakthrough times (see Table 2) and consider outflow performance in relation to tubular constraints. The horizontal well will delay the water breakthrough time substantially even for a 300-ft horizontal well.

Figure 18 expands on the 300-ft horizontal case and varies rate projections for that length. The actual horizontal well drilled reached a horizontal length of 310 ft and its production is also plotted on this figure. The well was brought on production slowly and gradually increased to a maximum rate of 18 MMCF/D. It is now being produced at a constant rate of approximately 14 MMCF/D. No water was produced over the production period of 645 days.

Should the well performance continue to track similarly to the projection, it is expected that water breakthrough will occur within the next year. This assumes that the well rate will be maintained at the 14 MMCF/D figure.

As mentioned earlier, there are restrictions due to tubing size and capacity to lift the water to the surface. The water-gas ratios as shown in Figure 19 are the model results and were not subjected to tubular constraints.

We may summarize the predictions as follows:

- a) In this case, the actual horizontal performance is tracking well enough to predict future water breakthrough time.
- b) Horizontal well length has an impact on rate and well performance.
- c) Horizontal wells delay water coning over that of vertical wells and often produce with lower water gas ratios.

CONCLUSIONS

This paper exhibits the early production data (1-2 years) of horizontal wells in three oil and one gas reservoir. The

advantages of using horizontal wells over vertical wells are shown, and the horizontal well design and production forecast are illustrated in each case. The main conclusions are listed as follows:

1. Performance prediction of horizontal wells can be accurately accomplished using finite difference simulators. A single well program, named "HVWELL", can automatically generate grid, rock and PVT data for simulators with minimal reservoir and fluid information. It was proven to be a robust tool for horizontal well design.
2. Horizontal wells showed great productivity improvement over vertical wells in the three oil reservoirs. The improvement ratios range from 3 to 6. However, the oil rate of horizontal wells generally declines much faster than that of vertical wells. The decline rate depends on the degree of pressure support and the horizontal well length.
3. Horizontal wells can effectively reduce gas and water coning. Carefully positioning horizontal wells between the GOC and WOC may maximize oil recovery by balancing gas and water coning.
4. In the high permeability gas reservoir, the short horizontal well not only increases the gas rate, but also greatly delays water breakthrough.
5. In order to accurately predict horizontal well performance, it is important to verify reservoir parameters (such as vertical/horizontal permeability ratio, relative permeabilities, etc) by history matching the adjacent vertical well performance.
6. Joshi's equation (or any other analytical equation) for calculating productivity improvement ratio (horizontal production rate/vertical well rate) can be used to predict the initial production rate for a horizontal well, if the production rates of the adjacent wells are available.

NOMENCLATURE

- h = net pay thickness, ft
 J_h = productivity of a horizontal well, STB/D/psi
 J_v = productivity of a vertical well, STB/D/psi
 K_h = horizontal permeability, md
 K_v = vertical permeability, md
 L = horizontal well length, ft
 r_e = external drainage radius, ft
 r_{eh} = external drainage radius for horizontal well, ft
 r_{ev} = external drainage radius for vertical well, ft
 r_w = wellbore radius, ft
 r_{we} = effect wellbore radius of a horizontal well, ft

ACKNOWLEDGEMENTS

The authors wish to express their thanks to Texaco and its management for permission to publish this paper. We thank Mr. Chester E. Hermes for his assistance in generating HVWELL panels, and also want to recognize members of Texaco Exploration and Production, East and West Regions, whose names are too numerous to mention, for their valued assistance and cooperation in this effort.

REFERENCES

1. Butler, R. M.: "The Potential for Horizontal Wells for Petroleum Production," Petroleum Society of CIM Paper No. 88-39-22, presented at the 39th CIM Annual Technical Meeting, Calgary, June 12-16, 1988.
2. Kossack, C. A. Kleppe, J., and Aasen, T.: "Oil Production From the Troll Field: A Comparison of Horizontal and Vertical Wells," SPE 16869, presented at the 62nd SPE Annual Technical Conference, Dallas, Texas, September 27-30, 1987.
3. Zaglai, B. M.: "Reservoir Simulation of Horizontal Wells in The Helder Field," SPE 19296 presented at Offshore Europe 89, Aberdeen, September 5-8, 1989.
4. Joshi, S. D.: "A Review of Horizontal Well and Drainhole Technology," SPE 16868 presented at the 62nd SPE Annual Technical Conference, Dallas, Texas, September 27-30, 1987.
5. Peaceman, D. W.: "Interpretation of Well-Block Pressures in Numerical Reservoir Simulation With Nonsquare Gridblock and Anisotropic Permeability," SPEJ, Vol. 23, June 1983, pp. 531-543.
6. Joshi, S. D., Horizontal Well Technology, 1991 PennWell Publishing Co.

APPENDIX

Productivity Improvement

Joshi's equation⁶ was used to account for the productivity and/or injectivity improvements over a vertical well.

Joshi's equation defines the productivity improvement of a horizontal well over a vertical well as:

$$\frac{J_h}{J_v} = \frac{\ln\left(\frac{r_{eh}}{r_w}\right)}{\ln\left(\frac{r_{eh}}{r_{wh}}\right)} \quad (1)$$

where J_h/J_v is the productivity improvement ratio. r_{wh} and r_{eh} are the external drainage radii for vertical and horizontal wells. We assume in this study that $r_{wh} = r_{eh} = r_e$, and

$$r_e = \sqrt{\text{Drainage Area} \cdot 43560/\pi} \quad (2)$$

r_w = effective wellbore radius, ft, of a vertical well, and r_{wh} is the effective wellbore radius of a horizontal well which is shown as,

$$r_{wh} = \frac{r_e(L/2)}{a[1 + \sqrt{1 - (L/2a)^2}][h\beta/2r_e]^{2\beta/L}} \quad (3)$$

h is thickness of the formation in feet and L is the length of the horizontal well, ft.

$$a = (L/2)[0.5 + \sqrt{0.25 + (2r_e/L)^2}]^{0.5} \quad (4)$$

$$\beta = \sqrt{\frac{K_h}{K_v}} \quad (5)$$

where K_h and K_v are horizontal and vertical permeabilities, respectively.

TABLE 1

SIMULATION INPUT VALUES				
Reservoir Properties and Description	Case 1	Case 2	Case 3	Case 4
Depth to Top of Formation, ft. subsea	700	4540	7965	1650
Initial Reservoir Pressure, psia	369	2418	3560	760
Connate Water Saturation, %	30	35	28	18
Reservoir Temperature, °F	88	133	216	91
Formation Thickness, ft - Gas, Oil, Water	0,65,0	60,100,600	0,30,0	40,0,110
Porosity, %	30	30.3	12	33
Permeability (horizontal), md	1150	810	2	6000
Permeability (vertical), md	115	16.2	1	600
Oil Gravity, °API	23.5	35	46.3	-
Oil Viscosity, cp	39.8	1.2	0.352	-
Gas Oil Ratio, SCF/STB	46	452	422	-
Bubble Point Pressure, psia	369	1975	1550	-
Formation Volume Factor, RB/STB	1.03	1.23	1.36	-
Joshi's Productivity Improvement Ratio ⁴	4.52	2.87	7.25	1.48
Horizontal Well Drainage Area, Acres	30.6	588	70.3	758
Drainage Area Dimensions, X & Y, ft	1040,1280	3200,8000	1320,2320	6000,5500
Horizontal Well Length	1270	1414	1500	310

TABLE 2

WATER BREAKTHROUGH TIME				
Rate (MMCF/D)	VERTICAL WELL	HORIZONTAL WELL		
		300 FT	500 FT	1000 FT
10	349 DAYS	1209 DAYS	NONE	NONE
15	29 DAYS	640 DAYS	724 DAYS	859 DAYS
20	12 DAYS	324 DAYS	415 DAYS	NONE

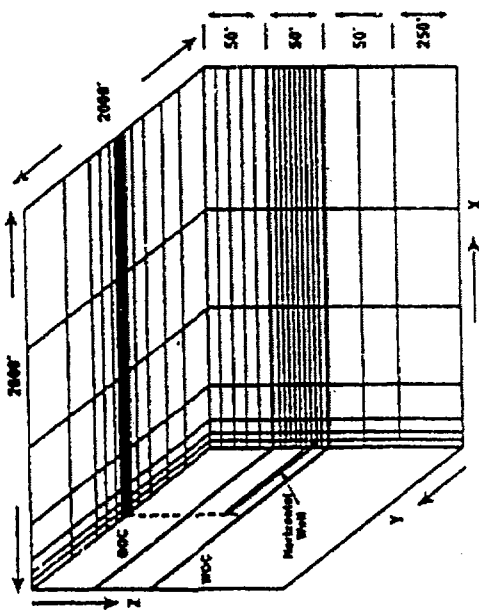


Figure 1
Grid dimension of 1/4 of horizontal well pattern

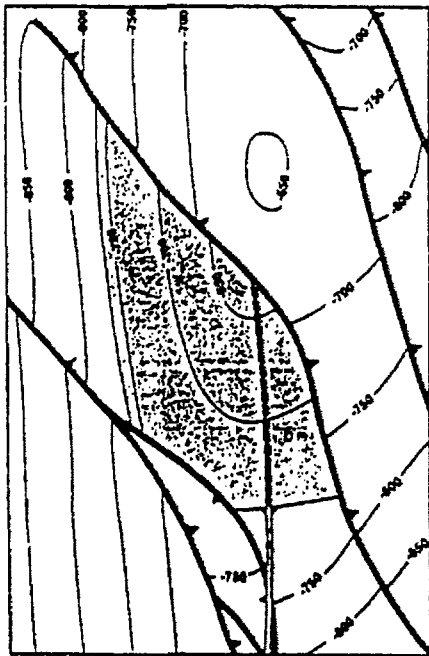


Figure 2
Case 1 - Structure map

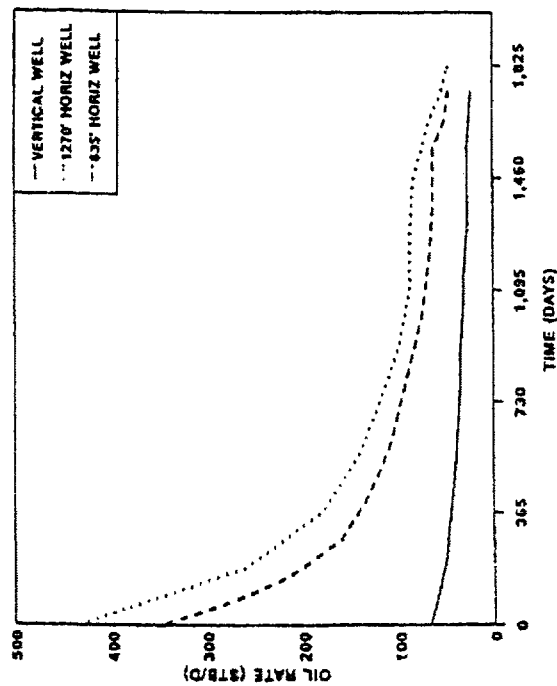


Figure 3
Case 1 - Oil rate projections for vertical & horizontal wells

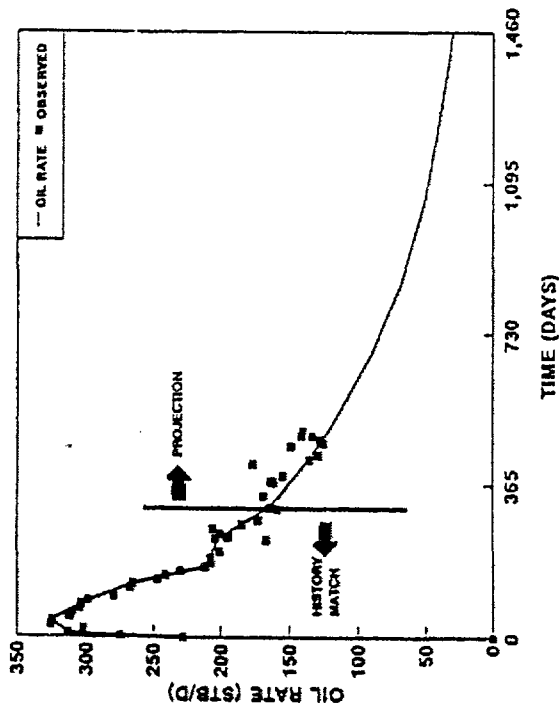


Figure 4
Case 1 - Observed & projected oil rates for 1270' horizontal well

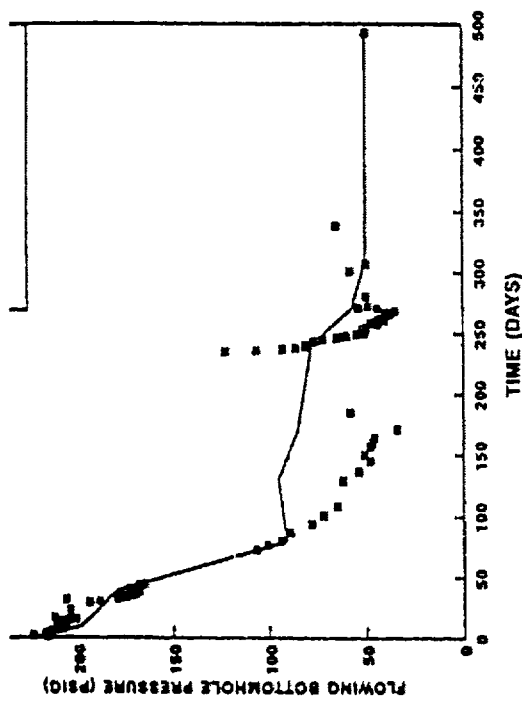


Figure 5
Case 1 - Observed & projected flowing
bottom hole pressure

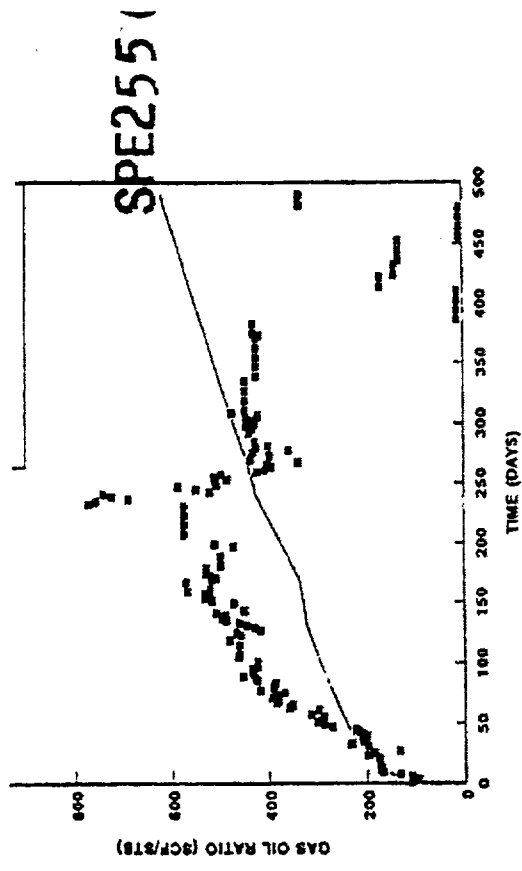


Figure 6
Case 1 - Observed & projected gas oil ratios

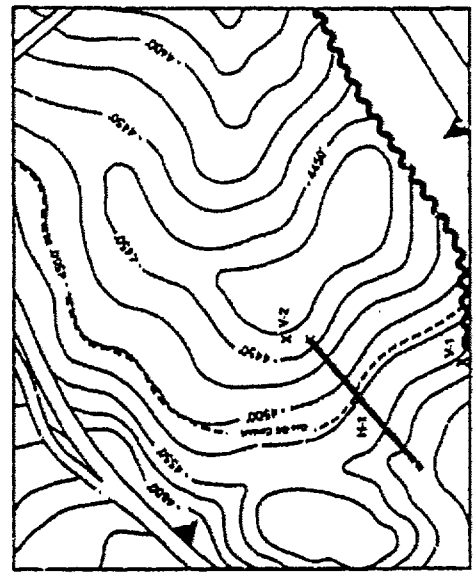


Figure 7
Case 2 - Structure map

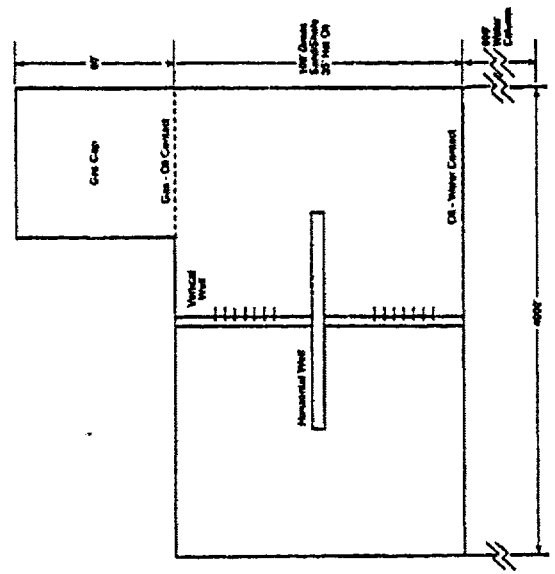


Figure 8
Case 2 - Model layout

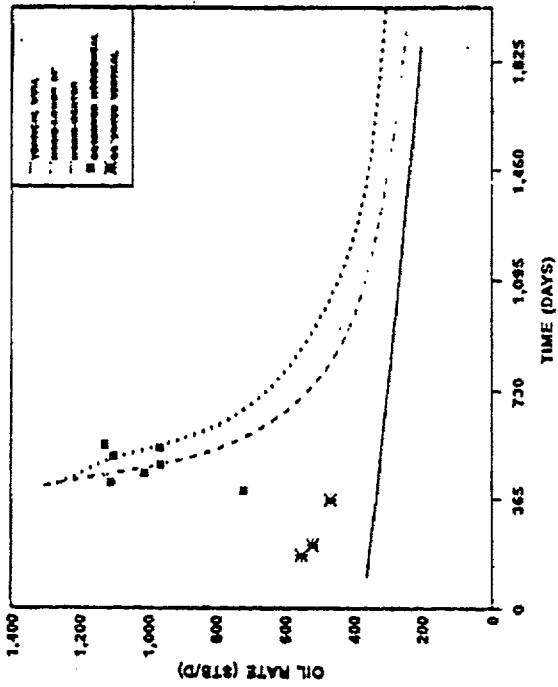


Figure 10
Case 2 - Observed & projected oil rates for vertical & 1400' horizontal wells

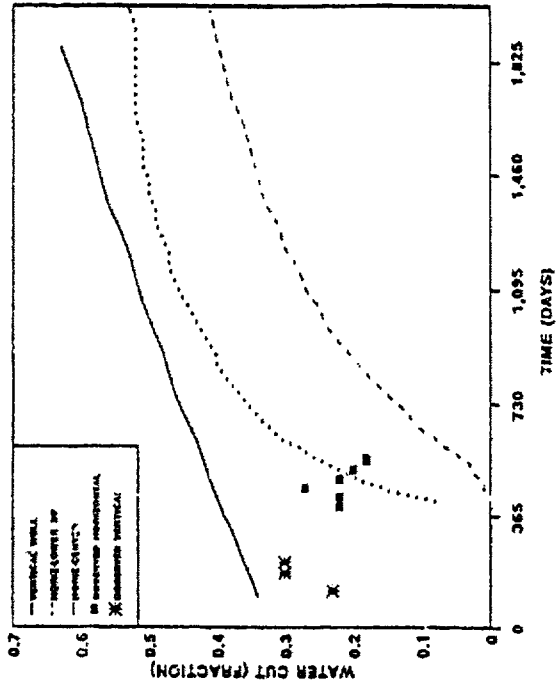


Figure 12
Case 2 - Observed & projected water cut for vertical & horizontal wells

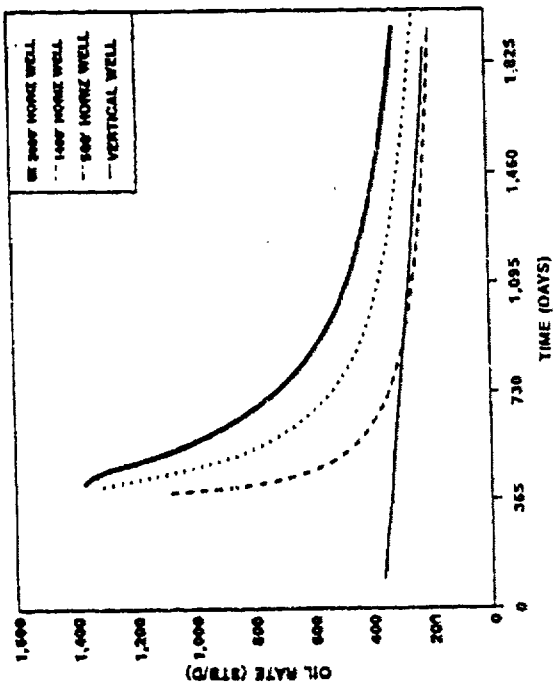


Figure 9
Case 2 - Oil rate projections for vertical and horizontal wells

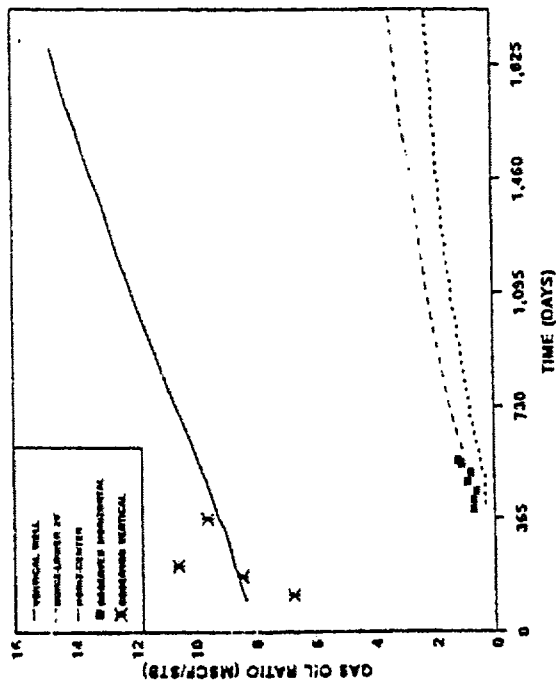


Figure 11
Case 2 - Observed & projected gas oil ratios for vertical & horizontal wells

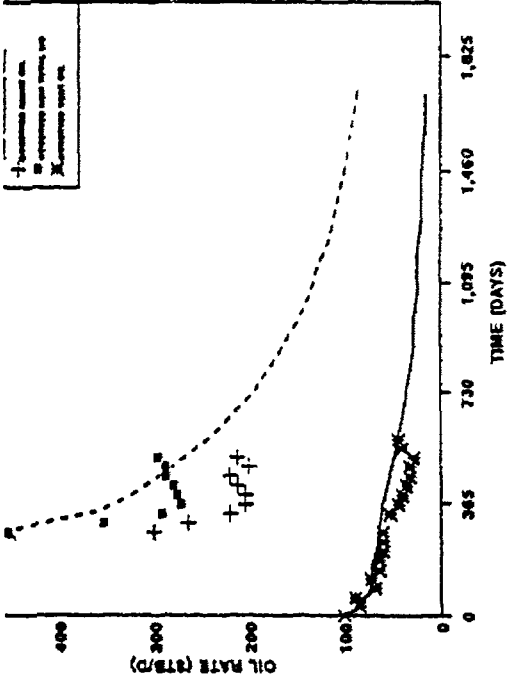


Figure 14
Case 3 - Observed & projected oil rates for vertical & 1500' horizontal well H-1

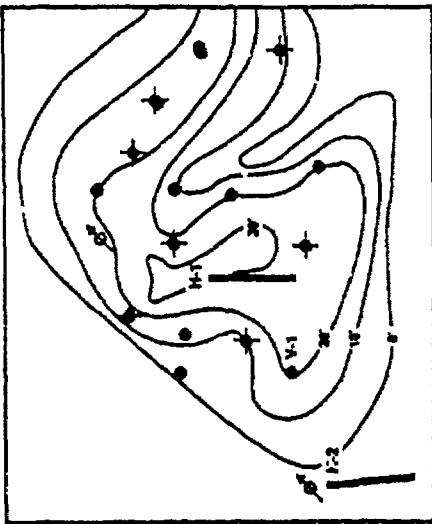


Figure 13
Case 3 - Structure map

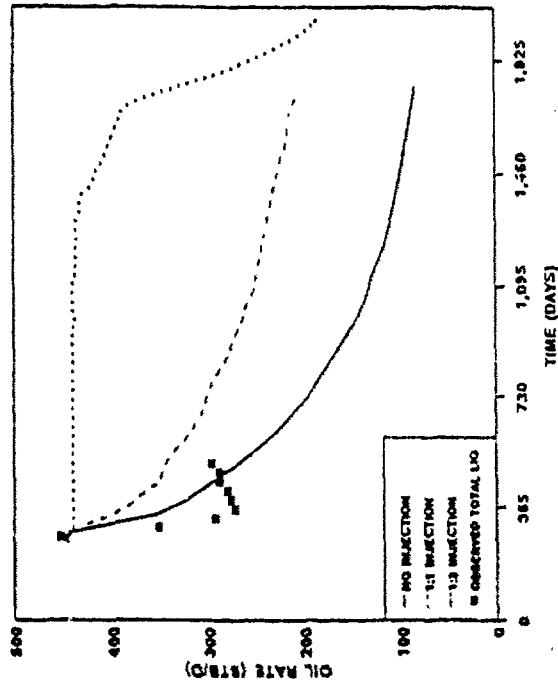


Figure 15
Case 3 - Oil rate sensitivity to water injection

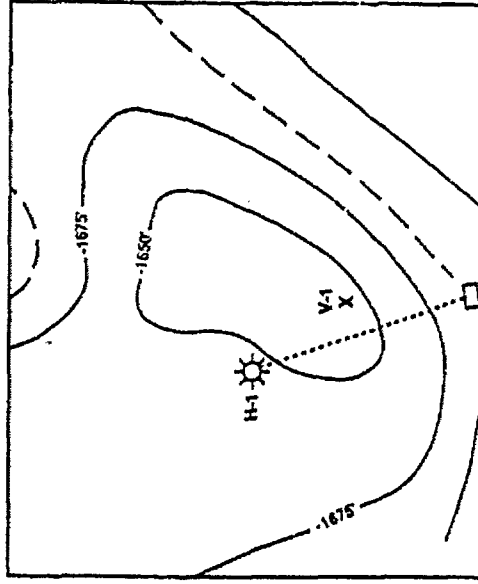


Figure 16
Case 4 - Structure map

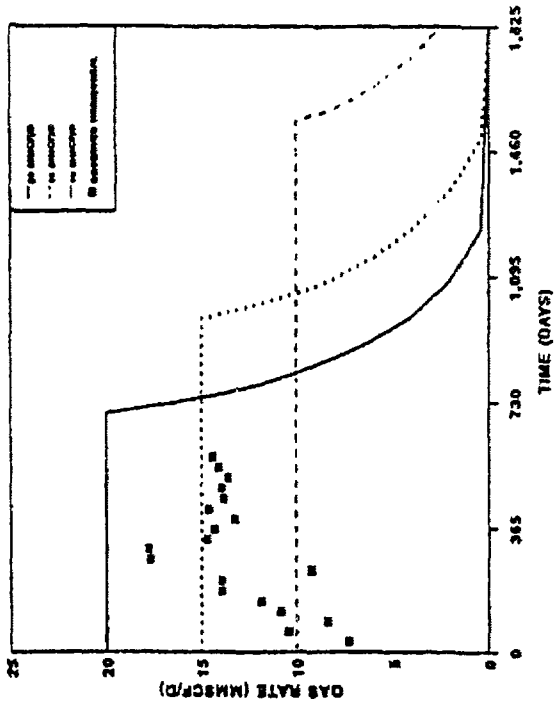


Figure 18
Case 4 - Observed & projected gas rates for
300' horizontal well

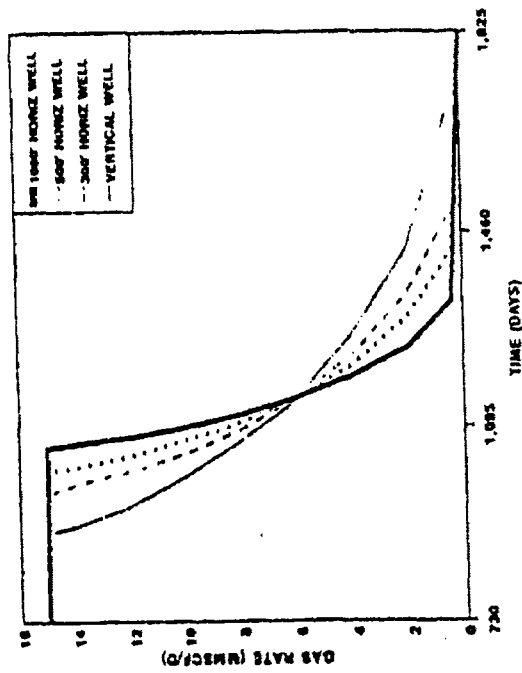


Figure 17
Case 4 - Projected gas rate for
vertical & horizontal wells

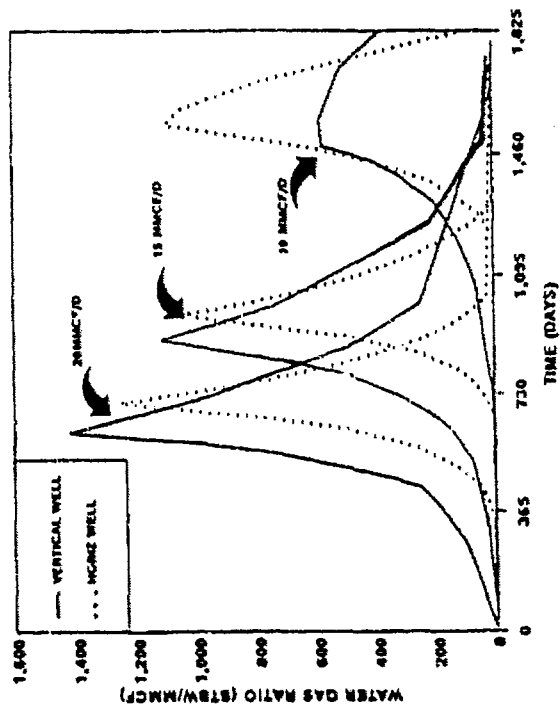


Figure 19
Case 4 - Projected water gas ratios for
vertical & 300' horizontal wells

SPE 21221

Seventh SPE Comparative Solution Project: Modelling of Horizontal Wells in Reservoir Simulation

by Long Nghiem, David A. Collins, and Ravi Sharma, *Computer Modelling Group*

SPE Members

Copyright 1991, Society of Petroleum Engineers, Inc.

This paper was prepared for presentation at the 11th SPE Symposium on Reservoir Simulation held in Anaheim, California, February 17-20, 1991.

This paper was selected for presentation by an SPE Program Committee following review of information contained in an abstract submitted by the author(s). Contents of the paper, as presented, have not been reviewed by the Society of Petroleum Engineers and are subject to correction by the author(s). The material, as presented, does not necessarily reflect any position of the Society of Petroleum Engineers, its officers, or members. Papers presented at SPE meetings are subject to publication review by Editorial Committees of the Society of Petroleum Engineers. Permission to copy is restricted to an abstract of not more than 300 words. Illustrations may not be copied. The abstract should contain conspicuous acknowledgment of where and by whom the paper is presented. Write Publications Manager, SPE, P.O. Box 833836, Richardson, TX 75083-3836 U.S.A. Telex, 730989 SPEDAL.

ABSTRACT

This paper reports the results of comparisons of simulation runs performed by fourteen organizations on a problem involving production from a horizontal well in a reservoir where coning tendencies are important. The effect of well length and rates on the recovery is examined. In addition, the paper also reports the techniques used by the different participants to calculate the inflow into the horizontal well and the wellbore hydraulics.

A variety of methods was used by the participants to model the inflow into the horizontal wells ranging from the use of productivity indices to grid refinement. A multitude of techniques was also used to calculate wellbore hydraulics while a few participants selected to represent the wellbore by a constant-pressure line sink.

All participants consistently predict a decrease in the coning behavior with an increase in well length. However, variations in the predictions were observed. Although the modelling methods from different participants can be grouped into different categories, no trend in the predicted results, according to the methods used, could be observed.

References and figures at end of paper.

INTRODUCTION

Recent interest in horizontal wells has been rapidly accelerating because of improved drilling technology, and the increased efficiency and economy of oil recovery operations. This paper presents a problem which deals with the effect of horizontal well lengths and rates on the recovery and selected results as submitted by the participants, compares various approaches for modelling horizontal wells in reservoir simulation, and discusses any large differences in the submitted results. This paper is the seventh in a series of comparative solution projects (CSP)¹⁻⁶ dealing with different aspects of reservoir simulation.

The objectives of this paper are:

1. To compare predictions from different participants.
2. To compare different approaches for calculating pressure drops in the wellbore. The inclusion of wellbore hydraulics in the simulation is preferable. However, participants can also represent the horizontal wellbore by a constant-pressure line sink.
3. To compare different approaches for calculating productivity indices for a horizontal well. Participants can also use local grid refinement around the horizontal well if they so desire.

In designing the problem, an attempt has been made to have the data as simple as possible while maintaining the practicality of the problem. The hope is that major differences in the simulation results are caused by different approaches for calculating pressure drops and productivity indices.

PROBLEM STATEMENT

The problem deals with oil recovery by bottom water drive in a thin reservoir where coning is important. Black-oil fluid properties and relative permeabilities from the Second SPE CSP² are used. However, reservoir and capillary-pressure data are different from those in the Second CSP.

Table 1 shows the reservoir data. Fluid property data are given in Tables 2 and 3, and relative permeabilities and capillary pressures are reported in Table 4. Initial conditions are also given in Table 1. The initial bubble-point pressure is equal to the gridblock oil pressure in each gridblock.

The reservoir is represented by a 9x9x6 grid system. The gridblock dimensions in the horizontal directions (x and y directions) are shown in Figure 1. The thicknesses in the vertical direction (z direction) are reported in Table 1.

Fluids are produced from a horizontal well drilled in the top layer (Layer 1). The well passes through the gridblock centers and the entire length is open to flow. Two lengths are considered:

- a) L=900 ft: well completed in Gridblocks (1,5,1), I=6,7,8
- b) L=2100 ft: well completed in Gridblocks (1,5,1), I=2,3,....,8

The flow direction in the horizontal well is from left to right in Figure 1. Fluids are removed from the portion of the well in Gridblock (8,5,1) to the surface. The horizontal wellbore has an inside diameter of 4.5 inches and an effective relative roughness of 10^{-3} .

A constant pressure line source is used to simulate the bottom water drive. The line source is completed in Gridblocks (1,5,6), I=1,2,....,9 as shown in Figure 2. Pertinent well data for both the injector and the producer are given in Table 5.

The horizontal well produces at a constant liquid (oil and water) rate. Three rates are considered: 3000

STB/day, 6000 STB/day and 9000 STB/day. The following eight cases are considered:

Case 1a:

L=900 ft
Liquid rate = 3000 STB/day
Simulation time = 1500 days
Reporting interval = 100 days

Case 1b:

Same as in Case 1a but with L=2100 ft

Case 2a:

L=900 ft
Liquid rate = 6000 STB/day
Simulation time = 1500 days
Reporting interval = 100 days

Case 2b:

Same as in Case 2a but with L=2100 ft

Case 3a:

L=900 ft
Liquid rate = 9000 STB/day
Simulation time = 1500 days
Reporting interval = 100 days

Case 3b:

Same as in Case 3a but with L=2100 ft

Case 4a:

Horizontal permeabilities = 3000 md for all blocks
Vertical permeabilities = 300 md for all blocks
Horizontal well length L = 900 ft
Liquid production rate = 9000 STB/day
Minimum bottom hole pressure of producer = 1500 psia
Water injection rate into the lower horizontal well = 6000 STB/day
Well index I_{we} for injector in each gridblock = 2.16×10^5 md.ft
Simulation time = 1500 days
Reporting interval = 100 days

Case 4b:

Same as in Case 4a but with L = 2100 ft

Cases 4a and 4b differ from the previous cases (Case 1a, 1b, 2a, 2b, 3a, and 3b) in the specification of reservoir permeabilities (Table 1) and in the injector constraint (Table 5). In the six previous cases, the permeabilities are ten times smaller and the injector operates at a bottom-hole pressure constraint of 3700 psia whereas a constant injection rate is maintained for Cases 4a and 4b.

Cases 1 to 3 examine the effect of rates and well lengths on the recovery. Since pressure is maintained, very little free gas is produced. In Case 4, the voidage replacement ratio is less than unity. A substantial amount of gas comes out of solution and is produced with the liquids. Table 6 summarizes the lengths of the producer and the injector/production schemes for the eight cases.

DESCRIPTION OF THE RESERVOIR SIMULATORS

This section describes the reservoir simulators used by the participants. The handling of wellbore hydraulics and of the inflow into the horizontal well are highlighted. Fourteen organizations participated in the Comparative Solution Project. The names and addresses of the participants are listed in Appendix A. Because of space limitations, the write-ups provided by the participants were condensed when required, with retention of the essential features.

ARTEP (Research association of Institut Français du Pétrole, Elf Aquitaine, Total-CFP and Gaz de France)

Sigma-Core, the ARTEP industrial simulator (presently jointly maintained and developed by Franlab) was used for the test examples of the present Project. Sigma-Core is a three-phase, three-dimensional black-oil and compositional model. Several different choices of space and time discretization techniques and matrix solvers are available.

In the runs for this CSP, a fully implicit, five-point difference scheme with upstream mobilities was used. The sparse linear equations were solved by D4 Gaussian elimination. The productivity indices were calculated by matching semi-analytical results (constant-pressure solution line source in a box shaped reservoir with one constant pressure boundary and three no-flux boundaries). The match consisted in reproducing the difference of pressure between the constant pressure boundary and the well and the repartition of well rates along the wellbore. Results are very close to those using Peaceman's formula¹⁴

with a circular permutation of the axes to account for the horizontal well. The values of the productivity indices in md.ft are:

Cases 1a, 2a and 3a:

$$\begin{array}{ll} I=6,8 & I_{we} = 6.52 \times 10^4 \text{ md.ft} \\ I=7 & I_{we} = 5.90 \times 10^4 \text{ md.ft} \end{array}$$

Cases 1b, 2b and 3b:

$$\begin{array}{ll} I=2,8 & I_{we} = 6.63 \times 10^4 \text{ md.ft} \\ I=3,7 & I_{we} = 5.94 \times 10^4 \text{ md.ft} \\ I=4,5,6 & I_{we} = 5.90 \times 10^4 \text{ md.ft} \end{array}$$

The values for Cases 4a and 4b are ten times the values of Cases 1a and 1b respectively.

A very flexible monitoring scheme of injection/production is available for wells, sectors and fields with several wellbore-hydraulic calculations suited for vertical, slanted or horizontal wells. The coupling between wellbore and reservoir is fully implicit.

The wellbore hydraulics used for the current project was from the Pepite model. Reference 7 outlines the main features of this model which can handle two-phase (liquid and gas) flow in pipes with the modelling of stratified and slug flow patterns and the transition from one pattern to the other. It was assumed that rates were constant between two adjacent centers of perforated gridblocks.

Chevron Oil Field Research Company

A fully implicit black-oil simulator with Cartesian local grid refinement capability⁸ was used. Local grid refinement was used to zoom in on the wellbore and replace it with a row of reservoir cells. Darcy's law, for axial flow in those cells, was replaced by a non-linear relationship between pressure drop and fluid velocity. The relationship was derived using Beggs and Brill's multiphase pipe flow correlation⁹. Relative permeability values were calculated, which ensured that the phase velocities in the wellbore were the same as those computed by the correlation (for wellbore gas saturations between 0 and 10%). These relative permeabilities were used for all cases. Flow from the reservoir to the wellbore was treated as cell to cell flow, eliminating the need for defining a productivity index. Flow out of the wellbore occurred in the last wellbore gridblock. The well bottomhole pressure was the pressure in the cell from which fluid was removed.

The multiphase relationships used for liquid (oil+water) and gas are:

$$k_{rj}(S_j) \left| \frac{dp}{dx} \right|_{m} = 4.46 \cdot 10^{-5} v_{sj} \mu_j + 6.235 \cdot 10^{-6} \rho_j v_{sj}^2$$

$j=1,g$

Here k_{rg} and k_{rl} are analogous to gas and liquid relative permeability functions, and v_{sg} and v_{sl} are superficial phase velocities.

Using Beggs and Brill's correlation for liquid saturations in the range from 0.9 to 1.0, and liquid flow rates from 9,000 to 200 reservoir bbl/day, and assuming distributed flow, a least squares fit gives:

$$k_{rg}(S_g) = S_g^{2.2404}$$

$$k_{rl}(S_l) = S_l^{2.9748}$$

For the 900-ft well, each gridblock in (6-8, 5, 1) is locally refined to 3 x 7 x 5 with $\Delta x = 3 \times 100$ ft, $\Delta y = 17$ ft, 8 ft, 4 ft, 2 ft, 4 ft, 8 ft, 17 ft, $\Delta z = 5$ ft, 4 ft, 2 ft, 4 ft, 5 ft. For the 2100-ft well, each gridblock in (2-7, 5, 1) is locally refined to 1 x 7 x 5 with Δy and Δz given as above; Gridblock (8, 5, 1) was locally refined to 3 x 7 x 5 as in the 900-ft well. For both the 900-ft and 2100-ft case, a 2 ft x 2 ft cell at the center of the refined region in the y-z plane represents the wellbore.

Computer Modelling Group (CMG)

The simulator used is IMEX which is an adaptive implicit, three-phase, black-oil simulator with pseudo-miscible options¹⁰. For this study, the hybrid grid refinement and wellbore frictional pressure and slip options^{11,12} were used.

The hybrid grid option results in curvilinear grid refinement within the Cartesian grid about the horizontal or vertical well. The grid is generated automatically based on the reservoir permeabilities, k_1 , k_2 , perpendicular to the well axis and user input number of subdivisions per gridblock. If $k_1 = k_2$ then a circular grid is created. If $k_1 \neq k_2$ then an elliptical grid is created. This provides an accurate and efficient means for modelling near wellbore phenomena allowing the use of coarser Cartesian grids near the wellbore.

The wellbore frictional pressure drop and slip option models the effects of pressure loss due to friction and liquid holdup in the well tubing within the

formation. This is done by coupling a two phase pipeflow correlation with the simulator in a fashion to allow the same primary variable set within the wellbore as within the simulator. Thus wellbore pressures and insitu saturations and bubble point pressures are calculated within a discretized wellbore. Wellbore insitu saturations and pressures were solved fully implicitly with the multiphase flow correlation coupled in an explicit fashion^{11,12}. This also provides an accurate means to model mixing within the wellbore and hence well backflow and crossflow through the wellbore.

When the above two options are used together, as done for this study, the inner grid is cylindrical in shape with the same dimensions as the wellbore. The well productivity then is calculated by using steady-state theory to calculate elliptical (or radial, depending on permeabilities) gridblock locations¹² and using curvilinear transmissibilities.

For the cases in this comparative solution project each Cartesian grid where the wellbore is located was divided into three in the elliptical direction and four in the hyperbolic direction. Dukler's correlation¹⁷ for multiphase flow in pipes was used in the present study.

ECL Petroleum Technologies (ECL)

Eclipse 100 is a fully-implicit, three-phase, general purpose black-oil simulator with gas condensate options. A series of special extensions to this simulator is available, collectively known as Eclipse 200. Two of these special extensions have been applied to this problem: Local Grid Refinement and Wellbore Friction.

The Local Grid Refinement option allows selected regions of a Cartesian grid to be replaced by finer-detailed local grids. The refined local grids are typically placed around wells that require coning effects to be resolved in more detail. The local grids may be Cartesian, 2-D radial (r,z), or 3-D radial with four sectors. Efficiency is enhanced by solving each local grid individually with its own timesteps and iterations, so that small timesteps can be used when necessary without holding up the progress of the global field simulation.

The Wellbore Friction option models the effects of pressure loss due to friction in the well tubing within the formation. It is primarily intended for use with horizontal wells, in which frictional losses may be significant. Eclipse treats the friction head terms in

each well-block connection as additional strongly-coupled variables, which it solves fully implicitly. The frictional pressure drop over a length L of tubing is

$$\Delta p_f = 2 \cdot f \cdot (L/D) \cdot \rho \cdot v^2$$

where f is the Fanning friction factor which, for turbulent flow in rough pipes, is calculated from Haaland's formula¹³. For multiphase flow, a homogeneous model is used, in which the mixture density and viscosity are the flow-weighted averages of the phase properties.

The well indices are calculated from Peaceman's formula for wells penetrating perpendicularly through the centre of rectangular gridblocks¹⁴.

In Cases 4a and 4b the grid was not refined. In Cases 1 to 3 the grid is refined as described below.

The aspect ratio of the well blocks in the yz -direction is approximately unity when transformed to an isotropic system, so a refinement that kept this aspect ratio was applied. The refinement was applied to the box of gridblocks consisting of the row of blocks containing the production well plus an extra block on either end. This box was refined as follows:

z -direction: 3 layers with $\Delta z = 8$ ft, 4 ft, 8 ft
 y -direction: 3 rows with $\Delta y = 24$ ft, 12 ft, 24 ft
 x -direction: 2 blocks at each end of the refinement box were refined into 4, with equal Δx values. The other blocks were not refined in the x -direction.

The refined blocks containing the production well thus had dimensions: $\Delta x = 300$ ft and 150 ft; $\Delta y = 12$ ft; $\Delta z = 4$ ft.

The well index calculated for each of these blocks was 9.75×10^4 and 4.88×10^4 md.ft. For Cases 4a and 4b where no grid refinement was used, the well indices were 5.194×10^5 md.ft.

Robertson ERC Limited (ERC)

The TIGRESS Reservoir Simulator has been used for this project. TIGRESS (The Integrated Geophysics Reservoir Engineering Software System) is an integrated software system which includes application modules for geophysics, geology, petrophysics, mapping, reservoir engineering, reservoir simulation and economics. It operates in a UNIX and X Windows environment with a database and user interface. The TIGRESS software is being developed by Robertson

ERC Limited with significant financial backing from ARCO British Limited, Enterprise Oil plc, Shell UK Limited and The UK Department of Energy. Because of their previous experience in writing the Pores Black Oil Simulator and Scorpio, a Chemical Flood Simulator, the mathematical aspects of the TIGRESS Reservoir Simulator have been developed by AEA Petroleum Services under contract to the TIGRESS consortium. AEA Petroleum Services also carries out the work for this project.

The simulator is based on a generalized compositional formulation which incorporates IMPES and fully implicit solution techniques¹⁵. Fluid properties can be calculated using either black oil or equation of state compositional models. The non-linear equations are solved by Newton's method. Linear equations are solved either by Line Successive Over Relaxation, or by ORTHOMIN with nested factorization preconditioning. Well block productivity indices are calculated using the method of Peaceman¹⁴, modified to allow for a horizontal well by interchanging the x and z axes. The simulator calculates the pressure drop in the wellbore using a modified version of the Beggs and Brill's correlation proposed by Brown¹⁶.

The calculations for this project used a fully implicit solution method and the ORTHOMIN linear solver. The reported results were obtained using the original $9 \times 9 \times 6$ grid. Some of the cases were repeated using local grid refinement in the central region of the model reservoir, but the results were found to be similar to those with the original grid.

HOT Engineering (HOT)

The test problem was solved with the Multipurpose Reservoir Simulation System SURE. SURE is a general non-isothermal compositional model which is formulated for any number of phases and components while the input data and results remain in well-known black-oil format. The available simulation models, from black oil to compositional, are defined blockwise. The models may therefore be changed with time as well as used simultaneously in one reservoir. The grid-refinement option allows construction of a reasonable grid system focusing on interesting areas. This may also be applied dynamically. Using grid gathering, blocks can be merged in aquifer areas. The dynamic implicitness, which was used for this test, reduces the number of implicit unknowns while providing the same quality as the fully implicit method. Direct Gaussian elimination procedure and an iterative solving method (ORTHOMIN) with incom-

plete factorization are available. The latter one was used for this test.

The calculation of pressure drops in horizontal well sections within SURE is based on the Dukler's correlation¹⁷ and is done explicitly. This is because it meets both our requirements by being sufficiently accurate in comparison to other models, and by having a moderate calculation demand.

This calculation model is based on a wide range of experimental data which supplies the necessary information to correlate the most significant variables in multiphase flow: liquid hold-up and friction factor. The calculations do not include the effect of different flow patterns on pressure losses, thus resulting in a simpler calculation model. The basic equation used in this correlation is the familiar Weisbach's friction loss formula. Dukler proposed a different formula for friction loss which includes mixture properties and liquid hold-up.

The productivity indices are calculated from Peaceman's method¹⁴. This gives a value of 5.19×10^4 md.ft for Cases 1, 2 and 3 and 5.19×10^5 md.ft for Case 4.

Integrated Technologies (INTECH)

The simulator used is the VIP-ENCORE simulator developed originally by the firm J.S. Nolen and Associates (now part of INTECH). VIP-ENCORE is the "black-oil" simulator module of the VIP-EXECUTIVE simulator software system. VIP-ENCORE is a three-phase, three-dimensional, vectorized, fully-implicit (or IMPES) simulator in which internally the hydrocarbon fluids are handled compositionally. Fluid data input can be in the conventional "black-oil" tabular form or as a two- or multi-component system defined by pressure-dependent k-values. The BLITZ matrix solver, also developed originally by J.S. Nolen and Associates, was used in the simulations described herein.

Wellbore hydraulics calculations for the horizontal section are not implemented in VIP-ENCORE. In lieu of that, the horizontal wellbore is simulated by a row of high-transmissibility blocks. The transmissibility used to simulate wellbore flow is that value which allows a match of the pressure drop obtained from a multiphase, horizontal flow calculation¹⁸. Because the pressure drop in the simulated wellbore is from block center to block center, the values reported are for 600 ft and 1800 ft, respectively, rather than the actual

wellbore lengths of 900 ft and 2100 ft. (In all cases investigated the pressure drop is very small - maximum 0.5 psi/100 ft).

Simulation of the wellbore with a row of high-transmissibility gridblocks provides two additional benefits. First, it provides a measure of grid refinement because in the y and z directions there are three blocks rather than one. Second, well productivity is determined by the transmissibilities of the block faces, so no "well index" or similar factor is required for each perforated gridblock. (It is necessary, however, to adjust transmissibilities at the wellbore, as described later).

The eight runs specified for the Seventh CSP were all made using a row of gridblocks for the wellbore. As a result, INTECH's grid dimensions were $9 \times 11 \times 8 = 792$ blocks rather than $9 \times 9 \times 6 = 486$ blocks. The "original" column and row of blocks containing the wellbore ($J=5$, $K=1$) are divided into three columns and three rows respectively with $\Delta y = 29.17$ ft, 1.66 ft, 29.17 ft and $\Delta z = 9.17$ ft, 1.66 ft, 9.17 ft. y- and z-direction spacing of the wellbore blocks is 1.66 ft which is the spacing necessary for the block pressure to equal the steady-state flowing pressure of the well (after Peaceman¹⁹.) All other guidelines (rates, pressures, wellbore lengths) were followed explicitly.

Adjustments (increases) in the y- and z-direction transmissibilities are needed because of the small cross-sectional areas to flow associated with the small Δy and Δz values used to simulate the wellbore along with the relatively long lengths of flow. Nine-point differencing in the vertical plane could help offset this problem, but that is not normally available. INTECH's approach was to use the transmissibilities determined from a finer grid ($9 \times 17 \times 12$) system. The transmissibility of each wellbore block face of the $9 \times 11 \times 8$ grid system was taken as the transmissibility computed at the face between two 1.66 ft blocks in both the y- and z-direction of the $9 \times 17 \times 12$ grid system. Use of these adjusted transmissibilities produced wellbore pressures very close to the method of Babu and Odeh²⁰.

Japan National Oil Corporation (JNOC)

JNOC coupled a fully implicit black-oil model to a model for multi-phase flow in pipes to include wellbore hydraulics in the calculations. The reservoir and wellbore equations are solved sequentially in the coupled model.

In the coupled model, the pressure drop in the wellbore is used instead of the hydraulic head as in the original black-oil model to calculate wellbore flowing pressures at the perforated blocks. The pressure drop was obtained from a previous calculation. Therefore for each horizontal multiblock well, there is one additional unknown, i.e. the well pressure at the last downstream block, just as in the original black-oil model.

The multi-phase pipe flow model calculates the pressure drop in the pipe from data on flow rates, well pressures and well geometry. The calculations are based on the Beggs and Brill correlation⁹ in which the flow regime is determined among six regimes (single-phase liquid, single-phase gas, bubble, stratified, intermittent and annular). The model allows precise calculations by dividing the wellbore element in each gridblock into several subsegments. In the current runs, ten subsegments were used for each wellbore element per gridblock.

The calculations of reservoir and wellbore equations are repeated until the updated well pressure is satisfactorily close to the value from the last calculations. From a practical point of view, iterations between the black-oil model and the wellbore model are required only if there is a drastic change in the production rate.

The productivity indices are calculated using the method of Peaceman¹⁴ for nonsquare gridblocks with anisotropic permeabilities. The calculated values are 5.194×10^4 md.ft for Cases 1, 2 and 3, and 5.194×10^5 md.ft for Case 4.

Marathon Oil Company

Marathon's simulator is fully implicit, three-dimensional and three-phase²¹. It can simulate single- or dual-porosity reservoirs using five-point or nine-point finite difference. For this study, nine-point finite difference in the yz plane (i.e. perpendicular to the horizontal well) was found to give essentially the same results as five-point, therefore the reported results are for five-point. The gas and oil phases are treated by use of a two-component formulation in which the maximum amount of dissolved surface gas in the oil phase and vaporized stocktank oil in the gas phase can be approximated as a function of pressure²².

The horizontal-well pressure drop calculations for this comparative study were obtained using the Mukherjee and Brill correlation²³. The oil, gas and water PVT data were input into an auxiliary program

to calculate tables of pressure drop as a function of oil rate, water-cut and gas-oil ratio using the specified empirical correlation. These tables were input into the simulator. Pressure drop between any two locations in the well is interpolated from the tables using total flow rate from all "upstream" locations in the well. Previous timestep values of flow rate are used to estimate the pressure drop (i.e. calculations are explicit). For this reason, timesteps were limited to be no greater than 10 days. Well connection factors for the producer were calculated using the method of Babu et al²⁴. From the rigorous formulation in Reference 24, a wellbore connection factor for each node was determined to be 5.19×10^4 md.ft for Cases 1, 2 and 3, and 5.19×10^5 md.ft for Case 4.

Phillip's Petroleum Company

Phillip's simulator is a general purpose three-dimensional, three-phase reservoir model that can be used to simulate vertical, inclined and horizontal wells. The model uses a fixed or variable degree of implicitness to solve for pressure, water saturation and gas saturation in saturated cells; and pressure, a water saturation and bubble point pressure in undersaturated cells. Results reported in this work were calculated using the fully implicit reservoir and wellbore pressure options. Productivity indices into each horizontal wellbore gridblock are calculated by Peaceman's method¹⁴.

The equivalent gridblock radius proposed by Babu et al²⁴ was compared to Peaceman's expression with good agreement between the two methods. The grid system specified in the problem statement resulted in an equivalent gridblock radius of 5.86 ft and a productivity index of 5.194×10^4 md.ft for Cases 1a through 3b, and a productivity index of 5.194×10^5 md.ft for Cases 4a and 4b. In this model, horizontal wells are treated as either a line source or a line sink, i.e. no wellbore hydraulics are included. Relative permeabilities were calculated using Stone's second method.

Time increment size was controlled by a dual set of constraints. The maximum saturation change per timestep was limited to 0.05, and the maximum time increment size was limited to 0.10 years to minimize time truncation error.

Reservoir Simulation Research Corporation (RSRC)

The simulator used by RSRC is based on a generalized compositional solution algorithm. This algorithm

supports the use of different fluid-property modules within one basic simulator. The algorithm uses a full Newton-Raphson solution technique which, due to fewer iterations per timestep, is more efficient than other commonly used methods. The calculations are structured so that no material-balance errors occur. The black-oil fluid-property option was used to solve the comparative solution problem. A detailed description of the simulator used in this study is presented in Reference 25. The simulator uses a fully implicit treatment of fluid mobilities at production wells and uses an implicitly calculated bottom-hole pressure to allocate well rates between layers for rate-limited wells.

The productivity index for the horizontal producer in this problem is calculated based on Peaceman's method^{14,26} modified to allow for a horizontal well by interchanging the x- and z-axes. Using the formula for interior wells¹⁴, the productivity indices are 5.19×10^4 md.ft for Cases 1, 2 and 3, and 5.19×10^5 md.ft for Case 4. Using the formula for edge wells²⁶, the respective productivity indices are 2.106×10^4 md.ft and 2.106×10^5 md.ft. It was found that the use of either productivity index produces similar results. The formula for edge wells was used in the simulation reported herein.

The pressure drop in the horizontal wellbore was not included in the simulation results reported.

Shell Development Company

The simulator used was the implicit black-oil version of Shell's multipurpose isothermal reservoir simulator. The unknowns solved for in the simulator are the reference phase pressure and the accumulation of Peaceman's formulas for a vertical well¹⁴ and transposing the x and z dependence in the formulas. The value of the productivity indices were 5.194×10^4 md.ft for Cases 1, 2 and 3 and 5.194×10^5 md.ft for Case 4.

The pressure drops within the wellbore are divided into a gravity and a viscous term. The gravity term uses either a no-slip assumption for the average density of a table of average density as a function of the surface flow rates passing through a completion interval. The average elevation of a completion interval can either be set to the gridblock elevation or be specified by the user. The pressure drop due to viscous forces is calculated from tables of pressure drop per unit length as a function of the surface flow rates flowing through a particular interval. The pipe length between two adjacent completion intervals must

be specified by the user. Although the tabular approach allows for a wide range of pressure drop correlations to be used by the simulator and hence requires an outside program to generate the input data, the Dukler's correlation¹⁷ can be used within the simulator to generate the tables.

Stanford University

The simulator used is a three-dimensional, three-phase research simulator with local grid refinement, hybrid grid and domain decomposition options. The wellbore hydraulics option in the simulator was not used for the runs reported here.

The productivity index was computed by using the analytical solution of the single phase differential equation reported by Babu et al²⁰ and numerical solution of the finite difference equations for single phase flow. In these calculations only the producer was considered. The resulting productivity indices are 5.08×10^4 md.ft for Cases 1, 2 and 3 and 5.08×10^5 md.ft for Case 4.

Calculations were made with maximum timestep size of 100 days for Cases 1, 2 and 3 and that of 50 days for Case 4.

Additional runs with local grid refinement and smaller timesteps were also made. The results however were not significantly different from those reported here.

TDC Reservoir Engineering Services

The TDC simulator, BLOS, is a standard 3-D, 3-phase, 3-component, IMPES, finite-difference based simulator. The model uses a two-point approximation for transmissibilities for enhanced spatial accuracy and a stabilized Runge Kutta time-integration scheme for increased timestep sizes relative to the normal IMPES limitation.

Flow coefficients for the horizontal well were computed using Peaceman's procedure¹⁴. The horizontal well was specified as constant potential, with inflow to each segment being determined by local mobility and pressure drop. We compute a well index of 5.19×10^4 md.ft for Cases 1, 2 and 3 and 5.19×10^5 md.ft for Case 4.

For the stated well parameters, we computed a wellbore pressure drop of approximately 0.011 psi/ft for an oil flow of 9000 STB/day. This would give a

maximum pressure drop of only 3 psi for the link closest to the offtake point. Outer intervals would have lower pressure drops. We, thus, elected to ignore the wellbore hydraulics in the simulations.

SUMMARY

The above descriptions shows a variety of methods for calculating inflow into the well. Participants use either Peaceman's approach¹⁴, Babu et al's approach^{20,24} or their own approach for calculating the productivity indices. These methods all give similar values. Four participants used grid refinement around the well. CHEVRON and ECL used Cartesian local grid refinement while CMG used elliptical local grid refinement. INTECH used finer Cartesian gridblock sizes for the whole row and column of gridblocks containing the wellbore. In CHEVRON, CMG and INTECH's approach, the inflow into the well is calculated from a direct discretization of the flow equations, whereas ECL used Peaceman's formula¹⁴.

Different correlations were also used to calculate the wellbore hydraulics. A few participants selected not to include wellbore hydraulics and represented the wellbore as a line sink with uniform pressure.

Table 7 summarizes the various methods for calculating well inflow and wellbore hydraulics. The symbols that will be used to identify the plots from the different participants are also shown.

RESULTS

Cases 1, 2 and 3

These cases examine the effect of well length and production rates on the recovery. Since pressure is maintained, very little free gas is produced. Refer to Table 6 for a summary description of these cases.

Figures 3 through 8 show the oil rate and cumulative oil produced for the different well lengths and rates. The results show that the use of a longer well reduces the water coning tendencies. Figures 9 through 14 show the corresponding water-oil ratios.

Table 8 shows the values of the cumulative oil produced at 1500 days predicted by the different participants. Some variations in the predicted results are observed. The last two rows of the table show the mean and standard deviation of the predicted cumulative oil.

When the problem was sent out to potential

participants the first time, three-phase relative permeability models were not specified. It was later suggested to participants to use the normalized Stone 2 relative-permeability model²⁷. However, some participants had already completed part of the runs with the Stone 1 three-phase relative-permeability model²⁸. The use of the Stone 1 model should give results similar to the Stone 2 model for Cases 1, 2 and 3 because very little free gas was produced. ECL, HOT and Shell's results for Cases 1, 2 and 3 were obtained with the Stone 1 model, whereas all the other participants used the normalized Stone 2 model.

Figures 15 through 17 shows the cumulative water produced. The variations between the participants are relatively small because the well produced at constant liquid rates with high water-oil ratios. Although not shown here, the amounts of injected water predicted by the participants are very similar. The bottom-hole pressure and pressure drop predicted are almost constant throughout the simulation. The values at 1500 days are shown in Tables 9 and 10 respectively. The results in Table 8 indicate that the standard deviation in the predicted bottom-hole pressure is higher for the shorter well. Table 9 shows a wide variation in the predicted pressure drop. A zero pressure drop corresponds to the use of a uniform-pressure line sink.

Case 4

Cases 4a and 4b were designed to yield a large amount of free gas flowing into the producer. Figures 18 and 19 show the oil rates and cumulative oil produced. There are larger variations in the cumulative oil produced than in Cases 1, 2 and 3. The mean and standard deviations of the cumulative oil produced at 1500 days are given in Table 8. As in the previous cases, there are larger variations for the shorter well.

Figures 20 and 21 show the water production rates. The water rates dropped sharply as the minimum bottom-hole pressure of 1500 psia was reached around 700 to 800 days. The cumulative water production is shown in Figure 22. There is reasonable agreement between different participants. Largest variations occur between 600 and 900 days.

The gas-oil ratios are depicted in Figures 23 and 24, and the cumulative gas production is shown in Figures 25 and 26. Gas production rates peaked around 700 to 800 days and then decreased. As free gas production increased, the decrease in bottom-hole pressure accelerated (Figures 27 and 28). The average

reservoir pressure exhibited a similar behavior. At around 700 to 800 days, the bottom-hole pressure reached its minimum value of 1500 psia. The reservoir pressure was then maintained and free gas production decreased.

Figures 29 and 30 show the predicted pressure drop along the wellbore. The pressure drop increased with increased free gas flow rates. There are sizeable variations in the peak pressure drop predicted. For the 900 ft well, three participants (HOT, INTECH and Marathon) predicted a peak pressure drop of less than 10.5 psia, six participants (ARTEP, CMG, ECL, JNOC and Shell) predicted a pressure drop between 27.6 psia and 32.9 psia whereas ERC predicted a value of 42.5 psia. For the 2100 ft well the predicted pressure drops are larger, with substantial variations among the participants. Chevron predicted substantially higher pressure drops than the values shown in Figures 29 and 30. The variations in pressure drop in Case 4 are much larger than the variations in Cases 1, 2 and 3 because of the large flow rate of free gas in the wellbore.

In Case 4, all participants but Shell used the normalized Stone 2 model for relative permeabilities. Shell used the Stone 1 model for all runs.

Observations

Although the modelling methods from the different participants can be grouped into different categories according to the approaches for calculating well productivity indices and for calculating wellbore hydraulics (pressure drop) (see Table 7), no trend in the predicted results corresponding to the methods used could be observed. Other factors such as truncation errors, convergence criteria, timesteps taken and implicit/explicit formulation could have masked any possible trends in the results.

It is not possible to identify the effect of wellbore hydraulics in the results. A recent study¹² shows that runs with and without wellbore hydraulics may give similar cumulative productions for the cases considered; however, the inclusion of wellbore hydraulics in the calculations yields a substantially different drainage pattern along the wellbore. Thus, information on rates and cumulative production per well element would be required. This information was not requested in the problem statement. The effect of wellbore hydraulics is more pronounced in high-permeability reservoirs than in low-permeability reservoirs. Indeed, the effect depends on the ratio between pressure drop and pressure drawdown, and

increases with this ratio.

Table 11 shows the total number of timesteps and Newtonian iterations from the participants. Runs with the shorter well seemed to require more timesteps and iterations than runs with the longer well for most participants although there were exceptions. This can be attributed to a stronger coning behavior associated with the shorter well which makes the problem more difficult to solve. Participants who used grid refinement may require more timesteps and iterations than would otherwise be required. This is due to small gridblocks used near the well.

Note that participants were requested to provide results at every 100 days. The plots were generated by joining these results by straight lines. Smoother curves could have been obtained if more frequent results were reported.

CONCLUSIONS

This Comparative Solution Project deals with the effect of varying the rate and the length of a horizontal well on the recovery of oil from a reservoir where coning is important. Two salient aspects of modelling a horizontal well were examined, namely 1) the calculation of inflow into the well, and 2) the handling of the wellbore hydraulics.

A variety of methods was used by the participants to address the above aspects. They all consistently predicted a decrease in the coning behavior with an increase in well length.

The calculation of inflow into a horizontal well has been a subject of much research and discussion recently²⁹⁻³³. The variety of methods used by the participants suggests that this is an area of active research. An important aspect to investigate would be the effect of grid spacing on the inflow calculation. In the current problem, the grid spacings of the well block in the y and z direction are respectively 60 ft and 20 ft, which are reasonably small.

The inclusion of wellbore hydraulics in a reservoir simulator has been mentioned in the literature. However, few details were given. In view of the variety of techniques used by the participants, publications discussing in detail the techniques used and their importance in reservoir simulation would certainly be welcome. A comparison of different multiphase flow correlations for horizontal wellbore flow in the context of reservoir simulation would also be desirable.

NOMENCLATURE

D	wellbore inside diameter
f	friction factor
I_{we}	well index
k_{rj}	relative permeability for Phase j
L	wellbore length
p	pressure
S_j	saturation of Phase j
v	velocity
v_{sj}	superficial velocity of Phase j
Δp_f	frictional pressure drop
Δx	grid spacing in x direction
Δy	grid spacing in y direction
Δz	grid spacing in z direction
μ_j	viscosity of Phase j
ρ_j	density of Phase j

Subscripts

l	liquid
g	gas

ACKNOWLEDGEMENTS

We thank all participants in this CSP for providing their results and modelling techniques to this paper. Their time and effort in making the runs and their prompt response to our requests are gratefully acknowledged. We also thank Dr. D. Nathan Meehan of Union Pacific Resources and Professor Khalid Aziz of Stanford University for their helpful comments in the design of the problem for this CSP. We are also indebted to Dr. Stephen H. Leventhal of Shell Development Company for performing the preliminary runs to test and check the data given in the problem description.

REFERENCES

- Odeh, A.S., "Comparison of Solutions to a Three-Dimensional Black-Oil Reservoir Simulation Problem," JPT, Vol. 33, January 1981, pp. 13025.
- Weinstein, H.G., Chappellear, J.E., and Nolen, J.S., "Second Comparative Solution Project: A Three-Phase Coning Study," JPT, Vol. 38, March 1986, pp. 345-353.
- Kenyon, D.E., and Behie, G.A., "Third SPE Comparative Solution Project: Gas Cycling of Retrograde Condensate Reservoirs," JPT, Vol. 39, August 1987, pp. 981-998.
- Aziz, K., Ramesh, A.B., and Woo, P.T., "Fourth SPE Comparative Solution Project: A Comparison of Steam Injection Simulators," JPT, Vol. 39, December 1987, pp. 1576-1584.
- Killough, J., and Kossack, C., "Fifth SPE Comparative Solution Project: Evaluation of Miscible Flood Simulators," paper SPE 16000 presented at the Ninth SPE Symposium on Reservoir Simulation, San Antonio, Texas, February 1-4, 1987.
- Firoozabadi, A., and Thomas, L.K., "Sixth SPE Comparative Solution Project: Dual-Porosity Simulators," JPT, Vol. 42, June 1990, pp. 710-715 and 762-763.
- Lagiere, M., Miniscloux, C., and Roux, A., "Computer Two-Phase Flow Model Predicts Pressure and Temperature Profiles," Oil and Gas J., April 1984.
- Wasserman, M.L., "Local Grid Refinement for Three-Dimensional Simulators," paper SPE 16013 presented at the Ninth SPE Symposium on Reservoir Simulation, San Antonio, Texas, February 1-4, 1987.
- Beggs, J.P., and Brill, J.P., "A Study of Two-Phase Flow in Inclined Pipes," JPT, Vol. 25, May 1973, pp. 607-617.
- Fung, L.S.-K., Collins, D.A., and Nghiem, L., "An Adaptive-Implicit Switching Criterion Based on Numerical Stability Analysis," SPERE, Vol. 4, February 1989, pp. 45-51.
- Collins, D., Nghiem, L., Sharma, R., Li, Y.-K., and Jha, K., "Field-Scale Simulation of Horizontal Wells," paper 90-121 presented at the 1990 CIM/SPE International Technical Meeting, Calgary, Alberta, June 10-13.
- Collins, D.A., Nghiem, L., Sharma, R., Agarwal, R., and Jha, K., "Field-Scale Simulation of Horizontal Wells with Hybrid Grids," paper SPE 21218 presented at the 11th SPE Symposium on Reservoir Simulation, February 17-20, 1991, Anaheim, California.
- Haaland, S.E., Trans. ASME, JFE, Vol. 105, 1983, p. 89.

SEVENTH SPE COMPARATIVE SOLUTION PROJECT:
MODELLING OF HORIZONTAL WELLS IN RESERVOIR SIMULATION

12

SPE 21221

- | | |
|--|---|
| <p>14. Peaceman, D.W., "Interpretation of Well-Block Pressures in Numerical Reservoir Simulation With Nonsquare Gridblock and Anisotropic Permeability," SPEJ, Vol. 23, June 1983, pp. 531-543.</p> <p>15. Mott, R.E., and Farmer, C.L., "A New Formulation for Generalized Compositional Simulation," Second European Conference on the Mathematics of Oil Recovery, Arles, France, September 11-14, 1990.</p> <p>16. Brown, K.E., "The Technology of Artificial Lift Methods," Petroleum Publishing Company, Tulsa, 1977.</p> <p>17. Dukler, A.E., Wicks, M., and Cleveland, R.G., "Frictional Pressure Drop in Two-Phase Flow: An Approach Through Similarity Analysis," A.I.Ch.E. J., Vol. 10, January 1964, pp. 44-51.</p> <p>18. Baxendell, P.B., "Pipeline Flow of Oil and Gas Mixtures," Proceedings Fourth World Petroleum Congress, Sec. II/E, Paper 4.</p> <p>19. Peaceman, D.W., "Interpretation of Well-Block Pressures in Numerical Reservoir Simulation," SPEJ, Vol. 18, June 1978, pp. 183-194.</p> <p>20. Babu, D.K., and Odeh, A.S., "Productivity of a Horizontal Well," SPERE, Vol. 4, November 1989, pp. 417-421.</p> <p>21. Gilman, J.R., and Kazemi, H., "Improvements in Simulation of Naturally Fractured Reservoirs," SPEJ, Vol. 23, August 1983, pp. 695-707.</p> <p>22. Vestal, C.R., and Shank, G.D., "Practical Techniques in Two-Pseudocomponent Black-Oil Simulation," SPERE, Vol. 4, May 1989, pp. 244-252.</p> <p>23. Mukherjee, H., and Brill, J.P., "Liquid Holdup Correlations for Inclined Two-Phase Flow," JPT, Vol. 35, May 1983, pp. 1003-1008.</p> <p>24. Babu, D.K., Odeh, A.S., Al-Khalifa, A.-J.A., and McCann, R.C., "The Relation Between Wellblock and Wellbore Pressure in Numerical Simulation of Horizontal Wells - General Formulas for Arbitrary Well Locations in Grids," unsolicited paper SPE 20161, October 1989.</p> | <p>25. Young, L.C., "Full Field Compositional Modeling on Vector Processors," paper SPE 17803 presented at the SPE Rocky Mountain Regional Meeting, Casper, Wyoming, May 11-13, 1988.</p> <p>26. Peaceman, D.W., "Interpretation of Well-Block Pressures in Numerical Reservoir Simulation: Part 3 - Off-center and Multiple Wells Within a Wellblock," SPERE, Vol. 5, May 1990, pp. 227-232.</p> <p>27. Aziz, K., and Settari, A., Petroleum Reservoir Simulation, Applied Science Publishers Ltd., 1979, London, p. 36.</p> <p>28. Stone, H.L., "Probability Model for Estimating Three-Phase Relative Permeability," JPT, Vol. 22, February 1970, pp. 214-218.</p> <p>29. Peaceman, D.W., "Discussion of Productivity of a Horizontal Well," SPERE, Vol. 5, May 1990, pp. 252-253.</p> <p>30. Brigham, W.E., "Discussion of Productivity of a Horizontal Well," SPERE, Vol. 5, May 1990, pp. 254-255.</p> <p>31. Babu, D.K., and Odeh, A.S., "Author's Reply to Discussion of Productivity of a Horizontal Well," SPERE, Vol. 5, May 1990, pp. 256.</p> <p>32. Peaceman, D.W., "Further Discussion of Productivity of a Horizontal Well," SPERE, Vol. 5, August 1990, pp. 437-438.</p> <p>33. Babu, D.K., and Odeh, A.S., "Author's Reply to Further Discussion of Productivity of a Horizontal Well," SPERE, Vol. 5, August 1990, pp. 438.</p> <p style="text-align: center;">APPENDIX</p> <p>Participants in the Seventh SPE Comparative Solution Project</p> <p>ARTEP
Institut Français du Pétrole
B.P. 311
92506 Rueil Malmaison Cedex
France
Contact: Patrick Lemonnier</p> |
|--|---|

Chevron Oil Field Research Company
1300 Beach Boulevard
P.O. Box 446
La Habra, California 90633-0446
U.S.A.
Contact: M.L. Wasserman

Computer Modelling Group
3512 - 33 Street N.W.
Calgary, Alberta T2L 2A6
Canada
Contact: Long Nghiem

ECL Petroleum Technologies
Highlands Farm, Greys Road
Henley-on-Thames, Oxon RG9 4PS
United Kingdom
Contact: Jon Holmes

Robertson ERC Limited
45 West Street
Marlow, Bucks SL7 2LS
United Kingdom
Contact: M.J. Allmen

HOT Engineering
Roseggerstrasse 15
A-8700 Leoben
Austria
Contact: Ludwig Ems

Integrated Technologies
10205 Westheimer
Houston, Texas 77042
U.S.A.
Contact: A.C. Carnes, Jr.

Japan National Oil Corporation
Technology Research Center
1-2-2 Hamada, Chiba City
Chiba 260
Japan
Contact: Takao Nanba

Marathon Oil Company
P.O. Box 269
Littleton, Colorado 80160-0269
U.S.A.
Contact: James R. Gilman

Phillip's Petroleum Company
141 Geoscience Building
Bartlesville, Oklahoma 74004
U.S.A.
Contact: Burt Todd

Reservoir Simulation Research Corporation
2525 East 21st Street, Suite 205
Tulsa, Oklahoma 74114-1747
U.S.A.
Contact: Hemanth Kumar

Shell Development Company
Bellaire Research Center
3737 Bellaire Boulevard
P.O. Box 481
Houston, Texas 77001
U.S.A.
Contact: Stephen H. Leventhal

Stanford University
Department of Petroleum Engineering
Mitchell Building 360
Stanford, California 94305-2220
U.S.A.
Contact: Khalid Aziz

TDC Reservoir Engineering Services
555 S. Camino del Rio, Suite A3
Durango, California 81301
U.S.A.
Contact: Michael R. Todd

Table 1 Reservoir Data and Initial Conditions

Layer	Thickness Δz (ft)	Depth to Center of Layer (ft)	Horizontal Permeability (md)	Vertical Permeability (md)	P _{int} (psia)	S _w	S _o
1(top)	20	3600	300	30	3600	0.711	0.289
2	20	3620	300	30	3608	0.652	0.348
3	20	3640	300	30	3616	0.527	0.473
4	20	3660	300	30	3623	0.351	0.649
5	30	3685	300	30	3633	0.131	0.869
6(bottom)	50	3725	300	30	3650	0.000	1.000

Initial bubble-point pressure = gridblock initial oil pressure

Permeability values for Cases 1 through 3. Horizontal and vertical permeabilities for Case 4 are 3000 md and 300 md respectively.

Table 2 Fluid Property Data
(From Reference 2)

Pressure (psia)	Solution GOR (SCF/STB)	Saturated Properties		Oil Viscosity μ _o (cp)	Gas Viscosity μ _g (cp)
		Oil FVF B _o (RB/STB)	Gas FVF B _g (RB/SCF)		
400	165	1.0120	0.00590	1.17	0.0130
800	335	1.0255	0.00295	1.14	0.0125
1200	500	1.0380	0.00196	1.11	0.0140
1600	665	1.0510	0.00147	1.08	0.0145
2000	828	1.0630	0.00118	1.06	0.0150
2400	985	1.0750	0.00098	1.03	0.0155
2800	1130	1.0870	0.00084	1.00	0.0160
3200	1270	1.0985	0.00074	0.98	0.0165
3600	1390	1.1100	0.00065	0.95	0.0170
4000	1500	1.1200	0.00059	0.94	0.0175
4400	1600	1.1300	0.00054	0.92	0.0180
4800	1676	1.1400	0.00049	0.91	0.0185
5200	1750	1.1480	0.00045	0.90	0.0190
5600	1810	1.1550	0.00042	0.89	0.0195

Oil compressibility for undersaturated oil (psia⁻¹)
 Oil viscosity compressibility for undersaturated oil (psia⁻¹)
 Stock tank oil density: P_{oil} (lb_m/ft³)
 Standard-condition gas density: P_{gsc} (lb_m/ft³)
 Water compressibility: c_w (psia⁻¹)
 Water formation volume factor at reservoir temperature and atmospheric pressure: B_o (RB/STB) 1.0142
 Water density at standard conditions: P_o (lb_m/ft³)
 Reference pressure for water FVF and densities: P_w (psia)
 Water viscosity: μ_w (cp)

Table 3 Property Equations

Water FVF: $B_w = K_o (1 - c_w (P_o - P_o^*))$ RB/STB

Densities: $\rho_o = (P_{o,at} + R_o P_{gsc}) / (5.6146) / B_o$ lb_m/ft³
 $\rho_g = (P_{gsc} / 5.6146) / B_g$ lb_m/ft³
 $\rho_w = \rho_o^* (1 + c_w (P_o - P_o^*))$ lb_m/ft³

Porosities: $\phi = \phi^* (1 + c_o (P_o - P_o^*))$

Table 4 Relative Permeabilities and Capillary Pressures

Water/Oil Functions			Gas/Oil Functions		
S _w	k _{rw}	P _{cwo} (psia)	S _g	k _{rg}	P _{cgo} (psia)
0.22	0.00	1.0000	0.00	0.0000	1.00
0.30	0.07	0.4000	0.04	0.0000	0.60
0.40	0.15	0.1250	0.10	0.0220	0.53
0.50	0.24	0.0649	0.20	0.1000	0.10
0.60	0.33	0.0418	0.30	0.2400	0.02
0.80	0.65	0.0000	0.40	0.3400	0.00
0.90	0.83	0.0000	0.50	0.4200	0.00
1.00	1.00	0.0000	0.60	0.5000	0.00
			0.70	0.8125	0.00
			0.78	1.0000	0.00

202 28261

Table 9 Bottom-Hole Pressure in psia at 1500 Days

Participants	1a	1b	2a	2b	3a	3b
ARTEP	3466.76	3575.78	3236.68	3470.49	3002.20	3364.74
Chevron	3464.77	3576.10	3239.19	3464.32	3012.13	3356.08
CMG	3446.32	3558.33	3210.46	3454.76	2970.39	3345.85
ECL	3485.03	3569.71	3326.22	3490.41	3170.46	3412.53
ERC	3439.96	3562.14	3199.89	3453.11	2949.06	3343.41
HOT	3511.65	3582.92	3382.08	3520.19	3256.18	3459.89
INTECH	3530.00	3601.00	3382.00	3541.00	3221.00	3479.00
JNOC	3471.72	3589.29	3251.86	3491.07	3020.84	3405.28
Marathon	3493.24	3593.85	3293.26	3509.80	3085.07	3433.56
Phillip's	3449.40	3572.40	3203.40	3460.20	2953.20	3351.90
RSRC	3567.80	3610.90	3444.10	3575.30	3318.90	3430.30
Shell	3448.75	3571.38	3201.16	3456.91	2948.98	3345.16
Stanford	3454.64	3572.29	3216.69	3464.30	2977.69	3359.93
TDC	3438.21	3544.40	3203.95	3452.69	2959.82	3343.16
Mean	3476.30	3577.18	3270.92	3486.04	3060.42	3395.06
Standard Deviation	37.96	17.45	81.54	37.87	127.79	60.28

Table 10 Total Pressure Drop in Wellbore in psia at 1500 Days

Participants	1a	1b	2a	2b	3a	3b
ARTEP	0.40	0.93	1.46	3.34	3.15	7.25
Chevron	1.03	1.42	3.89	5.41	8.57	11.97
CMG	0.46	0.98	1.70	3.57	3.68	7.73
ECL	0.42	0.95	1.53	3.49	3.33	7.55
ERC	0.33	1.05	1.13	3.50	2.25	7.30
HOT	0.21	0.45	1.10	1.50	1.97	3.06
INTECH	0.60	1.70	1.20	3.50	1.70	5.30
JNOC	0.45	1.05	1.86	4.31	4.14	9.58
Marathon	0.26	0.85	0.92	3.04	1.97	6.53
Phillip's	0.00	0.00	0.00	0.00	0.00	0.00
RSRC	0.00	0.00	0.00	0.00	0.00	0.00
Shell	0.48	1.09	1.69	3.74	3.57	7.77
Stanford	0.00	0.00	0.00	0.00	0.00	0.00
TDC	0.00	0.00	0.00	0.00	0.00	0.00

Table 11 Timesteps and Newtonian Iterations

Participants	1a	1b	2a	2b	3a	3b	4a	4b
ARTEP	39 ^(a)	39	45	39	47	42	50	49
Chevron ^(b)	104 ^(b)	94	120	100	124	107	186	171
CMG ^(c)	36	21	36	23	37	24	66	45
ECL ^(d)	84	63	96	78	120	92	247	246
ERC	24	23	25	25	25	25	31	33
HOT	58	61	62	76	61	66	135	134
INTECH ^(e)	23	21	23	23	23	22	35	34
JNOC	55	51	64	56	65	57	102	103
Marathon	26	25	24	27	24	25	149	149
Phillip's	39	38	42	43	51	45	459	943
RSRC	17	17	17	17	17	17	102	96
Shell	23	23	27	24	27	26	156	182
Stanford	31	31	33	31	34	33	82	72
TDC	92	106	105	104	105	114	392	356
Mean	22	21	23	22	24	22	48	47
Standard Deviation	53	48	57	53	57	53	130	134
Total number of timesteps	155	155	161	157	165	157	288	252
Total number of iterations	221	192	291	233	346	253	898	961
Use of grid refinement for all cases	57	46	47	47	47	47	47	50
Use of grid refinement with local timesteps and iterations for all cases except 4a and 4b	57	50	66	56	70	60	104	101
	58	36	158	44	182	71	1732	1264
	58	36	161	45	197	72	1733	1264
	42	42	45	43	42	43	55	47
	114	109	123	121	120	125	180	153
	20	19	22	20	22	21	49	43
	55	44	55	50	60	57	265	116
	318	96	632	272	951	421	901	541
	2093	189	4441	1796	6986	2882	7326	3366

(a) Total number of timesteps

(b) Total number of iterations

(c) Use of grid refinement for all cases

(d) Use of grid refinement with local timesteps and iterations for all cases except 4a and 4b

Figure 2 Water Injection in Bottom Layer (K=6)

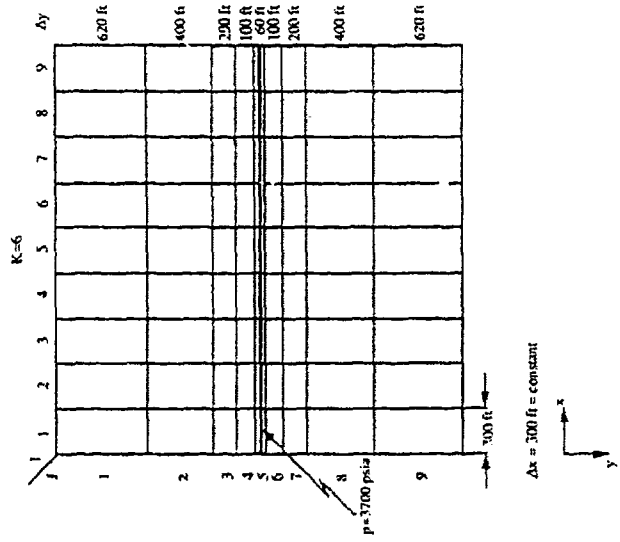


Figure 1 Horizontal Producer in Top Layer (K=1)

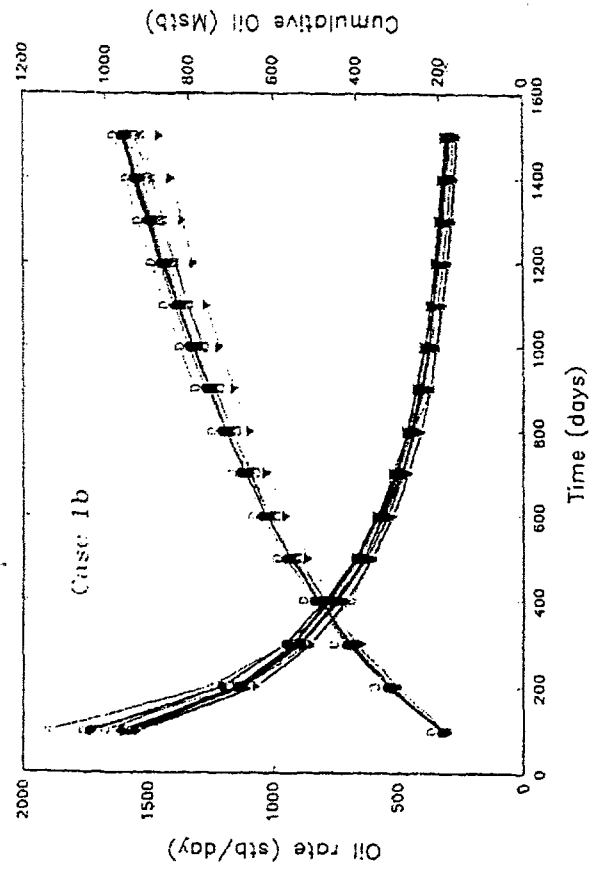
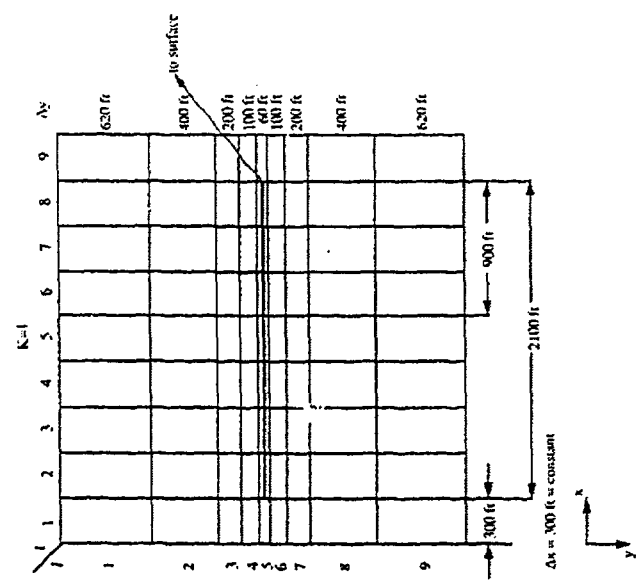


Figure 4: Oil rate (solid) and cumulative oil production (dashed) for Case 1b

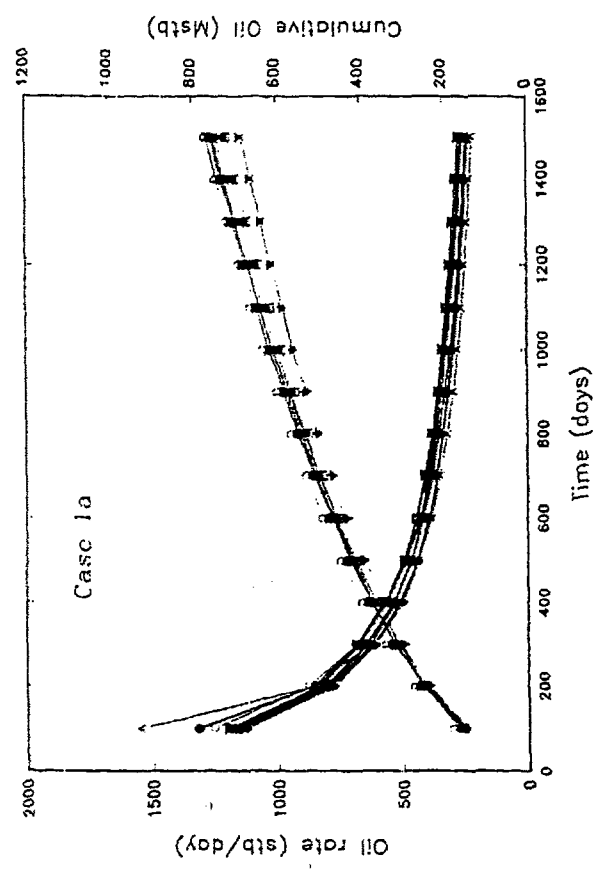


Figure 3: Oil rate (solid) and cumulative oil production (dashed) for Case 1a

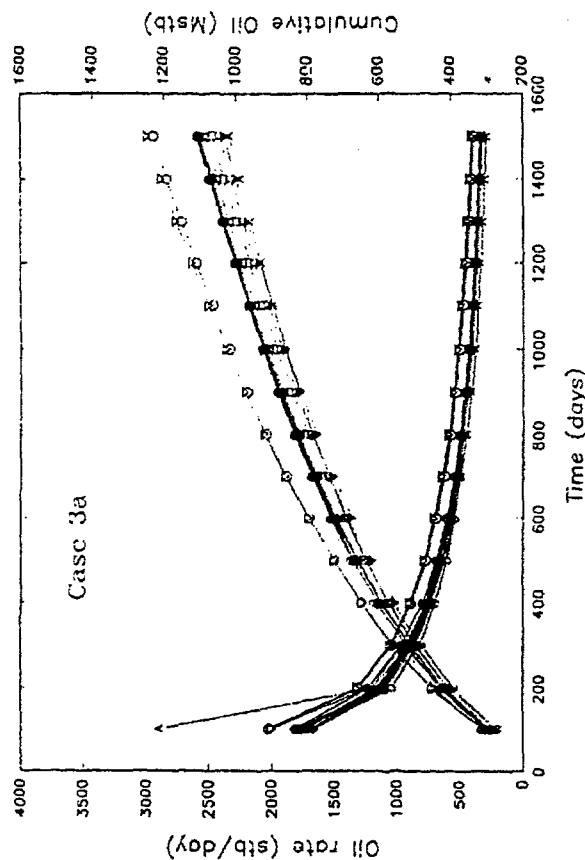


Figure 7: Oil rate (solid) and cumulative oil production (dashed) for Case 3a

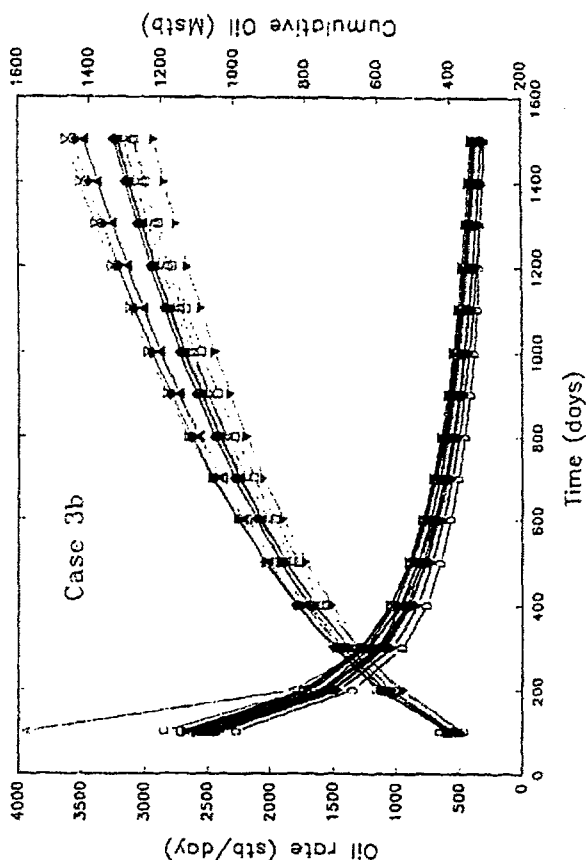


Figure 8: Oil rate (solid) and cumulative oil production (dashed) for Case 3b

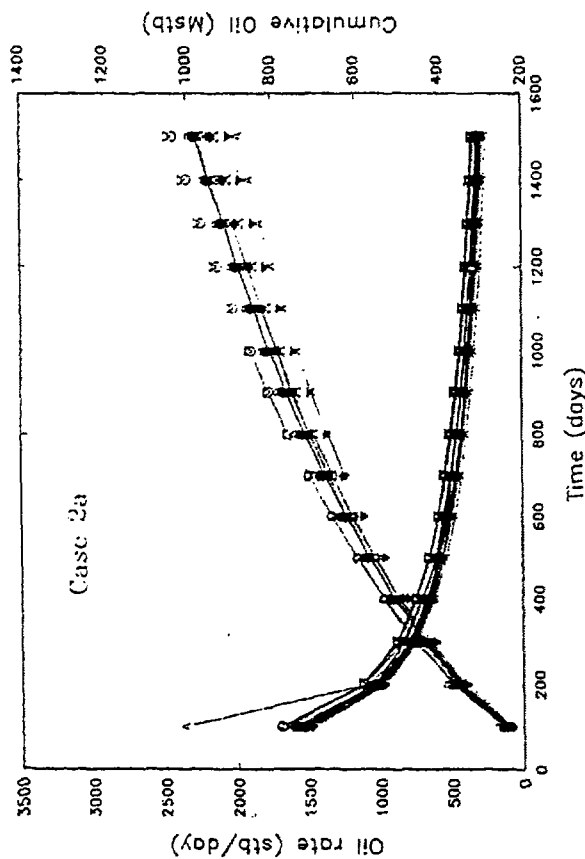


Figure 5: Oil rate (solid) and cumulative oil production (dashed) for Case 2a

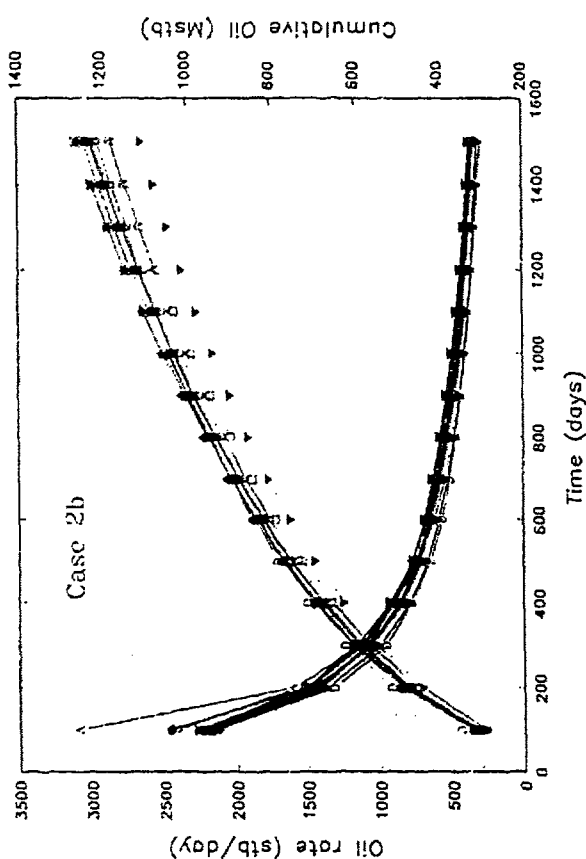


Figure 6: Oil rate (solid) and cumulative oil production (dashed) for Case 2b

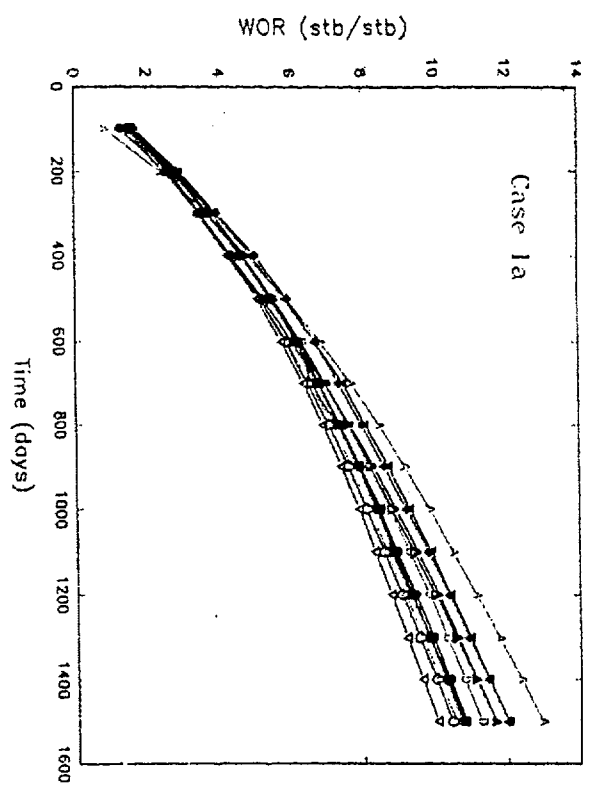


Figure 9: Water-oil ratio for Case 1a

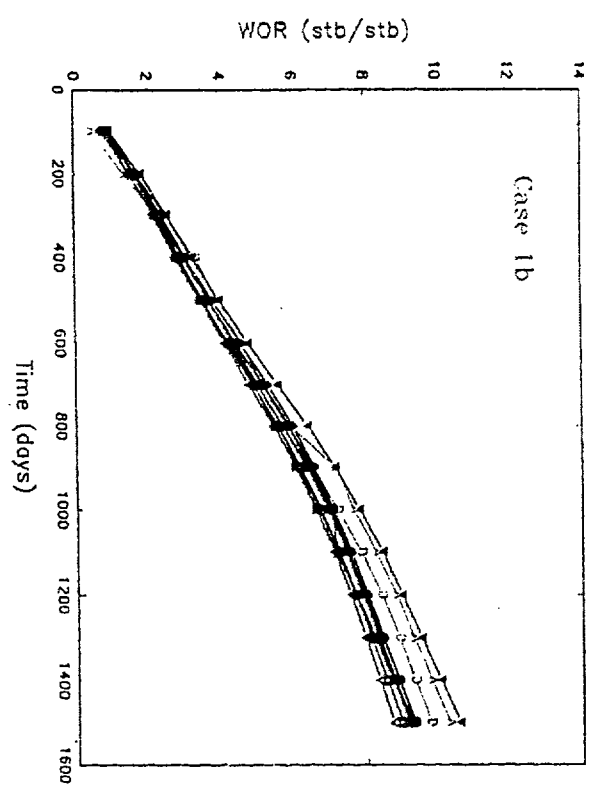


Figure 10: Water-oil ratio for Case 1b

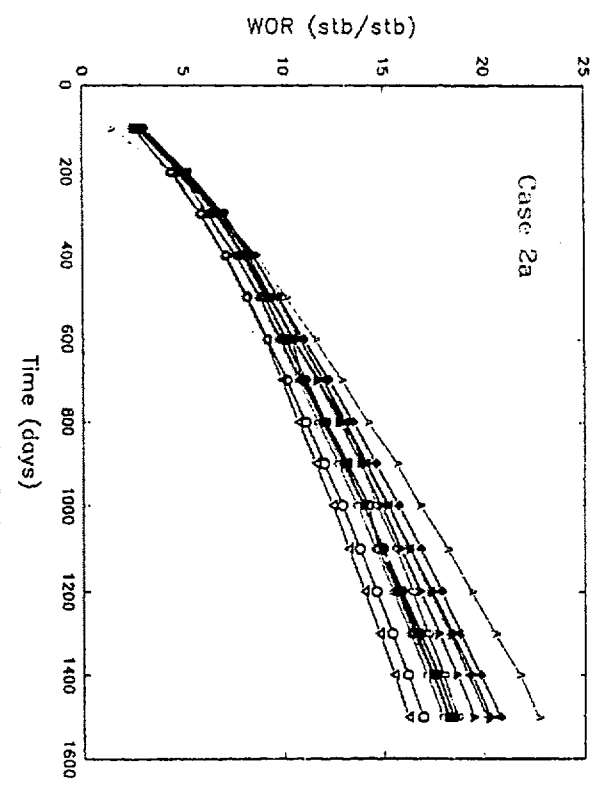


Figure 11: Water-oil ratio for Case 2a

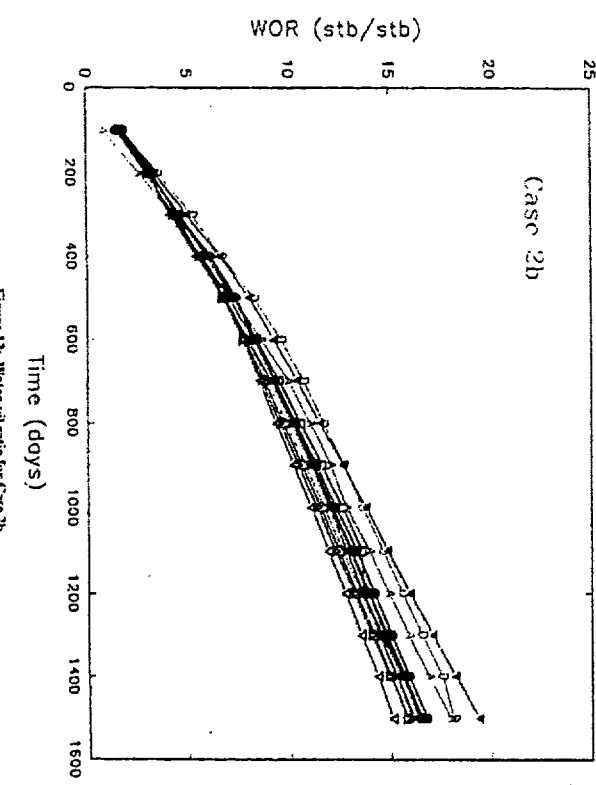


Figure 12: Water-oil ratio for Case 2b

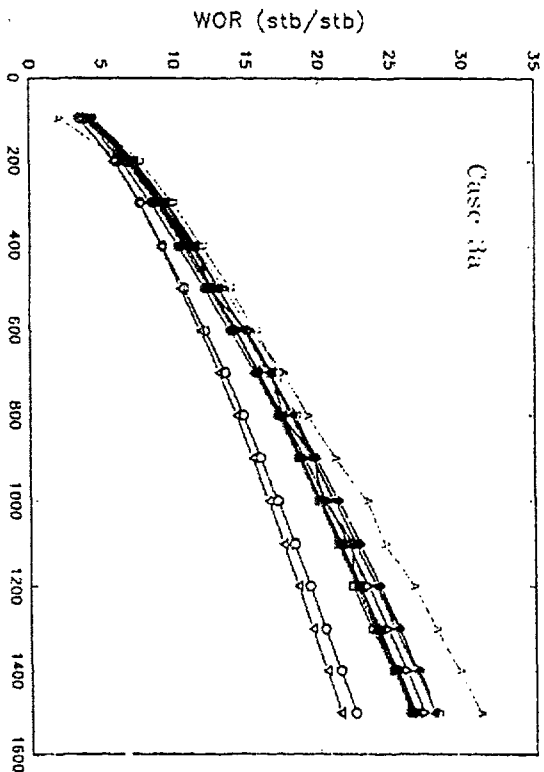


Figure 13: Water-oil ratio for Case 3a

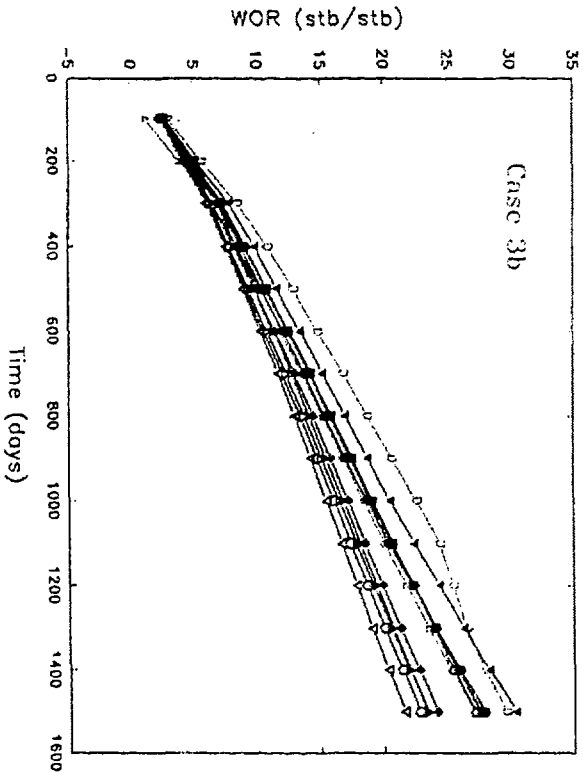


Figure 14: Water-oil ratio for Case 3b

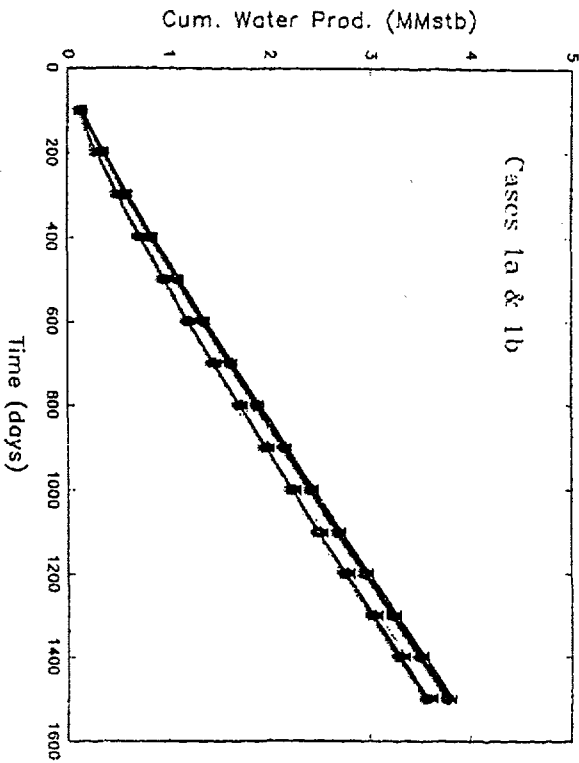


Figure 15: Cumulative water production for Case 1a (solid) and 1b (dashed)

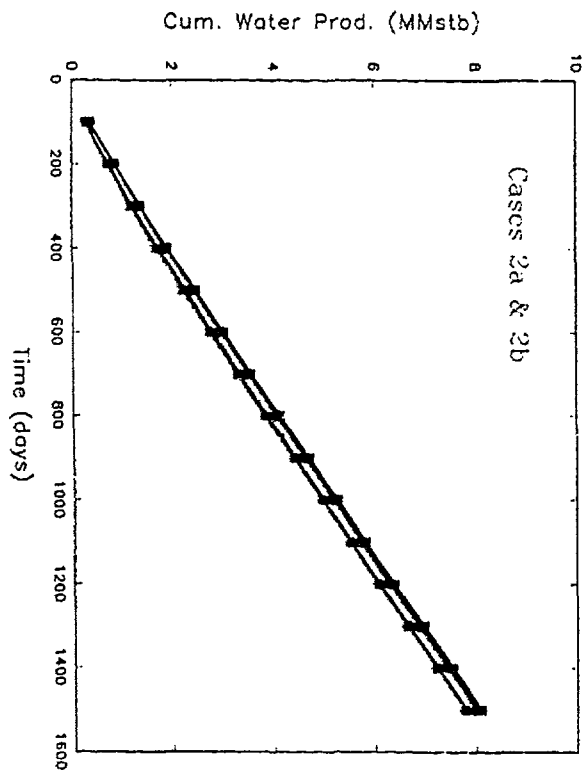


Figure 16: Cumulative water production for Case 2a (solid) and 2b (dashed)

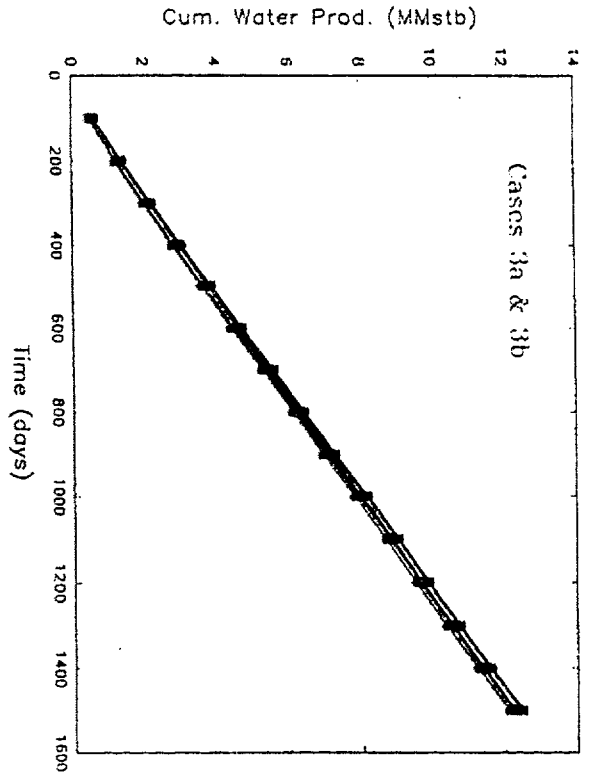


Figure 17: Cumulative water production for Case 3a (solid) and 3b (dashed)

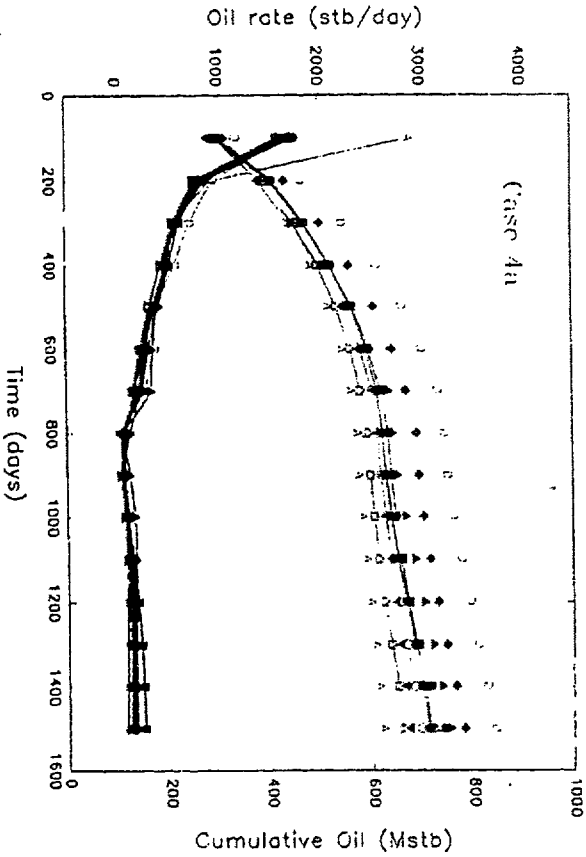


Figure 18: Oil rate (solid) and cumulative oil production (dashed) for Case 4a

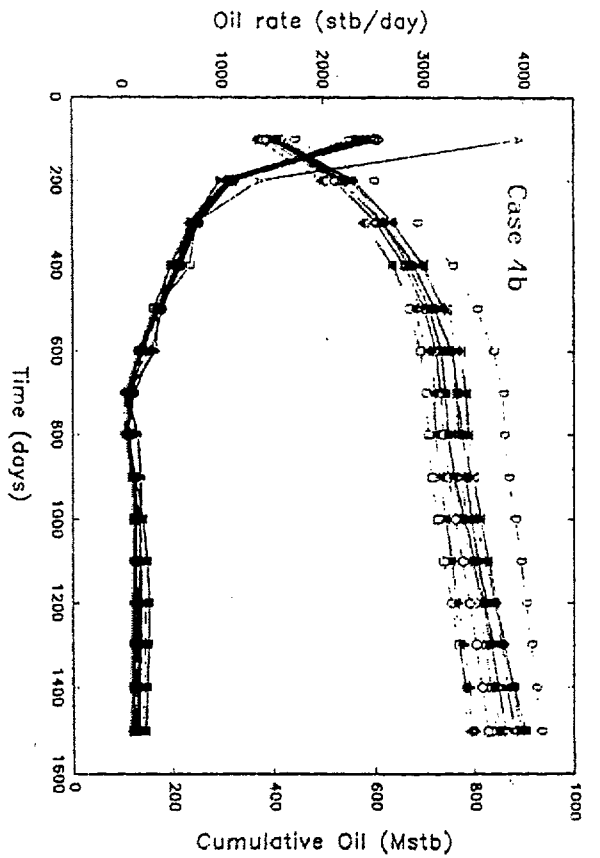


Figure 19: Oil rate (solid) and cumulative oil production (dashed) for Case 4b

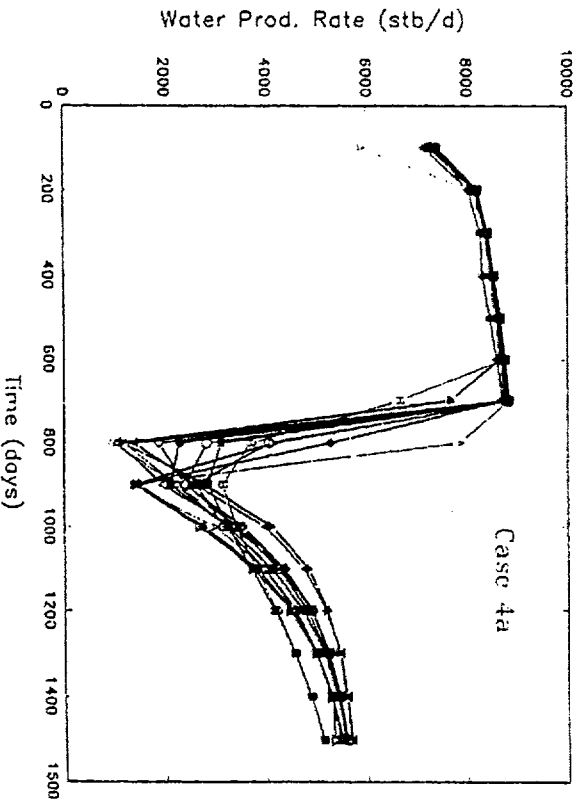


Figure 20: Water production rate for Case 4a

ML-21221

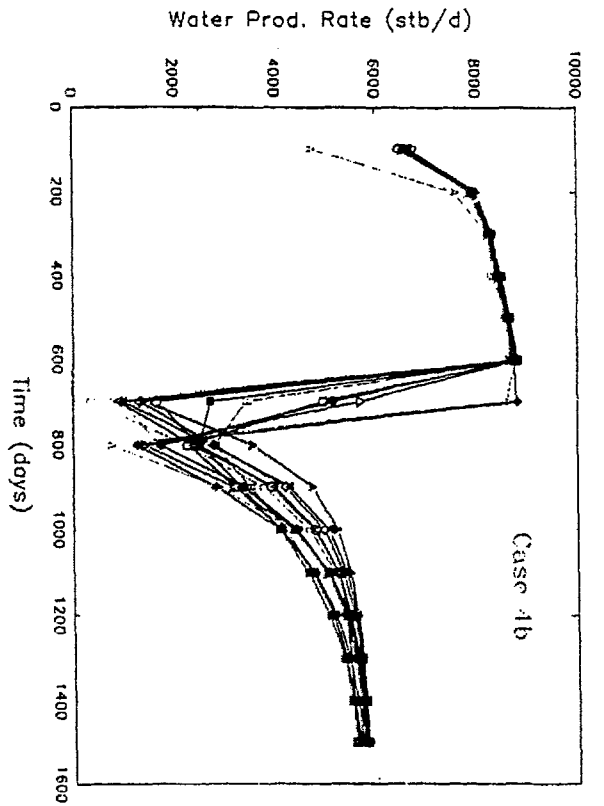


Figure 21: Water production rate for Case 4b

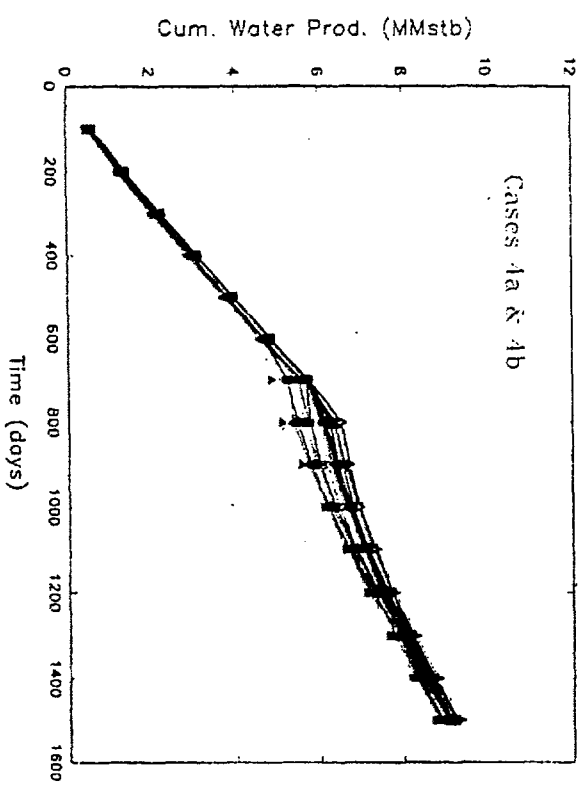


Figure 22: Cumulative water production for Case 4a (solid) and 4b (dashed)

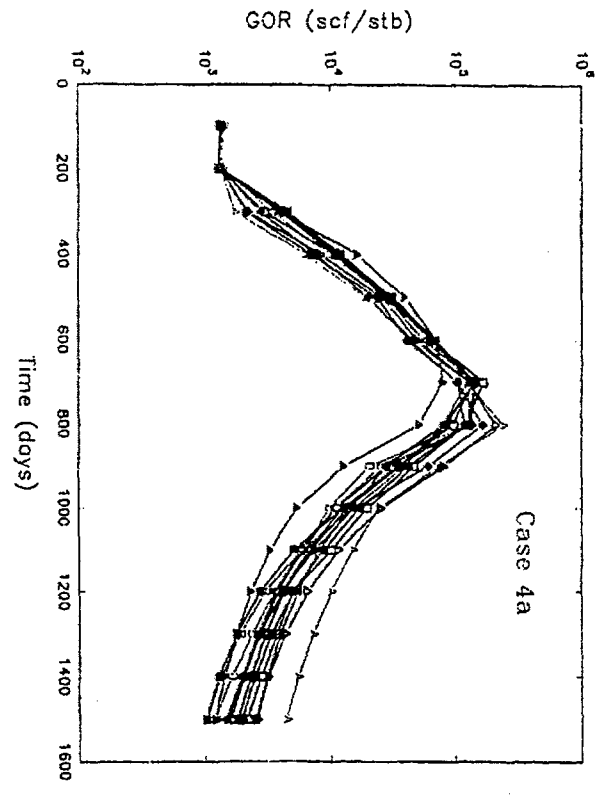


Figure 23: Gas-oil ratio for Case 4a

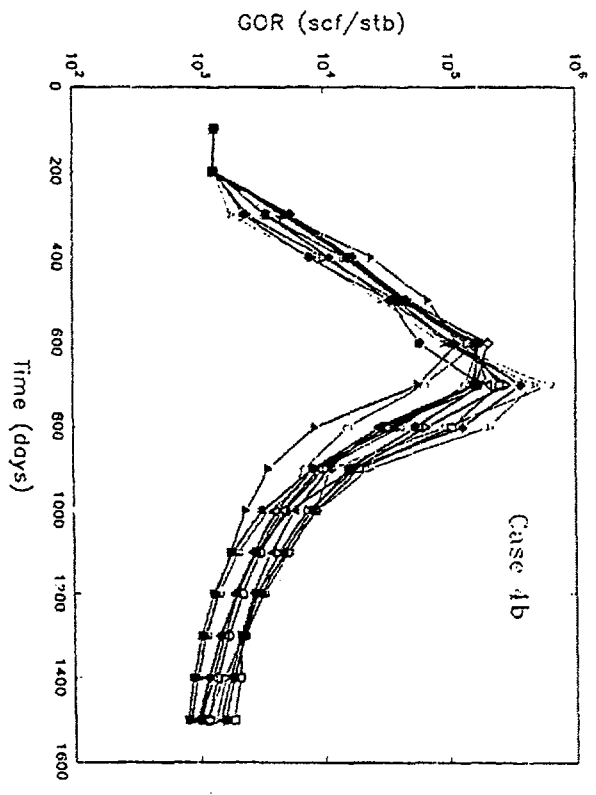


Figure 24: Gas-oil ratio for Case 4b

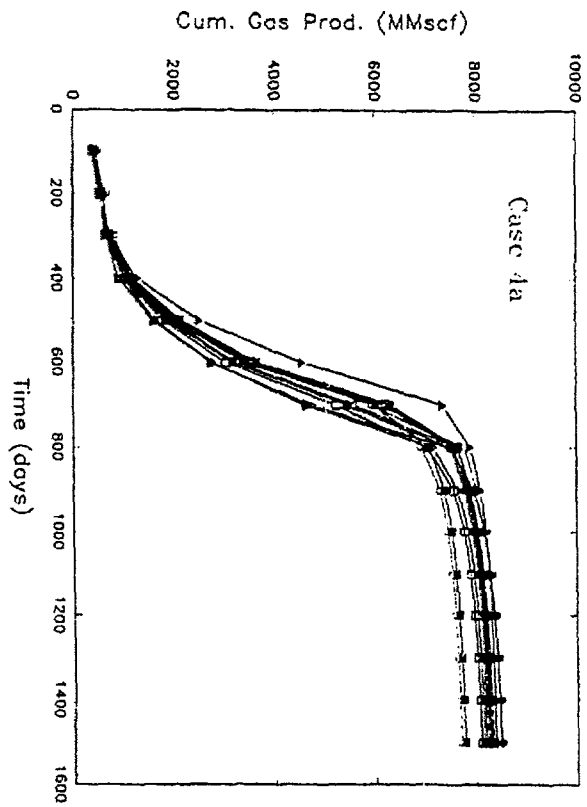


Figure 25: Cumulative gas production for Case 4a

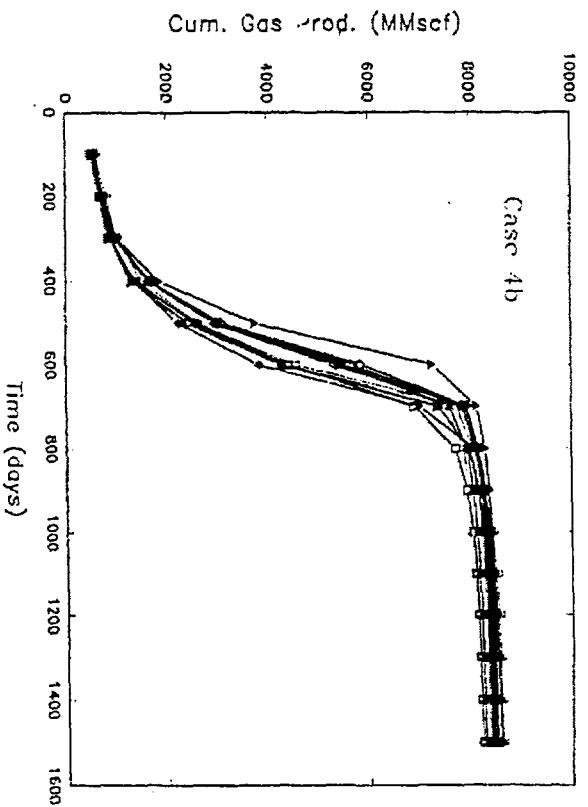


Figure 26: Cumulative gas production for Case 4b

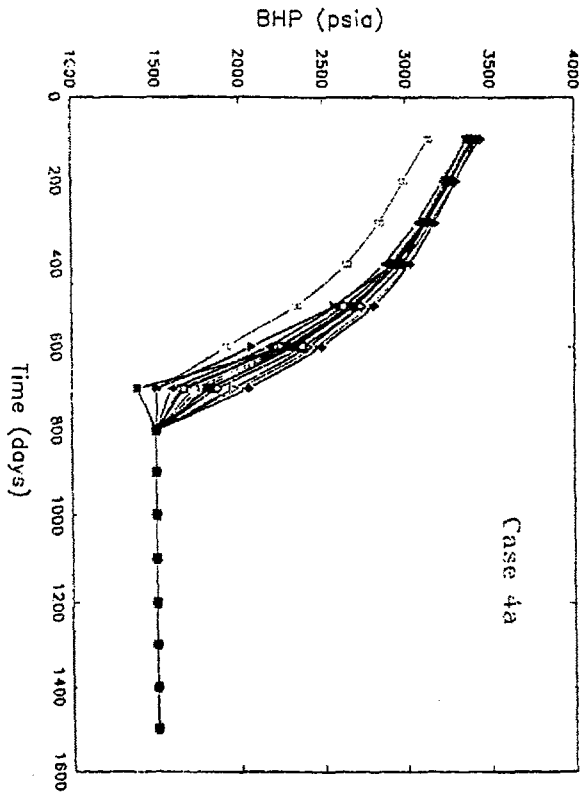


Figure 27: Bottom-hole pressure for Case 4a

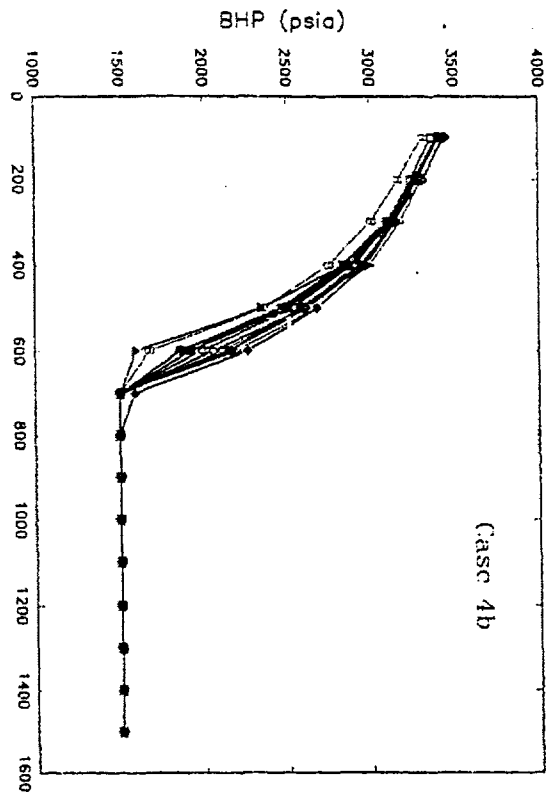


Figure 28: Bottom-hole pressure for Case 4b

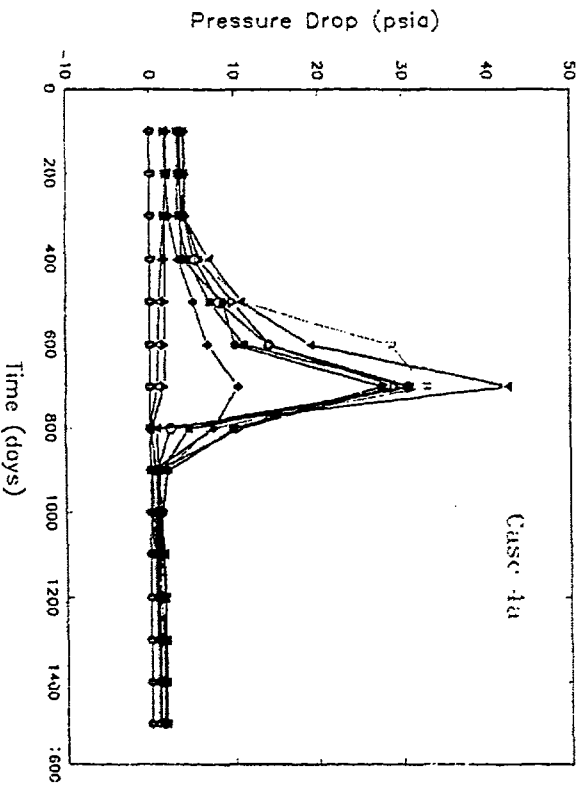


Figure 29: Total pressure drop along wellbore for Case 4a

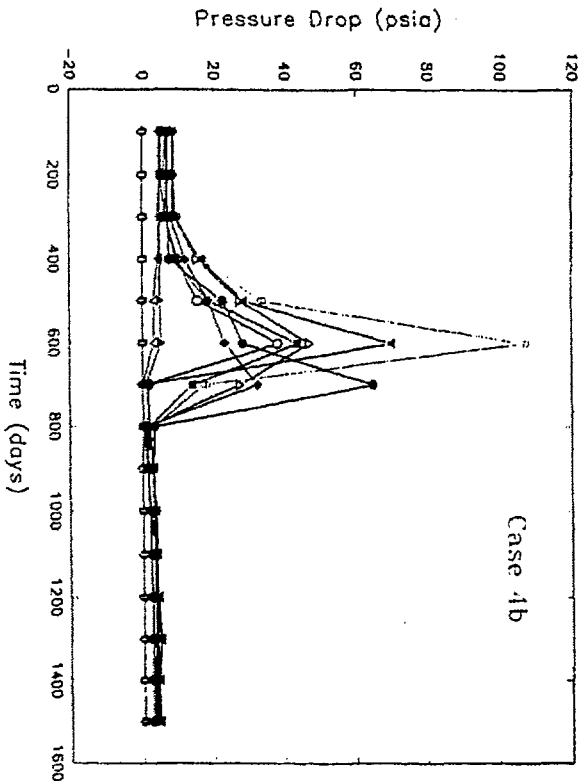


Figure 30: Total pressure drop along wellbore for Case 4b

SPE # 21221

TIGRESS

Robertson ERC Ltd

ADDENDUM

Seventh SPE Comparison Solution Project - Modelling Horizontal Wells
in Reservoir Simulation

Subsequent to our submission of the results of the Seventh Comparative Solution
Project, two small errors were discovered in our input data set which significantly
affected some of the solutions.

All eight cases have been re-run using the correct data and the results, where they
differed from the original ones, can be seen in Figures 3 - 17 and in Tables 8 - 10.

Figure 3: Oil rate (solid) and cumulative oil production (dashed) for Case 1a

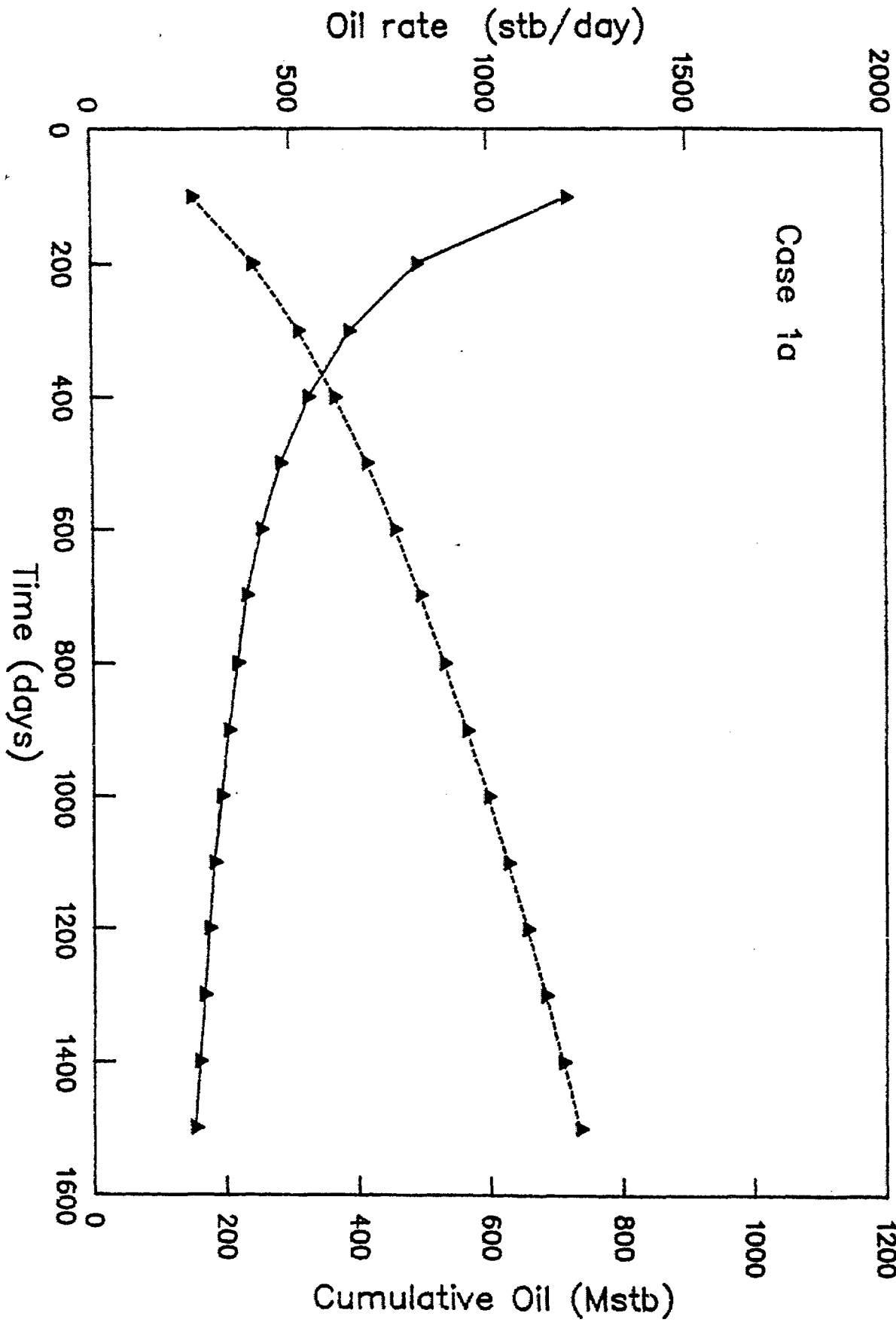


Figure 4: Oil rate (solid) and cumulative oil production (dashed) for Case 1b

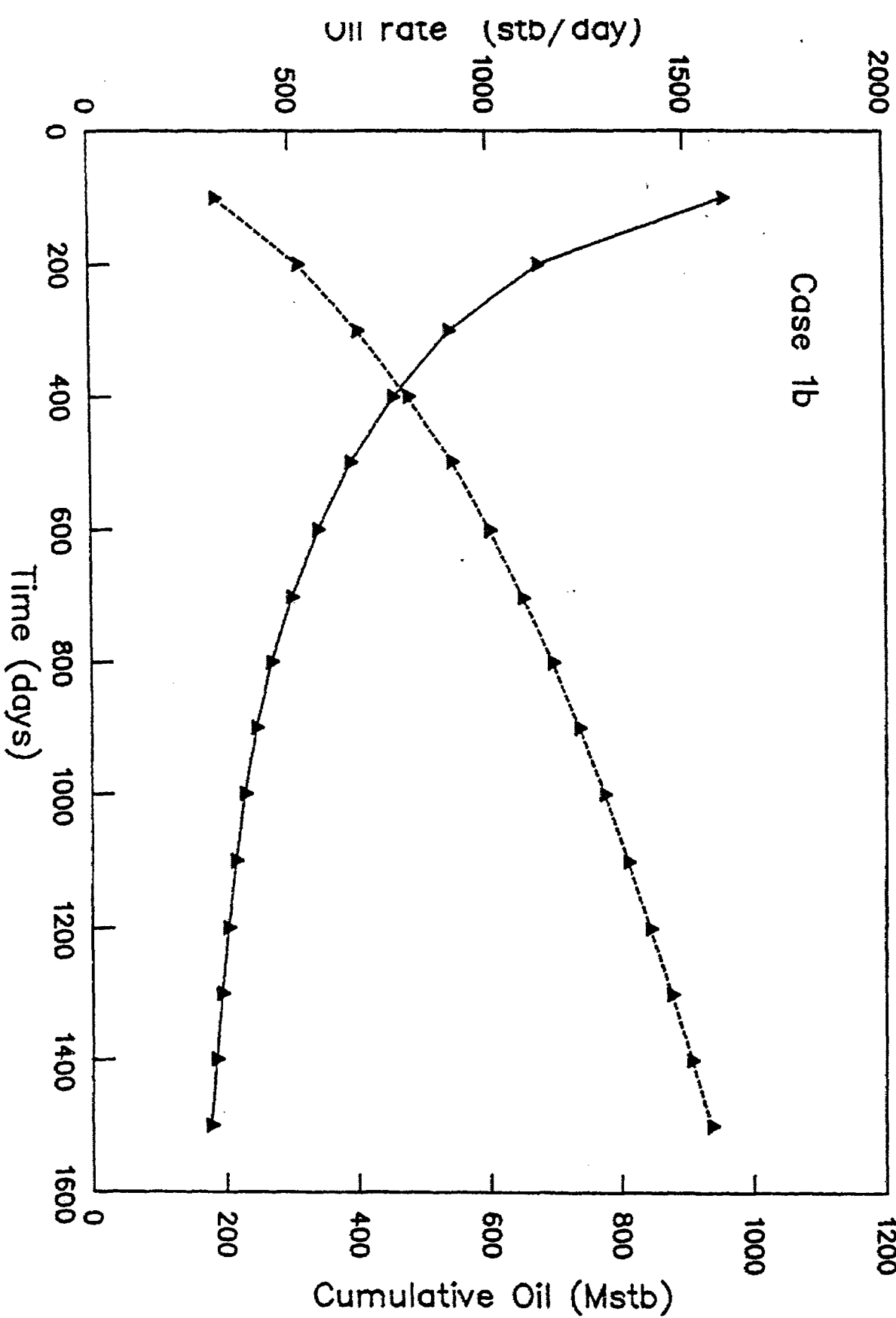


Figure 5: Oil rate (solid) and cumulative oil production (dashed) for Case 2a

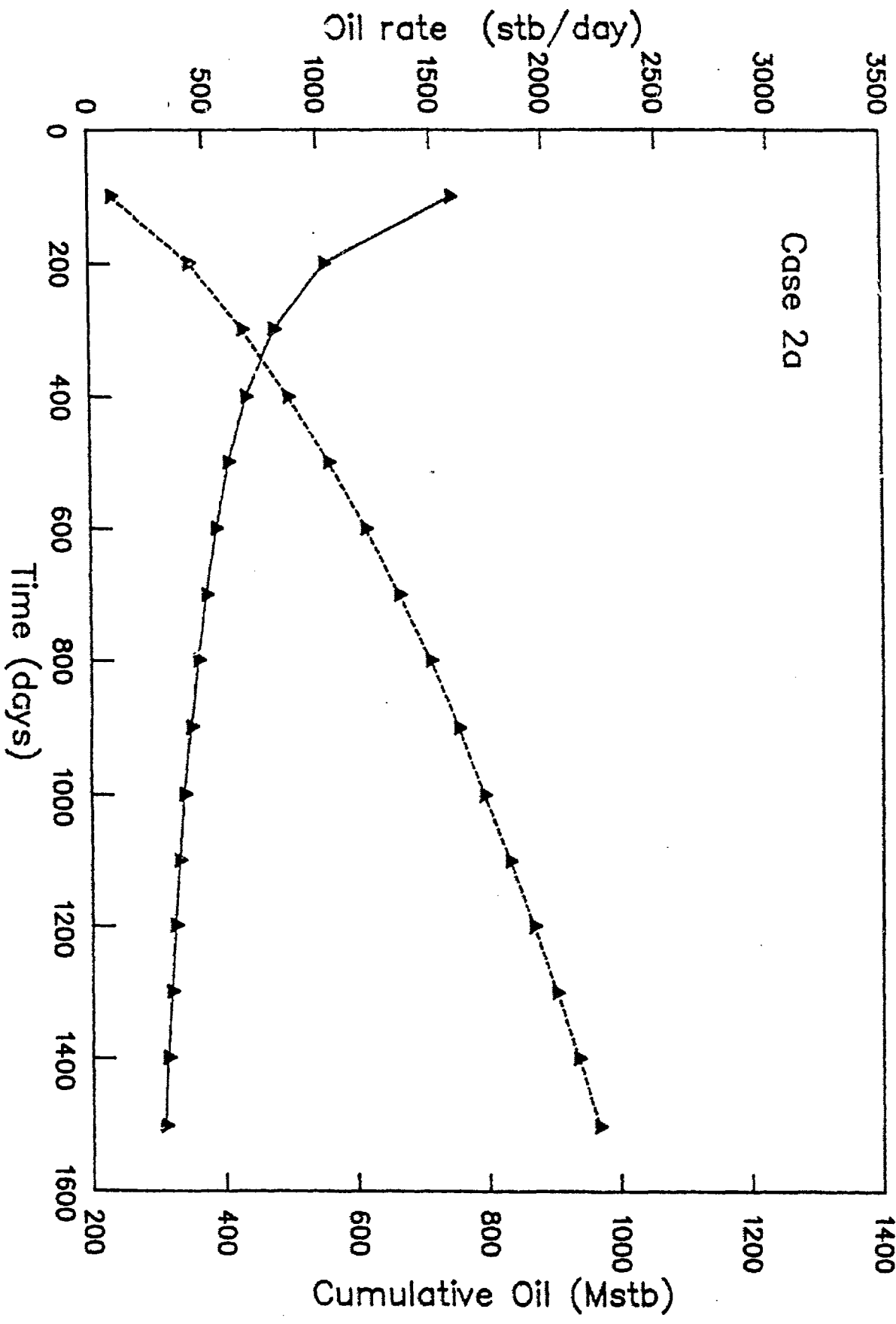


Figure 6: Oil rate (solid) and cumulative oil production (dashed) for Case 2b

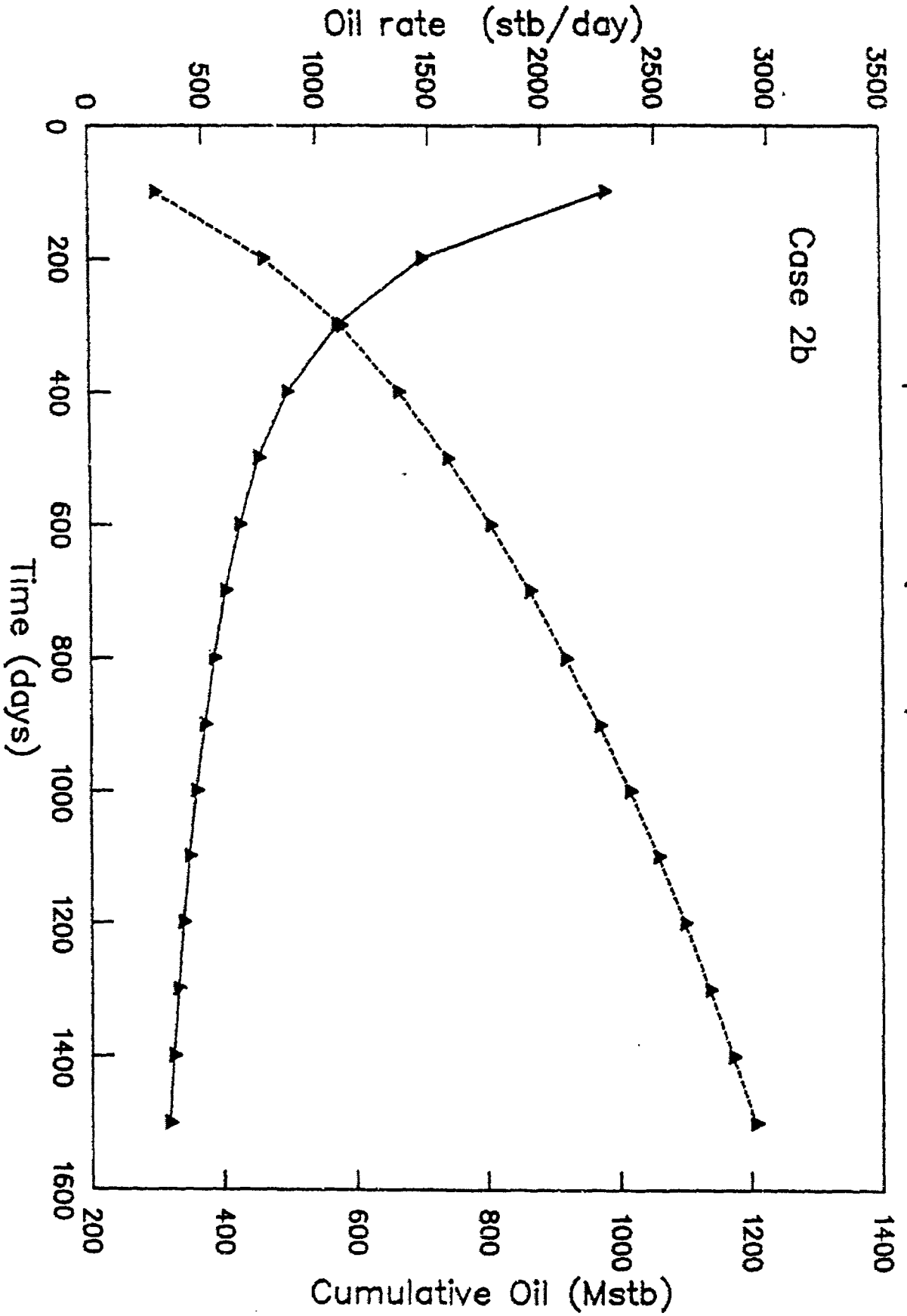


Figure 7: Oil rate (solid) and cumulative oil production (dashed) for Case 3a

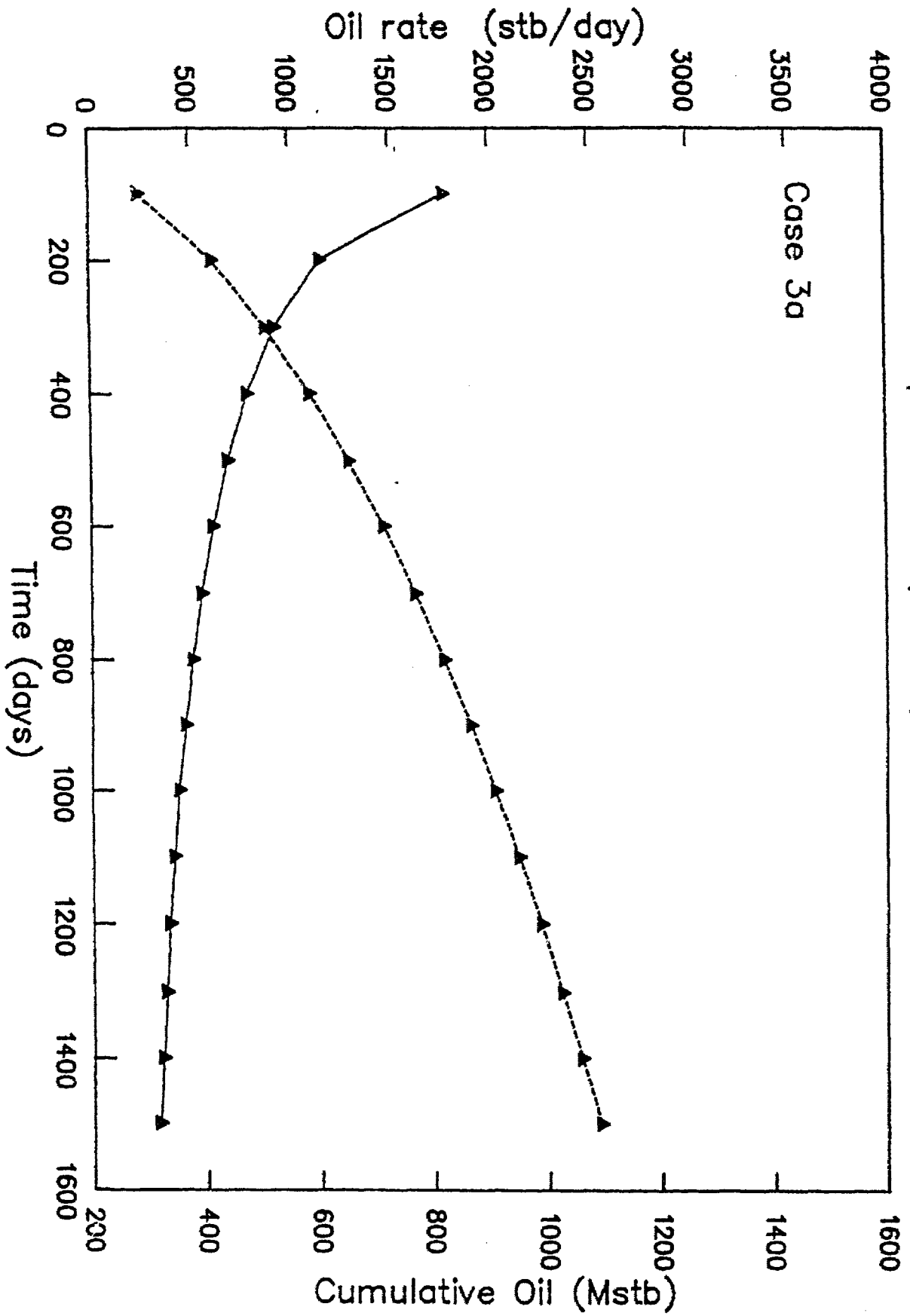


Figure 8: Oil rate (solid) and cumulative oil production (dashed) for Case 3b

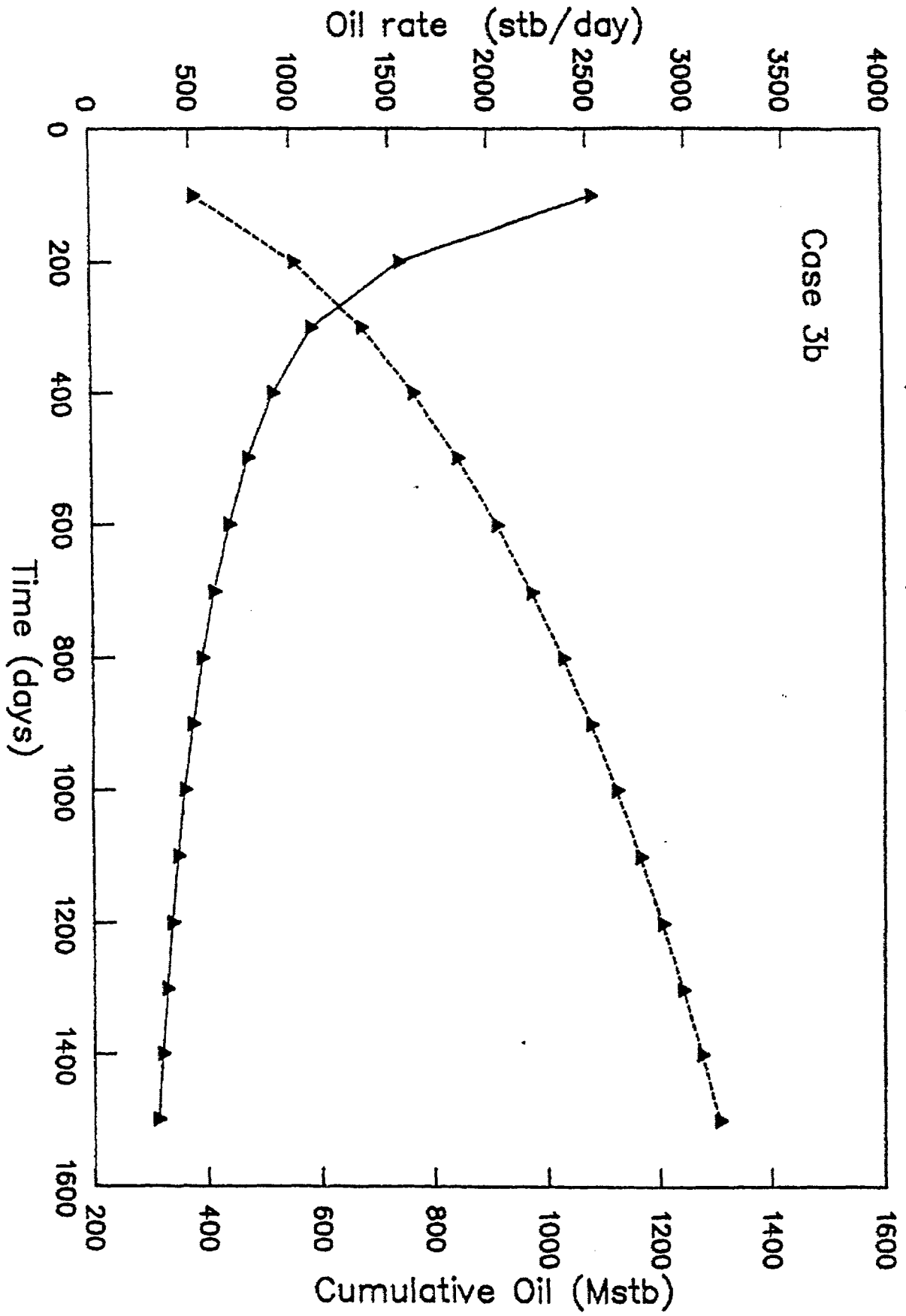


Figure 9: Water-oil ratio for Case 1a

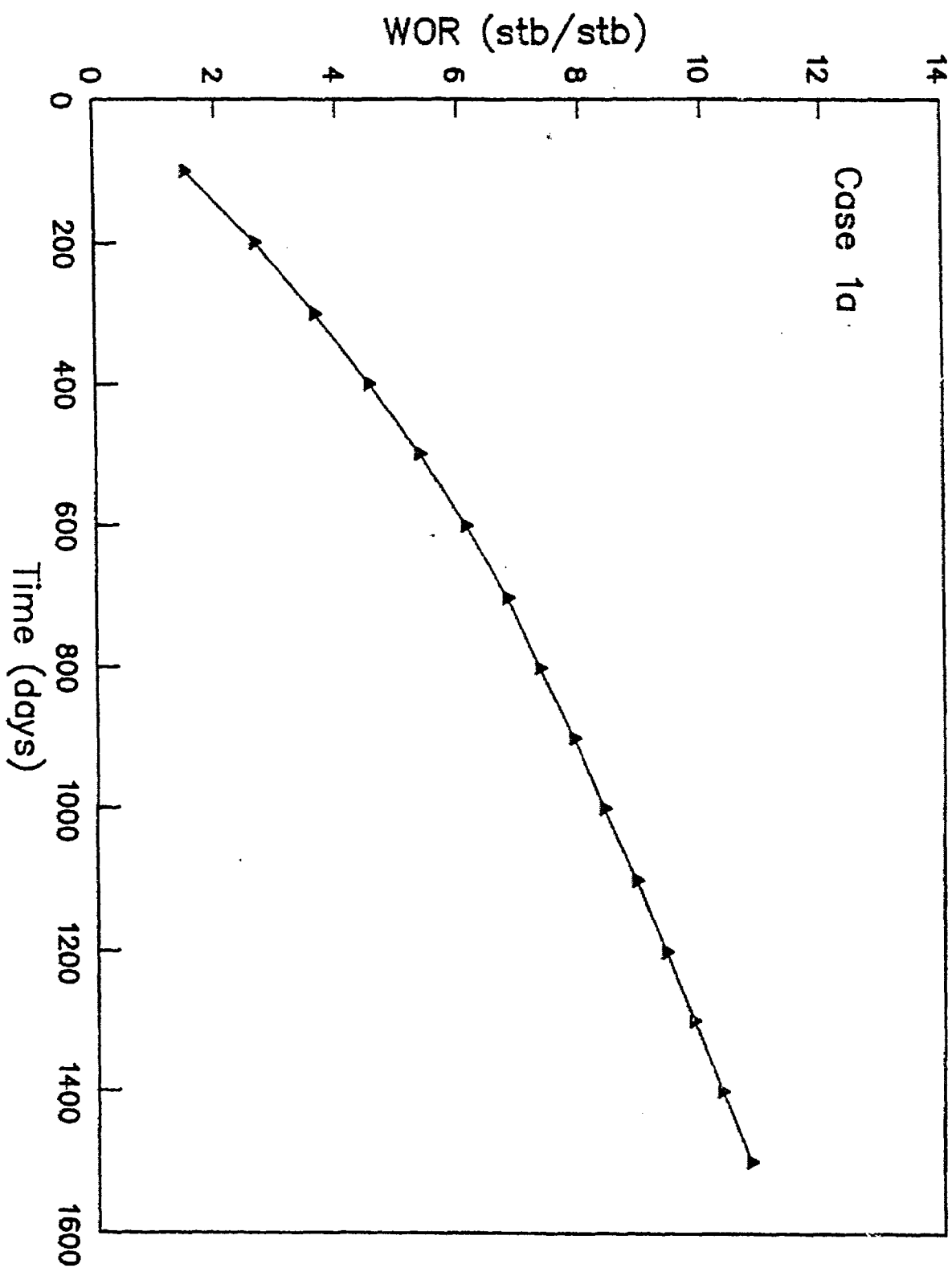


Figure 10: Water-oil ratio for Case 1b

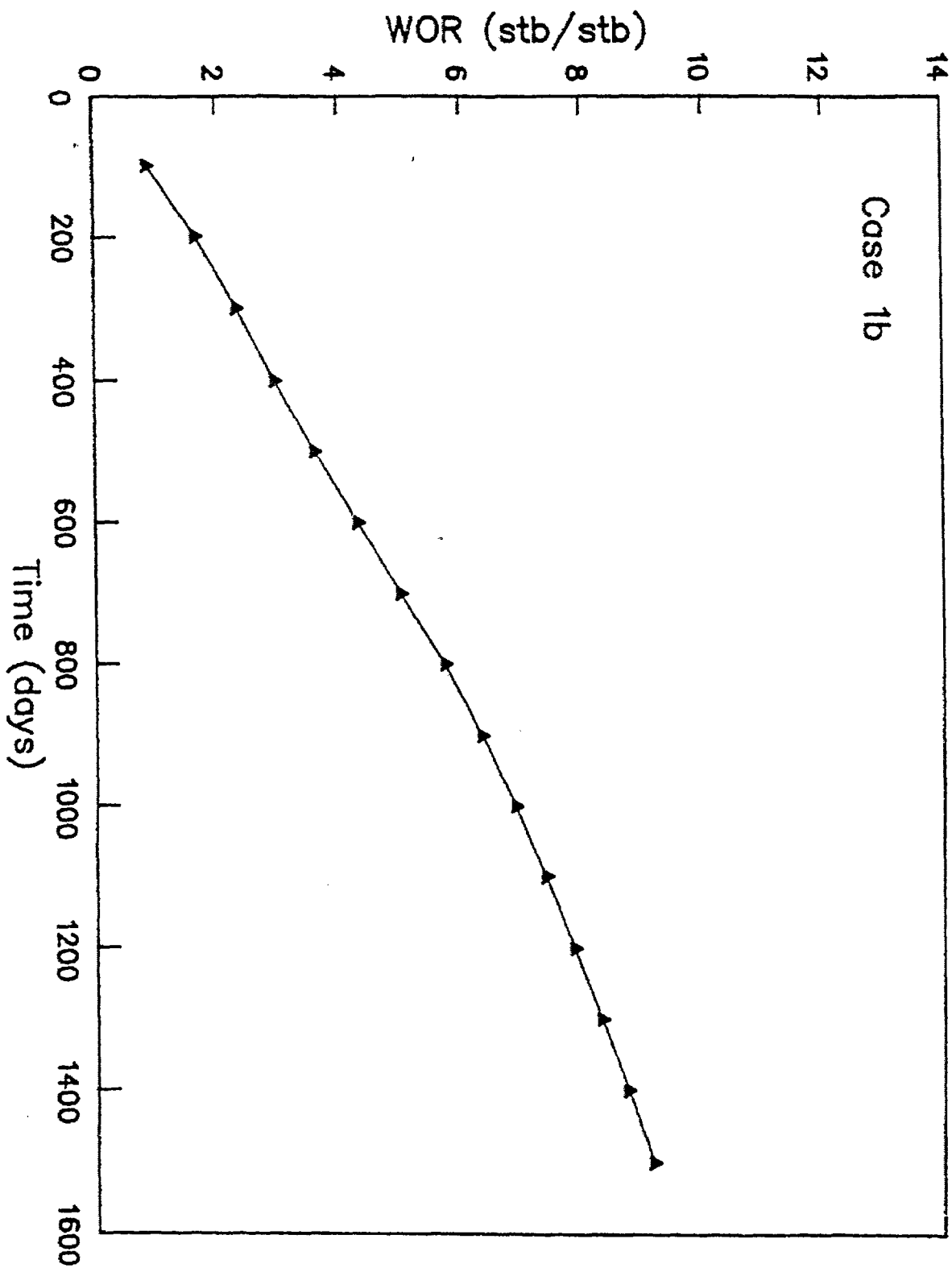


Figure 11: Water-oil ratio for Case 2a

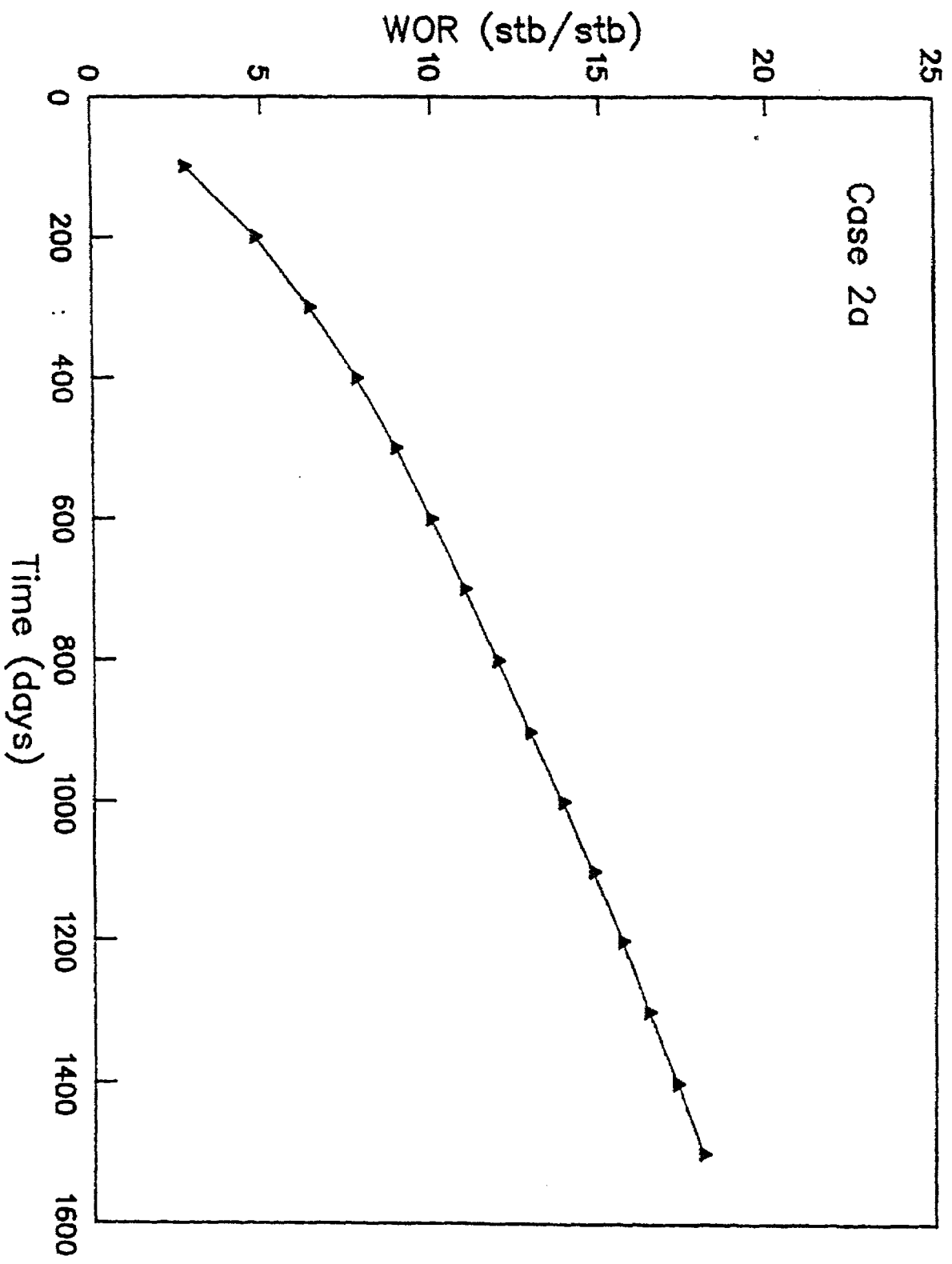


Figure 12: Water—oil ratio for Case 2b

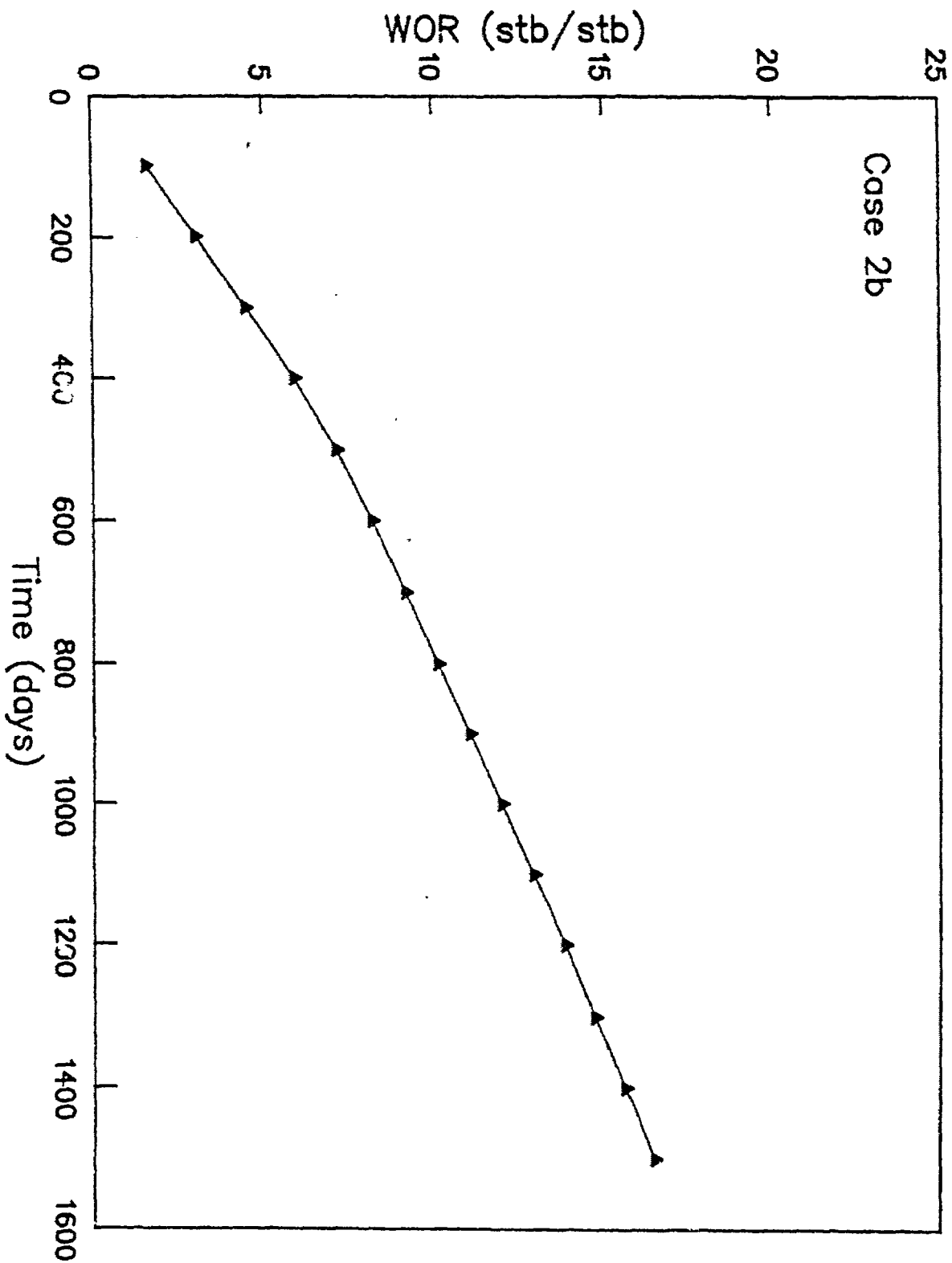


Figure 13: Water-oil ratio for Case 3a

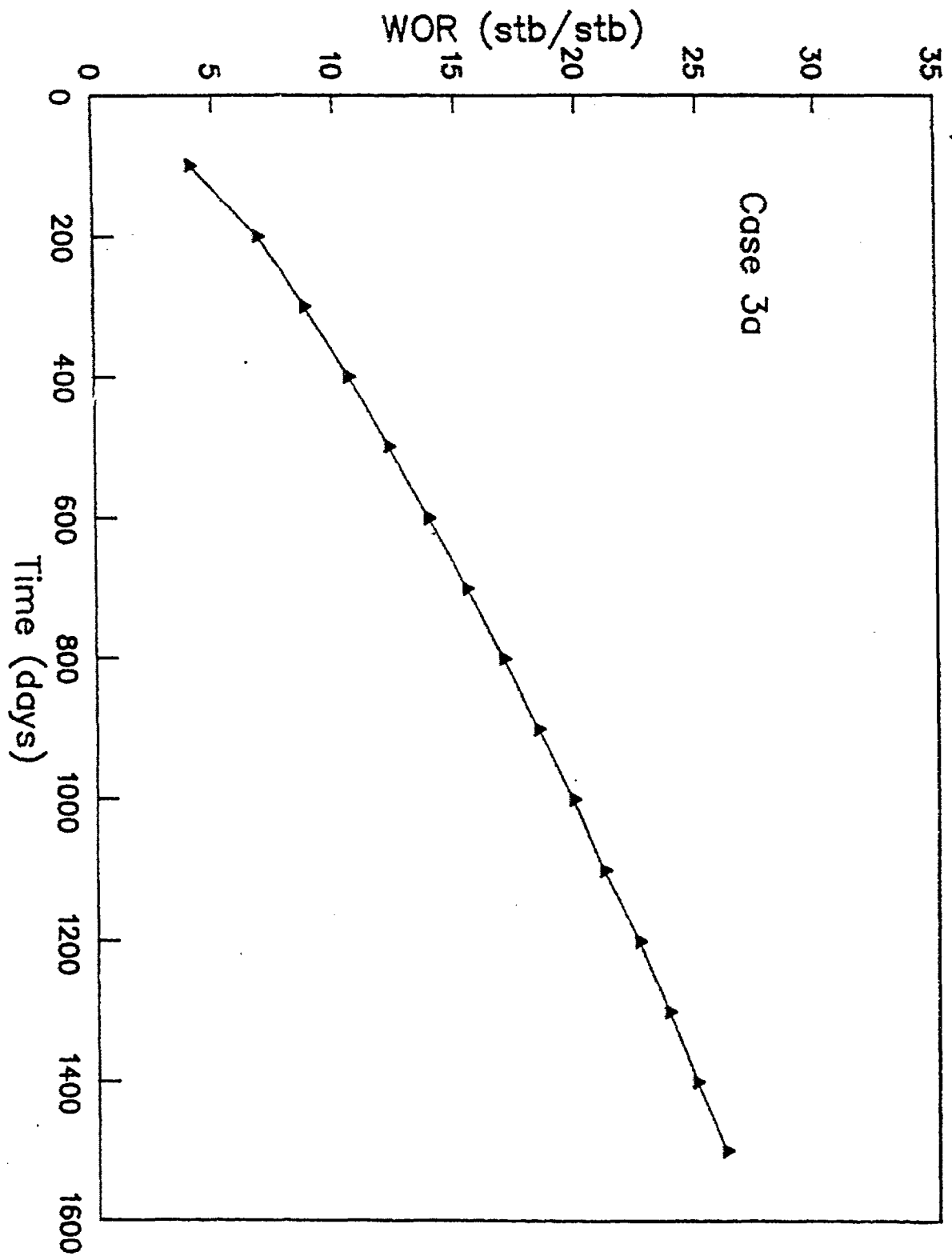


Figure 14: Water-oil ratio for Case 3b

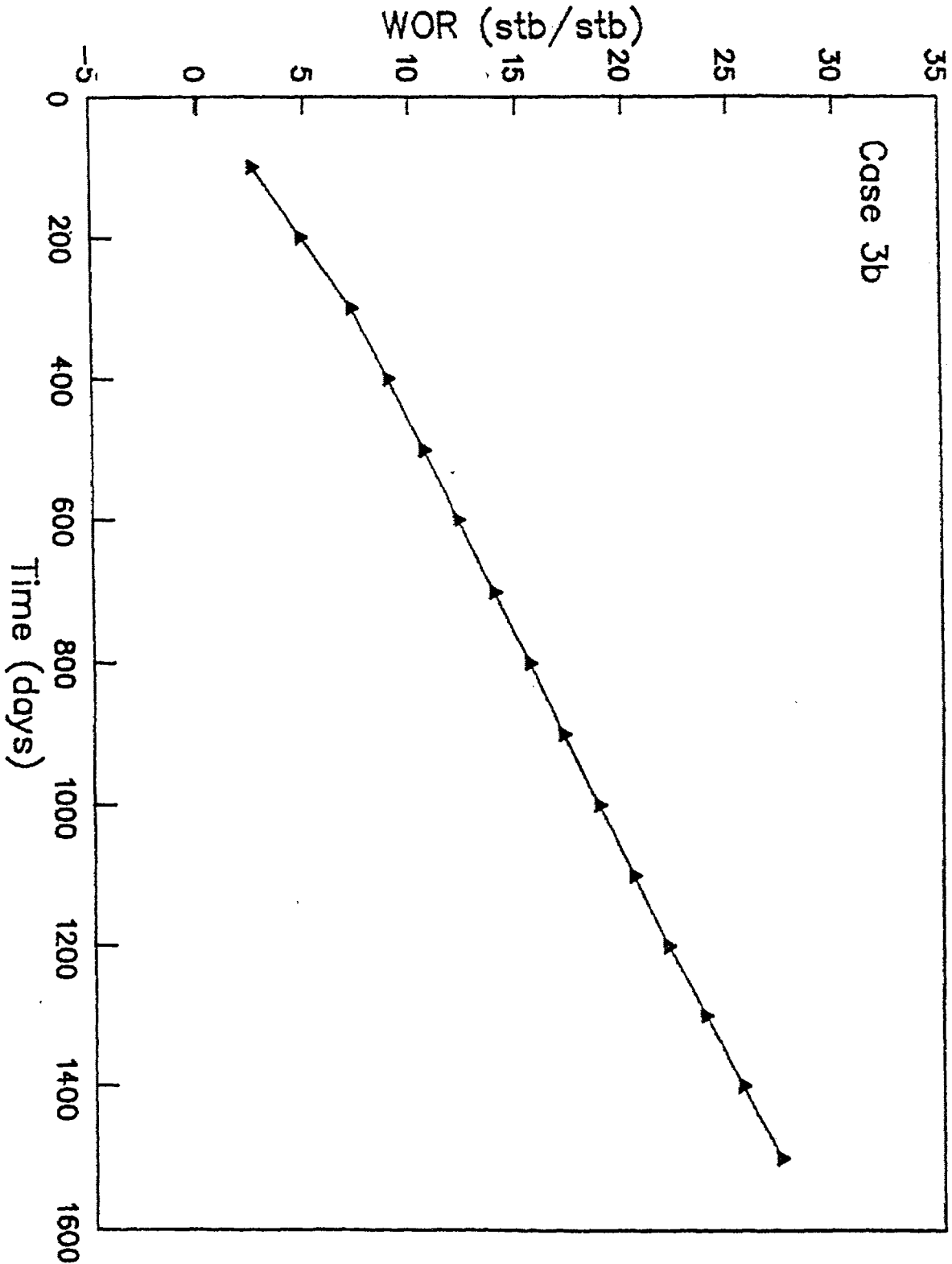


Figure 15: Cumulative water production for Case 1a (solid) and 1b (dashed)

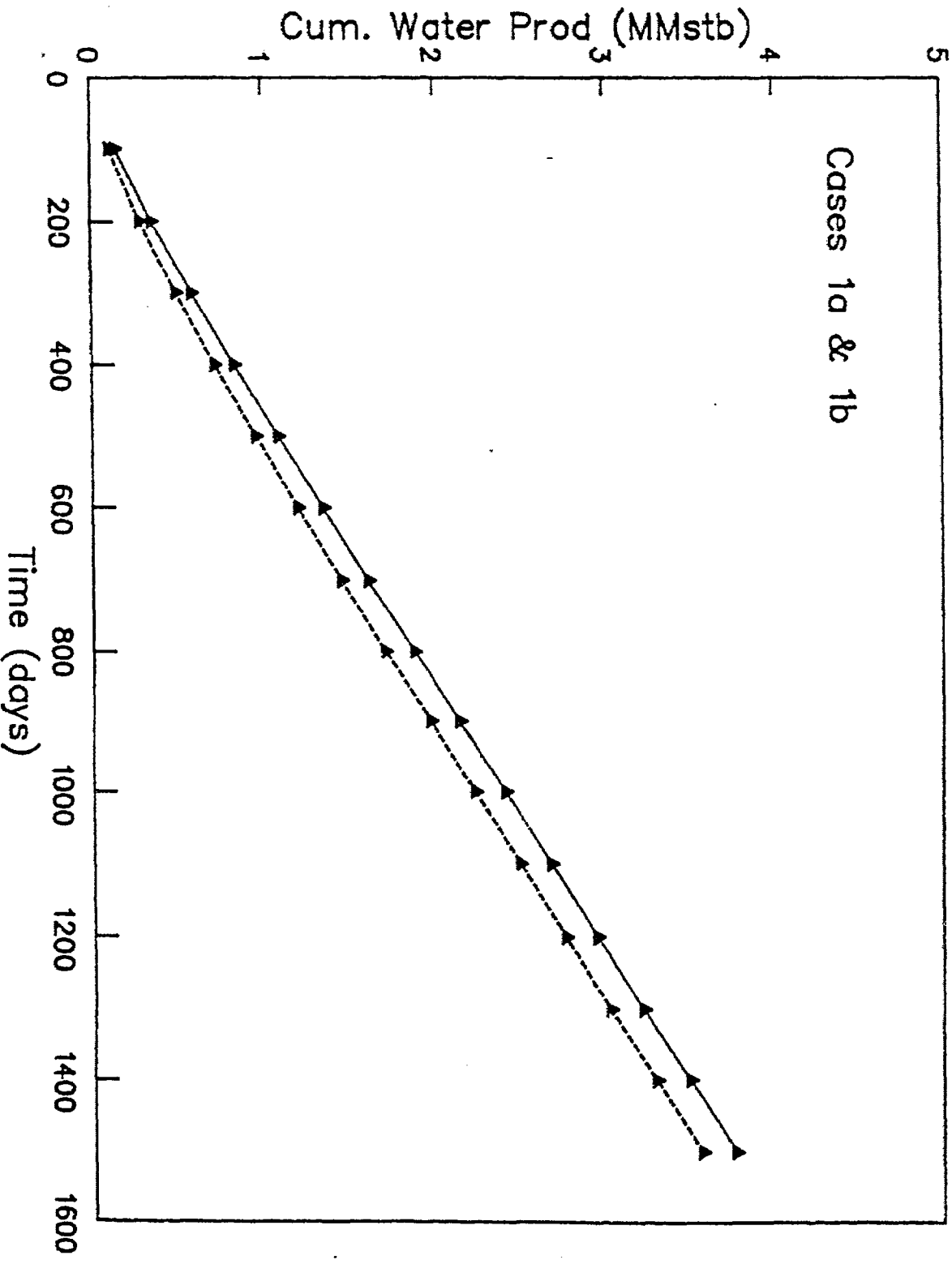


Figure 16: Cumulative water production for Case 2a (solid) and 2b (dashed)

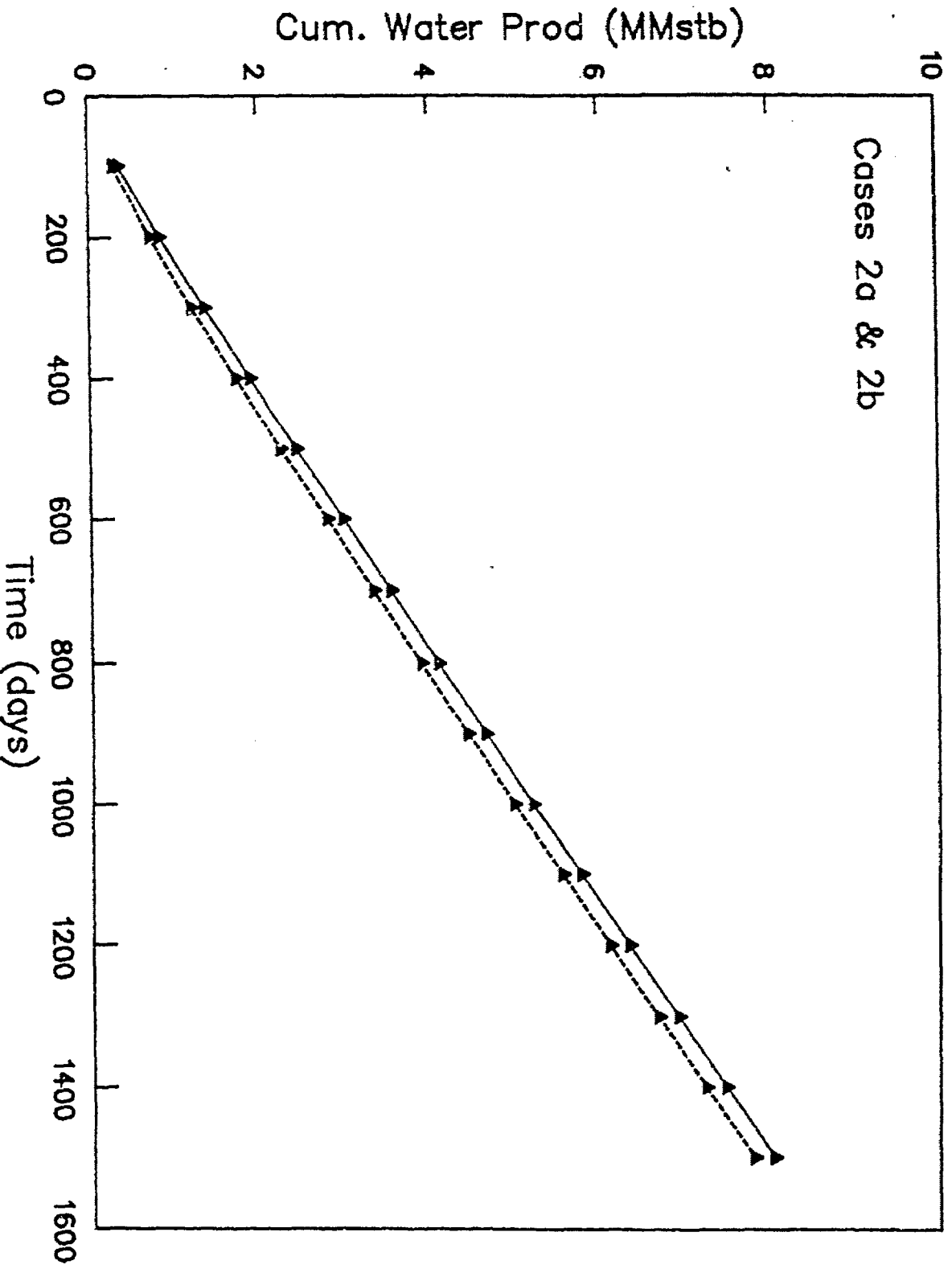


Figure 17: Cumulative water production for Case 3a (solid) and 3b (dashed)

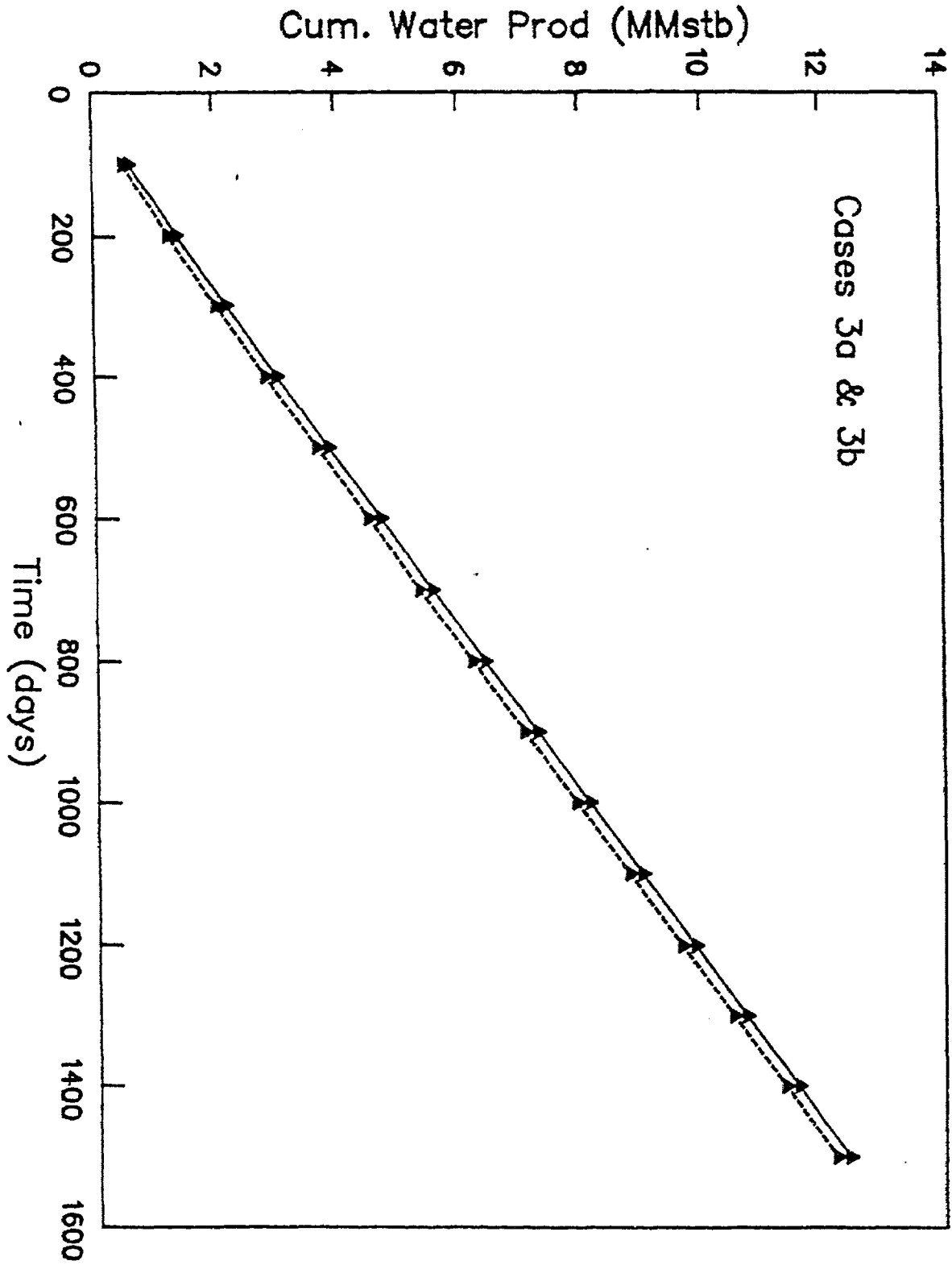


Table 8 Cumulative Oil Production in MSTB at 1500 Days

1a	1b	2a	2b	3a	3b
735.6	936.7	967.0	1206.2	1092.0	1306.8

Table 9 Bottom Hole Pressure in psia at 1500 Days

1a	1b	2a	2b	3a	3b
3444.88	3564.58	3202.85	3457.23	2952.26	3347.14

Table 10 Total Pressure Drop in Wellbore in psia at 1500 Days

1a	1b	2a	2b	3a	3b
0.33	1.05	1.13	3.49	2.25	7.30